UNIVERSITÀ DEGLI STUDI DI MILANO

Corso di Dottorato in Ricerca biomedica integrata

XXXI CICLO

Molecular mechanisms and therapeutic approaches in MN diseases

Tutor: Prof. Angelo Poletti

Co-tutor: Prof. Mariarita Galbiati

Coordinatore del Dottorato: Prof.ssa Chiarella Sforza

Tesi di Dottorato di:

Marco MERONI

Matr.n° R11236

Anno accademico 2017 – 2018

Contents

Contents

Introduction

Introduction

Motor neuron diseases (MNDs)

Motor neuron diseases (MNDs) are a heterogeneous group of disorders characterized by death of motor neuron cells. MNDs occur in both adults and children. In children, MNDs are usually characterized by familial forms of the disease; symptoms can be present at birth or appear before the child learns to walk. In adults, MNDs occur more commonly in men than in women, with symptoms appearing generally after the age of 40 [1].
MNDs may be sporadic or familial and are clinically classified according to whether they involve upper or lower motor neurons, or both. Upper motor neuron involvement leads to positive neurological features including spasticity, brisk reflexes, clonus, and extensor plantar responses, as well as negative features such as weakness and loss. Spasticity is defined as the velocity-dependent increase in muscle tone as assessed by passive movement of the limbs. The term is used to define the stiffness and other features due to the damage of descending motor pathways in the central nervous system. This damage, frequently in the spinal cord, leads to abnormal hyper-excitability of the tonic stretch reflex. Consequently, the patient with spastic legs complains of walking difficulty, weakness, fatigue, and reduced exercise tolerance. They may also have cramps of the legs due to spontaneous clonus. Lower motor neuron loss, on the other hand, leads to muscle wasting with fasciculation, weakness, and reduced or abolished reflexes [1].

Amyotrophic lateral sclerosis (ALS), also called Lou Gehrig's disease is a classical MND; it is a progressive fatal disorder that involve both upper and lower motor neurons. Symptoms usually appear first to the limbs, or swallowing muscles. Affected patients lose strength and the ability to move their arms and legs, and to hold the body upright. ALS is also characterized by other symptoms such as spasticity, spasms, muscle cramps, and fasciculations. At end stage of the disease muscles of the diaphragm and chest fail to function properly and patients lose the ability to breath without mechanical support. Usually ALS patients die from respiratory failure, within three to five years from the onset of symptoms. However, about 10 percent of affected individuals survive for ten or more years [2].
Rarely ALS patient present symptoms that involve the person's personality, anyway some recent studies report evidence that some patient with ALS may develop cognitive problems involving word fluency, decision-making, and memory.
ALS classical patient are people between 40 and 60 years of age, but also younger and older individuals can develop the disease. It is also known that men have a higher incidence than women. Familial forms of ALS represent only the 10 percent or less of ALS cases, with more than ten genes identified to date. [2].

Progressive bulbar palsy (PBP), also called progressive bulbar atrophy, involves the brain stem, which is the bulb-shaped region containing lower motor neurons needed for swallowing, speaking, chewing, and other functions. Limb weakness with both lower and upper motor neuron signs is almost always evident. Patients present symptoms include pharyngeal muscle weakness, weak jaw and facial muscles, progressive loss of speech, and tongue muscle atrophy. Moreover, PBS patient present high risk of choking, event that occurs when foods or liquids cross through the vocal folds reaching airways and lungs affected persons present also emotional lability such as unmotivated outbursts of laughing

or crying. Stroke and myasthenia gravis may have certain symptoms that are like those of progressive bulbar palsy and must be ruled out prior to diagnosing this disorder [1].

Pseudobulbar palsy, often confused with PBP because of many common, is characterized by degeneration of upper motor neurons that transmit signals to the lower motor neurons in the brain stem. Patients are affected by progressive loss of the ability to speak, chew, and swallow. Progressive weakness in facial muscles is also present leading to an expressionless face. Individuals may develop a gravelly voice and an increased gag reflex. The tongue may become static and unable to protrude from the mouth [3].

Primary lateral sclerosis (PLS) affects only the upper motor neurons involving arms, legs, and face. PLS depend on degeneration of one specific pool of nerve cells in the motor cortex, leading to slow and challenging movements. The disorder often affects the legs first, then the body trunk, arms and hands, and, finally, the bulbar muscles. Also, speech ability may be involved becoming slow. When affected, the legs and arms become inflexible, clumsy, slow and weak, leading to an inability to walk or carry out tasks requiring fine hand coordination. Difficulty with balance may lead to falls. Affected individuals commonly experience pseudobulbar symptoms and an overactive startle response. Generally, PLS occurs between ages 40 and 60, and like ALS also PLS is more common in men than in women, the cause is unknown ad the progression very slow, leading to progressive stiffness and clumsiness of the affected muscles. PLS is usually considered a variant of ALS but present some obvious difference such as the sparing of lower motor neurons, the slow rate of disease progression, and normal lifespan. PLS may be mistaken for spastic paraplegia, a hereditary disorder of the upper motor neurons that causes spasticity in the legs and usually starts in adolescence. Most neurologists follow the affected individual's clinical course for at least 3 to 4 years before making a diagnosis of PLS. The disorder is not fatal but may affect quality of life [1].

Spinal muscular atrophy (SMA) is a hereditary disease affecting the lower motor neurons. It is an autosomal recessive disorder caused by a mutation in the gene SMN1, which encode for SMN protein which have a key role in survival of motor neuron. Indeed, it is known that low level of SMN protein cause degeneration n motor neuron. In SMA patient's degeneration of the lower motor neurons, producing weakness and wasting of the skeletal muscles. There are three different classes of SMA, caused by defects in the SMN1 gene[4], based on ages of onset, severity, and progression of symptoms. .

SMA type I, also called Werdnig-Hoffmann disease, involve child within 6 months of age. Symptoms may include hypotonia, diminished limb movements, lack of tendon reflexes, fasciculation, tremors, swallowing and feeding difficulties, impaired breathing and often are present some skeletal abnormalities. SMN I children can't sit or stand and usually die because of respiratory failure before the age of 2 years[4].

Type II usually begin between 6 and 18 months of age. Also type two patient present respiratory difficulties, less than type one. So, despite the life expectancy is reduced, often patient reach adolescence or young adulthood. Children may be able to sit but are unable to stand or walk and may have respiratory difficulties.

Symptoms of SMA type III (Kugelberg-Welander disease) appear between 2 and 17 years of age and include abnormal gait, difficulty running, climbing steps, or rising from a chair, but they may have a

normal lifespan [4] . In this SMA type the lower extremities are most often affected and patients are characterized by some complications include scoliosis and susceptibility to respiratory infections [4].

Spinobulbar muscular atrophy (SBMA), also known as **Kennedy's disease**, is an X-linked recessive disease due to a mutation in the androgen receptor gene. Female are only a carrier of the disease and they have a 50 percent chance of having a son affected by the disease. The onset of symptoms is variable, and the disease may first be recognized between 15 and 60 years of age. Symptoms include weakness and atrophy of the facial and tongue muscles, leading to problems with chewing, swallowing, and changes in speech [5]. Early symptoms may include muscle pain and fatigue. Weakness in arm and leg muscles closest to the trunk of the body develops over time, with muscle atrophy and fasciculations. Individuals with Kennedy's disease also develop sensory loss in the feet and hands. Nerve conduction studies confirm that nearly all individuals have a sensory neuropathy (pain from sensory nerve inflammation or degeneration). The course of the disorder varies but it is generally slowly progressive. Individuals tend to remain ambulatory until late in the disease. The life expectancy for individuals with Kennedy disease is usually normal [6].

At the moment, there aren't specific tests to diagnose and discriminate between MNDs, although there are genetic tests for SMA, and SBMA. Indeed, in the early stages of the disease symptoms are variable and may be like those of other diseases, making diagnosis difficult. An important help could be a physical exam usually followed by a neurological exam. Neurological exam can give information about nerve function, sensory skills such as hearing, speech and vision ability, balance, coordination and changes in behavior or mood

Nowadays we don't have a standard treatment to face MNDs, only symptomatic or support treatment to help people be comfortable are available. Multidisciplinary clinics, with specialists from neurology, physical therapy, respiratory therapy, and social work are particularly important in the care of individuals with MNDs.

FDA approved specific treatment and drug for a few MNDs. Nusinersen (Spinraza) is the first drug approved to counteract spinal muscular atrophy in children and adults. The drug is administered by intrathecal injection into the fluid surrounding the spinal cord and can induce the expression of SMN protein, a key factor for motor neurons survival[4].

For ALS the FDA approved riluzole (Rilutek) that prolongs life by 2-3 months but don't show any effect on symptoms progression. The drug reduces the body's natural production of the neurotransmitter glutamate, which seems to be one of the cause of the disease leading to excitotoxicity.[2]

Muscle relaxants such as baclofen, tizanidine, and the benzodiazepines may help reducing spasticity. Botulinum toxin may be used to treat jaw spasms or drooling. Combinations of dextromethorphan and quinidine have been shown to reduce pseudobulbar affect. Anticonvulsants and nonsteroidal anti-inflammatory drugs may help relieve pain, and antidepressants may be helpful in treating depression. Some individuals may eventually require stronger medicines such as morphine to cope with musculoskeletal abnormalities or pain, and opiates are used to provide comfort care in terminal stages of the disease [1].

Usually pharmacological treatment is accompanied by rehabilitation exercise and physical therapy, to improve posture, prevent immobility, and reduce muscle weakness and atrophy. Also, simple stretching and strengthening exercises may help to reduce spasticity.

Now many researchers work to find specific treatment or therapy for MNDs taking advantage of all possible models and technique with the aim to prevent and repair the damage on the motor neuron.

Chapter 1

Introduction

Introduction

Kennedy's disease

Kennedy's disease, from the eponymous neurologist William R. Kennedy who first described the principal features in 1968, or spinal and bulbar muscular atrophy (SBMA) is a rare and fatal, progressive motor neuron disease (MND) involving different systems and manifesting as androgen insensitivity, diabetes, sensory neuropathy and automatic nervous system dysfunction [7].
SBMA has an estimated incidence of 1/400.000 inhabitants/year, anyway the prevalence of the disease can be vastly different from one area to another [8], for example Finland, present a particularly large number of affected patients [9]. Moreover, SBMA is often not properly diagnosed and frequently confused with other neuromuscular diseases, leading to underestimation of its true prevalence. The age at onset is between 30 and 50 years [10], and progression of the disease is very slow. The estimated disease duration is 27.3 years [11].

Pathogenesis

SBMA is an X-linked genetic disorder characterized by an abnormal CAG repetitions expansion. PolyQ expanded AR lead to motor neurons in the spinal cord and brain stem. However, we don't know which is the precise mechanisms, that probably involve many different pathway, behind the motor neuron degeneration and muscle atrophy [12].
In healthy conditions, after the interaction between its ligands testosterone and the more powerful dihydrotestosterone, the androgen receptor translocate in to the nucleus where interact with many target gene[13]. In SBMA the main cause of the disease depend on an alteration of the physiological function of AR, in addiction the pathological AR tend accumulate and form aggregate interfering with normal function of the cells[14].
This characteristic inclusions of polyQ expanded AR can be found in many tissue of SBMA patients not only in motor neurons, such as different parts of the nervous system but also in liver, skin, kidney proximal tubules, testis, prostate and scrotal skin, tissue where androgen receptor result more active and exert import function [14].
Cytoplasmic diffuse accumulations of mutated protein are also being found, but their role in the disease pathogenesis in not clear [15].
The inclusions have a granular aspect with a fibrillary pattern. Those containing mutant AR are usually positive for ubiquitin, suggesting that toxicity could be due to an abnormal response to the polyQ tract that avoid proteasomes degradation activity Androgen receptors inclusion are granular with fibrillar pattern, characterized by ubiquitination, suggesting a failing attempt of proteasome to degrade aggregates. [16].
It is known that not only AR is present in the inclusions, but also other protein such as the chaperones Hsp70 and Hsp90, CREB-binding protein (CBP) and other transcription factors are sequestered by aggregates. Loss of function of these proteins when sequestered in inclusions could be contributing to the disease pathogenesis interfering with physiological cellular function [17].

Androgen receptor

SBMA is due by a mutation on the androgen receptor (AR) gene, which code for the protein of 110-kDa, a steroid/thyroid hormone receptor family. This receptor mediates the effect of testosterone and dihydrotestosterone. Indeed, after the interaction between its ligand, androgen receptor interacts the androgen response element in the target genes ad regulate their expression. AR is essential for major androgen effects including normal male sexual d and pubertal sexual development [18]. The effects of AR include sex organs maturation, the growth of pubic hair, the enlargement of vocal cords, the production of sperms, the growth of muscle, and the development of masculine behavior. The expression of AR is not characteristic only of sexual organ but is widely expressed also in other tissue such as kidney, skeletal muscle, adrenal gland, skin, and central nervous system, suggesting it influences the majority of the tissues[19]. Androgen receptor is code by a 90kb DNA sequence that contains eight exons coding for specific function domains, located on the chromosome Xq11-12. The DNA binding domain is code by the exons 2 and 3 while the exons from 4 to 8 codes for the androgen binding domain. The N-terminal, transactivation domain, is characterized by the presence of a CAG trinucleotide repeat sequence [20].
Because of the presence of poly-glutamine repeats, N-terminal domain is a target of structural polymorphism. Indeed, the number of CAG repeat is highly variable cause of slippage of DNA polymerase during the DNA replication [21]. DNA polymerase process could lead to an increase of CAG repeat, causes of SBMA, or to a lower number of repetition associated with the increase of the risk of prostate cancer, hirsutism, male infertility, and cryptorchidism [22]. Therefore cause of SBMA is the expansion of the trinucleotide CAG repeat, which encodes the poly-glutamine tract, in the first exon of the AR gene [7]. The CAG repeats range size is usually from 9 to 34 in normal subjects, and from 38 to 62 in SBMA patients [23]. As documented in other poly-glutamine diseases, the CAG repeat size correlates with the age of onset in SBMA but does not appear to dictate the rate of disease progression [24].

The presence of polyQ tract on the androgen receptor leads to two mainly consequence, a loss of AR physiological function and a gain of toxic function, more evident in motor neurons cells. Moreover, it is known that androgens, through androgen receptor, exerts a trophic effect on neuronal cells. So, the loss of AR function may play a role in the pathogenesis of SBMA [25]. Expansion of the poly-glutamine tract slightly suppresses the transcriptional activities of AR, probably because it disrupts interaction between the N-terminal trans-activating domain of the receptor and transcriptional co-activators [15]. Although this loss of function of AR may contribute to the androgen insensitivity in SBMA.
It is known that the primary cause of neurodegeneration in SBMA is a gain of toxic function of the poly-glutamine expanded AR. Indeed, there are evidence of motor impairment in AR knockout mice and also in patient characterized by severe testicular feminization syndrome, lacking of AR function [26]. One of the main hallmark of SBMA are nuclear inclusions of poly-glutamine expanded AR that are found in the residual motor neurons and many other neuronal and non-neuronal tissue[27]. The consequence of this inclusions is not clear. Indeed there are evidence that indicate inclusions as a defense mechanisms against the pathogenic poly-glutamine protein, since sequestering mutant protein may lead to a reduction of its toxic activity [17]. On the other hand, diffuse accumulation of misfolded proteins appear to play an important role in the initiation of neurodegeneration in poly-glutamine disease [28]. The frequency of diffuse nuclear accumulation of the poly-glutamine expanded AR in spinal motor neurons strongly correlates with the length of the CAG repeat in the AR gene [13]. It

seems that polyQ androgen receptor principally accumulate in to the nucleus of motor neurons leading to functionality alteration and at the end cell death. But AR is widely expressed, so inclusions are detectable not only in central nervous system but also in pancreas and scrotal skin [29]. For instance, sensory neurons within the dorsal root ganglia often show AR aggregates in the cytoplasm, that appear to be associated with axonal degeneration of sensory nerves in SBMA [30], while the cytoplasmic deposits of AR in the pancreas likely correspond to diabetes. The presence of an abnormal number of CAG repetition interfere with the normal conformation of the protein and altered structure lead to aggregation. It is now widely accepted that accumulation of these abnormal proteins in neurons is the primary event in the pathogenesis of poly-glutamine diseases[31]. The oligomeric fibrils formed by the poly-glutamine-expanded AR are morphologically and functionally distinct from the annular oligomers formed by normal AR proteins [23]. Several experimental observations indicate that the formation of toxic oligomers or intermediates of abnormal poly-glutamine-containing protein initiates a series of cellular events which lead to neurodegeneration[32]. This hypothesis is also applicable in a mouse model of SBMA, in which soluble oligomers are detectable prior to the onset of neuromuscular symptoms[33]. Localization of misfolded proteins in to the nucleus is a key event for cells dysfunction and the consequence degeneration, in a poly-glutamine disease. Interestingly, in cell model of Huntington disease, has been proved that insertion of nuclear export signal to sequence of the mutant eliminates aggregate formation and cell [34], while a nuclear localization signal has the opposite effect [34]. Comparable result was obtained for poly-glutamine-expanded AR. Indeed, a mutation in the receptor's nuclear localization signal or the addition of a nuclear export signal to the protein, results in a lower toxicity suggesting that nuclear localization is essential for toxicity[12]. Nuclear accumulation of the poly-glutamine-expanded AR is followed by several downstream molecular events, that are thought to result in neuronal dysfunction and cell death (Figure 1). Ligand-dependent toxicity of poly-glutamine-expanded AR in SBMA is unique among poly-glutamine diseases in that the pathogenic

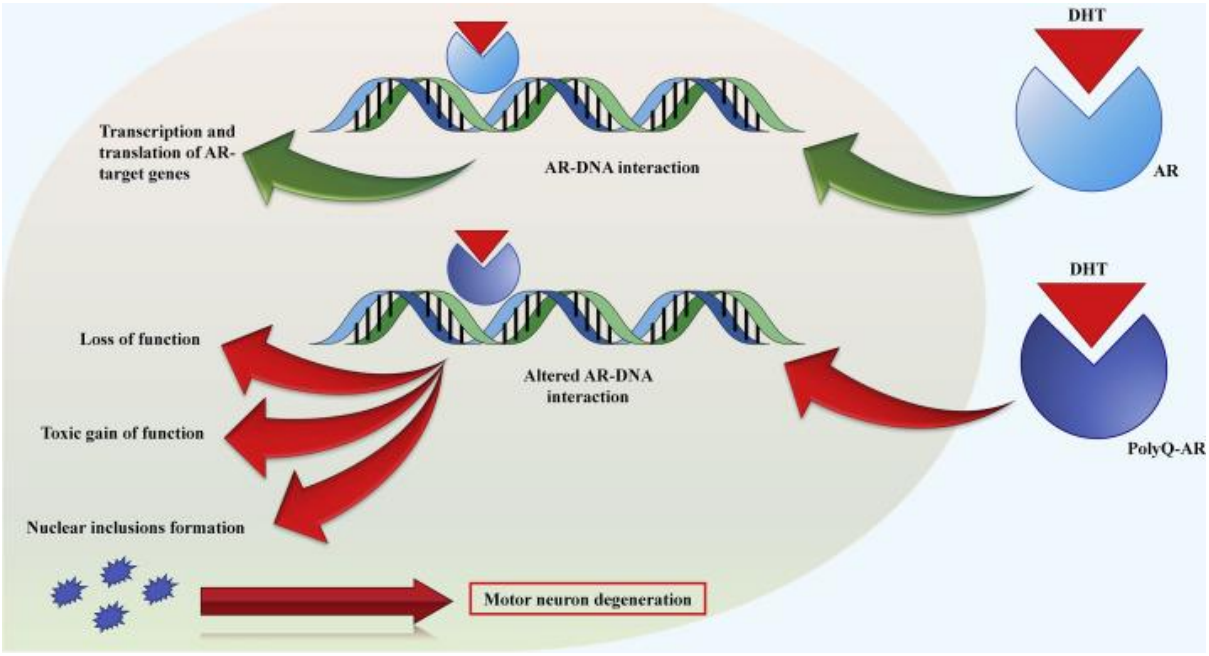

Figure 1 -Under normal conditions AR first interacts with dihydrotestosterone (DHT) or testosterone, then migrates to the cell nucleus, where it interacts with specific DNA sequences inducing transcription of androgen target genes. Polyglutamine AR also migrates to the nucleus after binding with its ligand and, once in the nucleus, it can no longer interact properly with AR target genes. Alteration of this pathway results in abnormal transcription and protein production by several genes, which may therefore lose their physiological function (Querin 2016).

protein, AR, has a specific ligand, testosterone, which alters the subcellular localization of the protein by favoring its nuclear uptake. Unbound androgen receptor is usually in a multi-heteromeric complex in the cytoplasm that inactive it functions. AR can translocate in to the nucleus only in ligand-dependent manner [35]. This ligand dependent mechanism play a key role in the pathogenesis of the disease and give an explanation for the gender difference which is a specific feature of SBMA [36]. The gender differences are also observable in animal model of Kennedy's disease. Indeed, in a mouse expressing the full-length human AR containing 97 CAGs (AR-97Q), neuromuscular symptoms are evident only in male mice, while not symptoms are detectable in female littermate [36]. Male AR-97Q mice show more abundant diffuse nuclear inclusion than females, in accordance with the symptomatic difference according to gender. Interestingly, because of surgical castration and androgen deprivation reduce the symptoms severity and the histopathological evidence. On the other hand, injection of testosterone also leads the females to develop the pathology. Since the nuclear translocation of AR is ligand-dependent, testosterone represent the trigger event to induce toxicity accelerating nuclear translocation of the poly-glutamine-expanded AR. This theory it has also been reported in animal model of the disease in which testosterone deprivation by castration reverses motor dysfunction in transgenic mice of SBMA [37]. Symptoms are minimal in homozygous females for expanded CAG repeat in the AR gene, while testosterone administration induced neuromuscular signs of SBMA patient. These observations support the ligand-dependent hypothesis[38]. Recent studies demonstrate that while nuclear localization induced by testosterone in necessary for the neurotoxicity, is not sufficient. For example, a mutation that inhibits the binding of mutated androgen receptor to DNA but not affect ligand binding, don't lead to neurodegeneration. This evidence suggest a role of DNA binding in the AR-mediated neurodegeneration[39].. In addition to nuclear translocation and DNA binding, testosterone mediates the interaction of the amino- and carboxyl-terminal domains (N/C interaction) of AR, which is also required for the toxicity of the poly-glutamine-expanded AR. The ligand-dependent interaction between the carboxyl-terminal AF-2 domain of AR and co-regulators is another requisite for the toxicity [39]. Post-translational modifications have been implicated in the neurotoxicity of the poly-glutamine-expanded AR. For instance, in cells the toxicity is decreased by phosphorylation of serine 215 and 792, by reduce affinity between AR and ligand[40]. It is also known that toxicity is further diminished in presence of insulin-like growth factor-1 (IGF-1), able to activate many cell survival pathways [41]. Moreover, the specific expression in muscle of IGF-1 is able to mitigates neuromuscular symptoms and ameliorates both muscle and spinal cord pathology, suggesting that studies on AR phosphorylation or androgen receptor manipulation may be a right way to find a therapy. In contrast, not all modifications lead to an amelioration. Indeed, the phosphorylation of AR at 514 induce activity of caspase-3 increasing AR N-terminal fragment via protein cleavage. Increase of N-terminal fragment amount enhancement of the pathogenic AR toxicity in a cellular model. Also other modification such as phosphorylation, acetylation and sumoylation seem to modify the toxicity of the poly-glutamine-expanded AR. Acetylation at lysin 630/632/633 stabilizes the poly-glutamine-expanded AR and enhances its cytotoxicity [42]. Sirtuin1 (SIRT1), a nicotinamide adenine dinucleotide dependent histone deacetylase, suppresses the nuclear accumulation and also toxicity of the pathogenic AR in primary motor neurons by de-acetylating the receptor [42], while mutation of lysine 630 or 632 and 633 delays the nuclear translocation and induces the formation of cytoplasmic aggregation of AR in a non-neuronal cell line [43]. Sumoylation seems also to increase polyQ AR solubility inhibiting formation of inclusion facilitating the clearance[44]. These observations suggest that acetylation and sumoylation are potential targets of therapy development, although their implication in animal models has yet to be clarified. Recent studies suggest that also transcriptional alteration could be involved in the

pathogenesis of SBMA and other poly-glutamine disease. For instance low levels of heat shock proteins (Hsps) were found in SBMA and HD animal models[45]. Other important factor such as the transcriptional co-activators CBP result sequestered in the protein inclusion in both mouse model and patient with poly-glutamine diseases[46]. CBP is an HAT, histone acetyltransferase, able to regulate gene transcription by altering the structure of the chromatin. It has already been showed that the activity of CBP as HAT is reduce in cells models of poly-glutamine disease, and this transcriptional dysregulation may due to a low histone acetylation and cause the pathogenesis of neurodegeneration. This hypothesis is confirmed observing that in the spinal cord of SBMA mice the histone H3 acetylation is drastically reduced [47]. Moreover, the presence of polyQ AR lead to dysregulation in expression of several growth factor genes, required for the neuronal survival [41]. Testosterone-dependent transcriptional dysregulation has also been studied using a Drosophila model of SBMA, in which the poly-glutamine-expanded AR enhances an androgen-dependent association of AR with Retinoblastoma protein [48]. This interaction appears to result in an aberrant E2F transactivation through the suppression of histone de-acetylation.

Another important factor in the neurodegeneration is represent by the obstruction of axonal transport, complication that often occurs in MNDs. For example, mutation in the gene coding for dynein and dynactin 1, protein that regulate axonal trafficking, are already known. In humans SMBA patient and also in rodents models, the mRNA expression of dynactin 1 is reduced, leading to the disruption of retrograde axonal transport[49].Alteration in axonal trafficking of motor neurons and the blockade of endosomal trafficking are also documented in a knock-in mouse model of SBMA carrying AR113Q [28]. These deficits are partially rescued by the local administration of VEGF PolyQ androgen receptor cytoplasmic inclusion were found also in the axons, where can alter the kinesin localization, one of the most important motor for anterograde transport, and so alter also organelles transport[35]. Also fast axonal transport could be affected by the presence of aggregate and inclusion, in both anterograde and/or retrograde direction[50]. Furthermore, the poly-glutamine-expanded AR activates c-Jun N-terminal kinase (JNK), leading to the inhibition of kinesin-1 microtubule-binding activity and eventual disruption of anterograde axonal transport [51]. It is noteworthy that JNK inhibitors reverse the suppression of neurite outgrowth by pathogenic AR in cultured cells [51].

Mitochondrial impairment is also observed, and it also involves activation of caspase in neurodegenerative polyQ disease. Indeed, N-terminal fragments of the poly-glutamine-expanded AR may activate an apoptotic pathway via activation of JNK in primary cortical neurons [7]. This system depends on Bax, a key apoptosis factor able to induce the release of cytochrome C from the mitochondria. Furthermore, polyQ AR bind to testosterone seems to altered the membrane depolarization ability of mitochondria leading to an increase of reactive oxygen species, which is treated with the antioxidants co-enzyme Q10 and idebenone [52]. It is also demonstrated that the poly-glutamine-expanded AR represses the transcription of subunits of peroxisome proliferator-activated receptor gamma coactivator-1, a transcriptional co-activator that regulates the expression of various nuclear-encoded mitochondrial proteins, suggesting a link between poly-glutamine-mediated transcriptional dysregulation and mitochondrial dysfunction [52].

Phenotype and symptoms

The main clinical feature of SBMA is a muscular weakness reported in the 97% of the cases. Symptoms usually appears at the age of 35-40 years[24]. The age of onset could correlate between the number of CAG, while seems not affect the disease progression[53]. Lower limb weakness is the most common symptom, followed by upper limb weakness. However, recently many other symptoms have been observed, also before the onset of muscle weakness, classically considered the primary sign on the disease. For instance, many patient present hand tremor, usually is first manifestation noted by patients and appears at a median age of 35 years. Since is a postural high-frequency tremor that may result in impairment of daily activities as writing and eating [5]. Other early symptoms could be muscle cramps, myalgia, breast enlargement, premature exhaustion during physical exercise and foot numbness. Also leg tremor has been observed in a small court of patient, characterized by a high number of CAG repetition in the androgen receptor gene. Kennedy disease affect mainly proximal lower-limb muscles, so the characteristic manifestation of the disease are represent by difficulty in climbing stairs and getting up from a chair[5].

The progression of pathology forces the use of walking aids (handrails, canes, frames and wheelchairs) and bulbar-related symptoms (dysarthria and dysphagia) and erectile dysfunction are reported between the ages of 50 and 60 years.

In every stage of the disease are reported fatigue and a reduced tolerance of effort that can limit activities of daily living [54].

A peculiar feature of SBMA is an involvement of brain-stem motor nuclei. This implication result in symptoms such as weakness of the masseter muscles leading to tremors of the mouth when is hang open. Also tongue is affected characterized by fasciculations with irregularities at the edges or deep furrowing in the midline due to wasting [55]. Weakness and atrophy in mouth muscle are usually associated with vocal-cord paresis, leading to dysarthria and dysphonia, chewing difficulties and pharyngeal paresis[56]. Swallowing dysfunction is found in 80% of cases and is characterized by incomplete food bolus clearance through the pharynx [57]. Patient are also characterized by nasal voice cause of palatal atrophy and also laryngospasm which pathogenesis still is unknown[58,59].

Like other NMD also in SBMA respiratory muscles may be progressively involved, while complete respiratory failure is uncommon [60].

Androgen receptor inclusion were find not only in the spinal cord and brain stem, but are present also in the cells of dorsal root ganglia, affecting sensory system, vibratory sensation and reduction of sensory function in the extremities and several patient present symptoms of weak or absent deep tendon reflexes [61].

The presence of sensory neuropathy may also be associated with neuropathic pain that is mainly localized distally in the lower limbs, associated with frequent foot numbness and tingling, as reported in up to 58% of patients [62].

Because of wide androgen receptor expression in many parts of nervous and non-neuronal tissue, SBMA is not just a classical neuromuscular disease, indeed patient are also characterized by the presence of non-neurologic symptoms [45].

Endocrine symptoms, depending on AR loss of function, are usually present like as gynecomastia, reduced fertility due to testicular atrophy, azoospermia, oligospermia, erectile dysfunction and reduced libido [63].

Abdominal obesity, dyslipidemia, liver dysfunction and glucose intolerance can be also detected in some patients, and frequently patients show metabolic syndrome [64]. While gynecomastia and other

symptoms of androgens insensitivity are due to the loss of AR function, the remaining non-neuronal symptoms depend to toxicity of mutant ARs in those tissues [65]. Several patients show also signs of primary cardiomyopathy and 40% present urological involvement, such as lower urinary tract obstruction in the absence of prostatic hypertrophy. These complication lead to patient catheterization [66]. At the moment the mechanism that cause al this non-neuronal and non-endocrine is still not clear [67].

Extensive accumulation of mutant ARs in the brain of SBMA patients have been demonstrated, and recent studies have focused on the consequences of SBMA on the central nervous system [13].

Indeed, is common for patients with SBMA to have some specific psychological characteristics, such as diffidence, marked emotional sensitivity and concentration problems [68]. Such observations are supported by evidence of altered theory of mind functions related to empathy, which is linked to complex frontal lobe functioning [69]. Magnetic resonance and electrophysiological studies have revealed subclinical abnormalities in the primary motor cortex and other frontal areas of the brain in SBMA patients [70,71]. A recent study using positron emission tomography (PET) also identified hypometabolism in the frontal regions in 10 patients with SBMA [72].

Muscle and non-cell autonomous disease

Traditionally, SBMA has been reported as a cell autonomous primary MND, neuronal death is due to a toxic gain of function by PolyQ expanded AR.

More recently, it has been proposed the hypothesis of a primary myopathy component trigger to the pathology development [73]. Indeed, there are evidence of muscle involvement such as high creatine phosphokinase serum levels and the presence of myogenic changes in muscle biopsies from patients [74].

Clues of mixed neurogenic and myopathic processes have also been reported in mouse models of SBMA [75]. Histopathological analyses of muscle tissues from transgenic and knock-in mice expressing polyQ-expanded AR have revealed both neurogenic and myopathic involvement [14,41,76].

Moreover in knock-in mouse mode of Kennedy's disease muscle features are evident earlier then motoneurons alteration, suggesting a primary role of muscle in SBMA pathogenesis [77].

It is also known that androgens have an important role in skeletal muscle, for example in their development and anabolic action. Androgens in healthy man induce muscle strength, endurance and size improving muscle performance. Low level of AR activity in SBMA patient have as a consequence a reduction of muscle tissue and an increase of adipose tissue [78].

It is also possible that polyQ AR induce a toxic response in the satellite cells, responsible for the regeneration and development of muscle, leading to deterioration of SBMA muscle. Indeed, while androgens and AR result in hypertrophic effects on muscle, in SBMA patient have a detrimental role [79].

PolyQ expansion in AR has been proposed to cause toxicity in muscle due to an alteration of gene expression. Another important pathway of toxicity in SBMA muscle could be the alteration of RNA splicing. However, it remains to be established how these toxic pathways contribute to the pathogenesis.

Damage to motor neurons can also be a consequence of damage in other cell types, such as muscle and glial cells, following a non-cell-autonomous toxic process.

These cells secrete important factors with trophic support activity, which is essential for motor neuron maintenance in adulthood [73].

Two important classes of molecules, which have trophic support activity and can protect neurons by initiation of apoptotic pathways and promoting activation of pro-survival pathways, are that of neurotrophin and growth factors. It is known that expression of neurotrophin and growth factors is altered in mouse models of SBMA [80]. This observation highlights the idea that altered trophic support to motor neurons from neighboring tissues may be responsible for non-cell autonomous damage in SBMA.

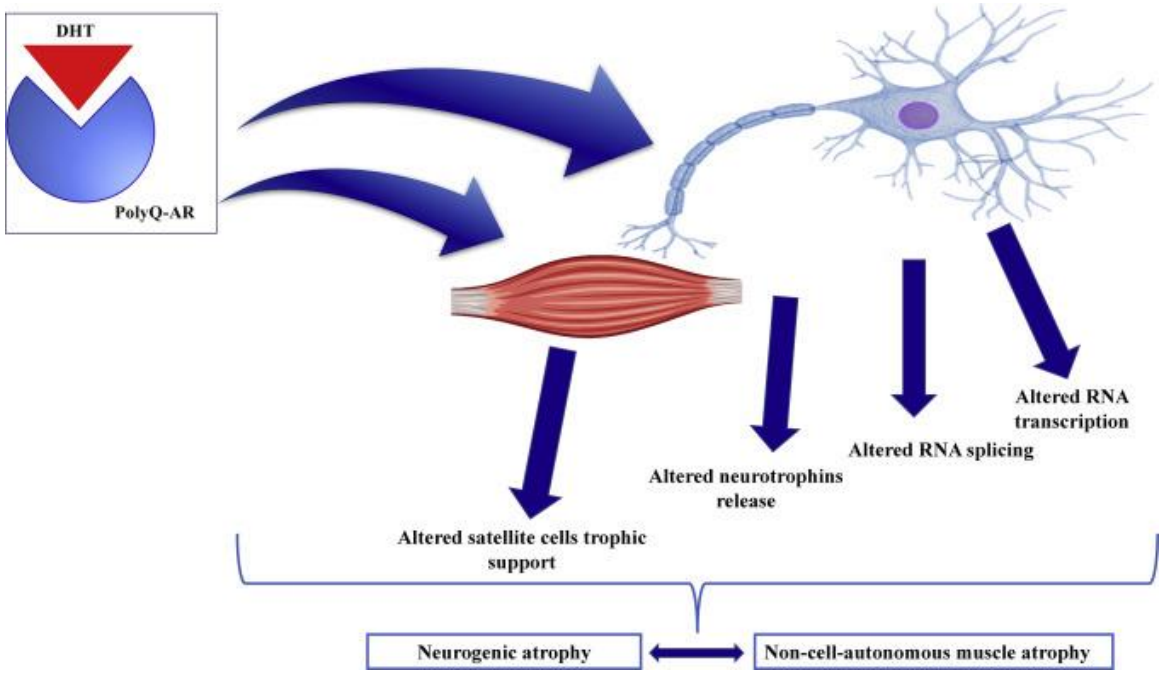

Figure 2 -In the pathogenesis of SBMA, damage to motor neurons can result both from cell-autonomous and non-cell-autonomous toxic processes, the latter arising in other cell types such as skeletal-muscle cells. These cells are highly androgen-sensitive and may alter several physiological pathways after interactions with mutated polyQ-AR (Querin 2016).

Diagnosis

The main way for SBMA diagnosis is a genetic test that can estimates the number of CAG repetition in the androgen receptor gene. If the sequence results longer than 38 repetition the subject is considerate an SBMA patient[81]. A second strong approach is the familial history of the patient, could be very useful for e first selection and then deepen the analysis by genetic test. Unfortunately neurological symptoms are not specific only for SBMA, but endocrine features can be really helpful for the diagnosis [1024]. An increase of creatine phosphokinase levels may also be an important clue, since all patients show very high levels, up to 38 times the normal value, which decrease with progression of the disease [82].

Also, endocrine-related symptoms, like as glucose intolerance or dyslipidemia in association with lower motor neuron abnormalities, can suggest a diagnosis of SBMA.

The diagnosis is often confirmed on electromyography usually performed during the routine analysis of motor neuron disease, showing a chronic neurogenic pattern with fasciculations that extend beyond the regions affected by weakness [73].

Also, involvement of sensory system is a clue of SBMA, reduction of sensory sensitivity, in addition, muscle biopsy can also be performed, particularly when myopathy is initially suspected. Signs of neurogenic atrophy have been described in all patients, including aggregation of type I and II fibers, target fibers, atrophied fibers and sub-sarcolemma nuclei clumping. Myopathic alterations are more often found in patients with a higher grade of disability [81].

Therapy and symptomatic treatment

Now are available only palliative or symptomatic approach usually focused on rehabilitation and exercise to treat SBMA, no specific treatment has yet been found. One of the main goal to face SBMA is preserve muscle and strength as long as possible taking advantage of physical activity or physiotherapy exercises[81].

Assist devices for walking are usually necessary, in the most serious cases also a wheelchair could be necessary. Muscle cramps are frequent and may be persistent and affecting SBMA patient quality of life [24].

The most part of the symptomatic approaches is necessary to treat neuropathic pain, using classical painkillers drugs such as antiepileptics and amitriptyline.

Treatment of neuropathic pain is based on the classic drugs used for this indication, such as antiepileptics and amitriptyline. Speech therapy aims to improve voice modifications and dysarthria. Behavioral measures can be established to reduce the risk of aspiration in patients presenting significant dysphagia. Nutritional control is useful for weight control [24].

Aspiration pneumonia is the predominant cause of death and hospitalization in SBMA [83]. However, patient usually don't present diaphragm weakness, and only in a few patients are detectable ventilation alteration. Expert suggest also regular cardiological monitoring because of increased cardiovascular risk that correlate also with diabetes ad metabolic alteration[81].

Young patient can also present reduced fertility, so assisted reproductive technology could be used along with genetic counseling for couples that are planning pregnancy.

Experimental treatments

In the past several experimental treatments seemed to ameliorate the condition of SBMA models in preclinical studies, or were able to delay disease progression, unfortunately none of these attempts reached the same result in human trials and in patients. Obviously one of the first target for a therapy is to restore or at least to preserve muscle functionality. It is known that in animal model β-agonist drugs may induce muscle development and anabolism. For instance, clenbuterol, a β-agonist, can increase muscle strength and resistance, but only for few months. Moreover, in mouse clenbuterol treatment shows the ability to induce satellite cells activity, leading to an increase of muscle development[84]. The real efficiency and the safety of this treatment still are to be confirmed.

A second possible strategy is representing by androgen reduction therapy since disease phenotype depends on androgen. In mouse models the use of leuprorelin [85], a drug widely used in prostate cancer, showed evidence of reducing nuclear inclusions. Another possibility, is to inhibit the action of the enzyme 5α-reductase, for example using dutasteride, so limiting the conversion of testosterone in the more power dihydrotestosterone Both strategies didn't show any significant improvement of muscle strength in clinical trials [84].

An additional strategy promising in mice but not in patients consist in the use of histone deacetylase inhibitor or microRNA to reduce androgen receptor mRNA expression or increase mRNA degradation[86].

Since polyQ expanded AR toxicity is possible only after the interaction between AR and ligand, its inhibition, using, for example, the non-steroidal antiandrogen flutamide, may be an ideal target for therapy in SBMA. However, no benefits were detectable in transgenic mice.

Since the main toxicity of PolyQ AR is due to aggregate formation, also protein degradation system could be a possible approach to counteract the pathology, for example through the enhancement of autophagy pathway [87]. Nevertheless, at the moment this may be unsuccessful in SBMA, as toxic mutant protein is localized into the nucleus [88].

Therapeutic potential of autophagy

Autophagy plays a critical role in maintaining homeostasis, adapting to stress in both normal and pathogenic cells [89].
In prevention of neurodegenerative diseases [90,91], the role of autophagy is highlighted by removing protein aggregates which is not possible via proteasomal degradation. Many studies demonstrate the presence of ubiquitin-containing inclusions occurred via elimination of Atg5 or Atg7 in murine central nervous system during embryonic development. These symptoms are also found in many neurodegenerative diseases like Alzheimer disease [92].
For the physiological function of the cells a key mechanism Is the balance between synthesis and degradation, possible through two major pathways such as autophagy and proteasome. The primary aim of proteasome is to degrade single proteins, while autophagy can sequester big aggregate of protein and organelles
[93].
There are three primary types of autophagy: microautophagy, macroautophagy and a mechanistically unrelated process, chaperone-mediated autophagy that only occurs in mammalian cells [94]. Both micro and macroautophagy can be selective or nonselective and these processes have been best characterized in yeast [95]. As noted above, the most distinctive feature of macroautophagy is the formation of the double-membrane bound phagophore and autophagosome. In contrast, during microautophagy the cargos are sequestered by direct invagination or protrusion of the yeast vacuole membrane [96]. Nonselective autophagy is used for the turnover of bulk cytoplasm under starvation conditions, whereas selective autophagy specifically targets damaged or superfluous organelles, including mitochondria and peroxisomes, as well as invasive microbes.

Microautophagy is characterized by the sequestration of the materials to degrade by the vacuole through membrane invagination[97]. Microautophagy is widely study in yeast were is involved in the homeostasis of several substrate, including peroxisomes (macropexophagy) [97], damage organelles, lipid droplets and also big portion of nucleus[98].
The substrate of microautophagy are characterized by the presence of a KFERQ-like motif recognized by HSPA8 [99]. Microautophagy activity requires some components of the macroautophagy machinery for cargo targeting and internalization, including Atg7, Atg8, and Atg9 [97]. Microautophagy depends also on multiple endosomal sorting complexes required for transport (ESCRT) systems [100]. In addition, the selective uptake of KFERQ-containing proteins by late endosomes during endosomal microautophagy depends on HSPA8, reflecting its ability to directly interact with phosphatidylserine on the outside endosomal membrane [101]. In a similar way, is known that in Saccharomyces cerevisiae the chaperone ATPase Hsp104 is necessary to interact with lipid droplets[102]. Another main character of the microautophagy are the chaperones from the HSP70 protein family, but their role is still not clear. Notable, the yeast orthologue of mammalian NBR1, autophagy cargo receptor apparently underlies an ESCRT-dependent and ubiquitination-dependent microautophagic pathway [103]. So, microautophagy could be a type of autophagy in which the cargo is directly internalized in small

vesicles that form at the surface of the lysosome/vacuole or late endosomes via ESCRT-dependent mechanisms.

Chaperone-mediated autophagy (CMA) is a second type of autophagy characterized by the direct delivery of cytosolic proteins targeted for degradation to the lysosome [104]. The main difference between CMA and macro and microautophagy is that in CMA the substrates reach the lysosomal through a protein-translocation complex at the lysosomal membrane without intervention of membrane invagination or vesicles. Moreover, CMA is able only to degrade protein taking a KFERQ-like motif and recognized by HSPA8[105]. CMA has been shown to operate on many of cytosolic proteins, exerting a lot of regulatory function, such as metabolic regulation, genome integrity preservation [106], aging, neurodegeneration, and oncogenesis [107]. It is known that 30% of cytosolic protein are substrate for CMA[108]. The peculiar mechanism that allowed substrates to translocate across lysosomal membrane involve specific isoform of LAMP2, LAMP2A. Thus, chaperone-bound autophagy substrates bind LAMP2A monomers on the cytosolic side of the lysosome, which stimulate the formation of an oligomeric LAMP2A translocation complex [104]. While unfolding and dissociating from chaperones, CMA substrates are translocated into the lysosomal lumen through oligomeric LAMP2A complexes that are stabilized by a lysosomal pool of heat shock protein HSP90, and a cytosolic pool of glial fibrillary acidic protein (GFAP) [104]. It remains to be determined to what level CMA is conserved in lower organisms, since the splice variant of LAMP2 that is essential for CMA appeared relatively late in evolution [109].

Macroautophagy is the variant of autophagy best characterized indeed molecular machinery that executes and regulates macroautophagy in organisms is also present in yeast, nematodes, flies, and mammals has been the subject of intense investigation throughout the past two decades [110]. Macroautophagy present easily distinguishable morphological features. Indeed, whereas microautophagy and CMA are not associated with major morphological changes in vesicular compartments, macroautophagic responses involve vesicles that can occupy a considerable part of the cytoplasm [111]. These changes depend on formation of a double-membraned vesicles, known as autophagosomes. The potential of macroautophagy depend on the ability to sequester big protein aggregate or entire organelles. It is also know that macroautophagy has a fundamental role in the regulation of cell death [89], muscular fiber atrophy and neurodegeneration [112]
The macroautophagic responses involving the formation of autophagosomes, their fusion with lysosomes, and lysosomal degradation have been associated with the activity of two ubiquitin-like conjugation systems [110]. First ATG7 and ATG10 are involved in inducing the association of ATG5 with ATG12 which leads to a multiprotein complex characterized by the presence of autophagy-related 16-like 1 (ATG16L1) [93]. The next system is promoted by ATG3 and ATG7, which together with the ATG12-ATG5:ATG16L1 complex conjugates phosphatidylethanolamine to microtubule-associated protein 1 light chain 3 beta, best known as LC3B [113]. LC3-II, the lapidated form of LC3, is generated on developing autophagosomes and allows binding to several autophagy receptors [114]. The assembly and activation of a multiprotein complex including ATG13, ATG101, RB1 inducible coiled-coil 1 (RB1CC1 or FIP200) and unc-51-like autophagy activating kinase 1 (ULK1) at ATG9-containing membranes promotes the autophagosome formation. This mechanism is followed by ULK1-dependent ATG9 phosphorylation [115]leading to the elongation of pre-autophagosomal membranes upon incorporation of phospholipids from other organelles such as mitochondria[116]. This process permits the recruitment of a multiprotein complex with Class III phosphatidylinositol 3-kinase (PI3K) activity, which contains

BECLIN1 , phosphatidylinositol 3-kinase catalytic subunit type 3 (PIK3C3), phosphoinositide-3-kinase regulatory subunit 4 (PI3KR4) [117], the sensor of membrane curvature ATG14, and nuclear receptor binding factor 2 (NRBF2)[118] . On activation, VPS34 produces phosphatidylinositol 3-phosphate (PI3P), which is essential for the expansion of autophagosomal membranes until closure by engaging PI3P-binding ATG proteins and members of the WIPI family [119].

One of the main characters of the autophagic process is the macroautophagy regulations is MTOR complex 1 (mTORC1). mTORC1 is able to regulate autophagy by the inactivation of ATG13 and ULK1 by phosphorylation[120], or also preventing the nuclear translocation of transcription factor EB (TFEB), a key transcriptional regulator factor of lysosomal biogenesis and macroautophagy [121]. mTORC1 inactivation act by AMP-activated protein kinase (AMPK), which responds to reduced ATP levels and consequent AMP accumulation [122]. AMPK also catalyzes activating phosphorylation events on ULK1 and BECN1 [123].

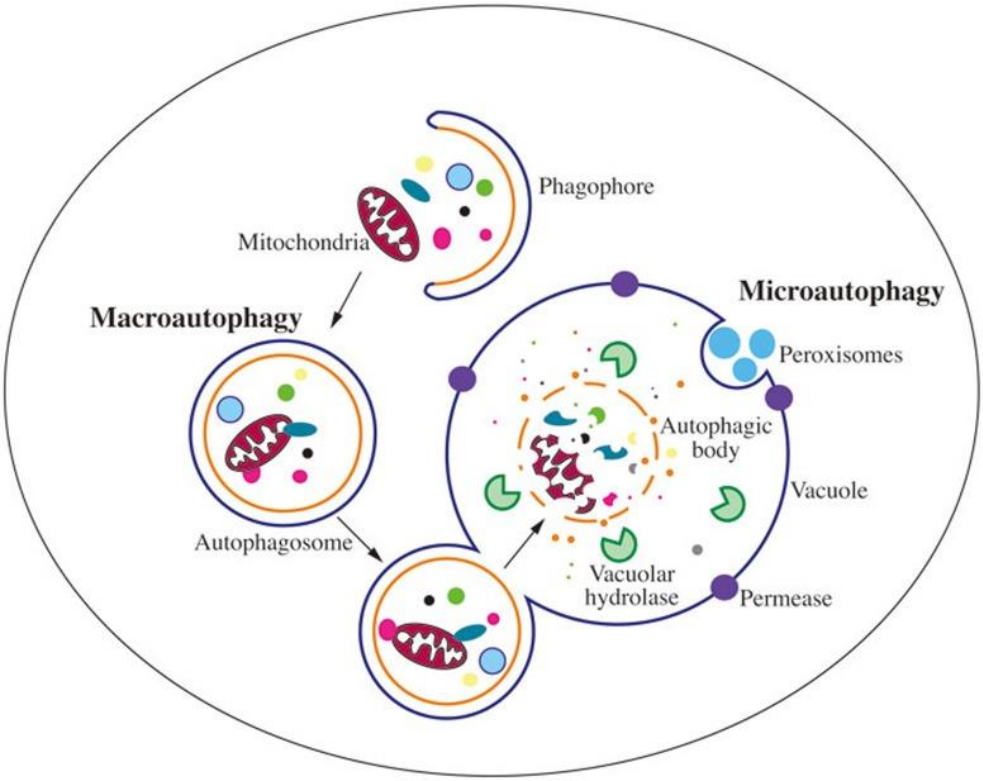

Figure 3 -Schematic depiction of the two main types of yeast autophagy. In macroautophagy, random cytoplasm and dysfunctional organelles are sequestered by the expanding phagophore, leading to the formation of the autophagosome. The autophagosome subsequently fuses with the vacuole membrane, releasing the autophagic body into the vacuole lumen. Eventually, the sequestered cargos are degraded or processed by vacuolar hydrolases. In microautophagy, cargos are directly taken up by the invagination of the vacuole membrane, followed by scission, and subsequent lysis, exposing the cargo to vacuolar hydrolases for degradation (Feng 2014).

In mammalian cells, ULK1 directly phosphorylates BECN1, resembling AMPK in its VPS34-stimulatory effects and ATG14 [106]. The autophagy-specific Class III PI3K complex is regulated by several interactors, including the VPS34 activator autophagy and beclin 1 regulator 1 (AMBRA1) as well as the BECN1 inhibitor BCL2, which also interacts with ATG12 [124]. Once autophagosomes have enclosed autophagy substrates, they can fuse with late endosomes or lysosomes to form amphisomes or autolysosomes. The molecular machinery that is responsible for these fusion events involve dozens of proteins, most of which are shared with the endocytic pathway [125]. In this setting, an important role is the activation of the GTPase RAB7A, which is required for autophagosome maturation [126], the PI3P-binding protein

tectonin beta-propeller repeat containing 1 (TECPR1), ectopic P-granules autophagy protein 5 homolog (EPG5), inositol polyphosphate-5- phosphatase E (INPP5E) [127], and other soluble N-ethylmaleimide-sensitive factor activating protein receptor (SNARE) proteins, as well as homotypic fusion and vacuole protein sorting (HOPS) complexes [128]. ATG14, LAMP2B as well as phosphorylated and lipidated LC3 are also involved in the formation of autolysosomes [129]. On the other hand, RUN and cysteine-rich domain containing BECLIN 1 interacting protein (RUBICON) negatively regulates the fusion of autophagosomes with lysosomes upon interacting with VPS34 [130]. Degradation of autophagy substrates proceeds through the lysosomal lumen that is acidified, upon disassembly of the inner autophagosomal membrane supported by the ATG conjugation systems [131]. Lastly, mTORC1 reactivation inhibits macroautophagy as it promotes leading to autophagic lysosome reformation (ALR), a process essential to regenerate the lysosomal compartment [132].

Trehalose

Trehalose is a natural disaccharide sugar found broadly but not abundantly among miscellaneous organisms including bacteria, plants, insects, yeast, fungi, and invertebrates. By preventing protein denaturation, it plays various protective roles against stress conditions such as heat, low temperature, oxidation, desiccation and dehydration [133].

In preliminary research the protective role of trehalose was attributed to its nature of chemical chaperone, able to directly interact with proteins, inducing the correct folding. This protective activity of trehalose was observed not only in yeast, where trehalose is easily find, but also in mammals, where it is not endogenously synthesized. For instance, trehalose now is use to prevent crystallization of hydrated protein in cryopreservation of cells[134].

A second important role of trehalose is the ability to induce the autophagy pathway in an mTOR-independent manner, observable analyzing others important autophagy factors such as LC3-II and Atg5, which are associated to autophagosome structure[135].

Additionally, it was demonstrated that trehalose decreases the damage of the blood brain barrier caused by MPTP, a neurotoxin which causes permanent symptoms of Parkinson's disease, through the recovery of the levels of tight junctional proteins [136]. The protective role of trehalose was observed in the treatment of many neurodegenerative disorders, usually characterized by inclusion formation or anomalous proteins folding, leading to neuronal dysfunction [137]. Aggregation of proteins in neurons and glia takes place through several mechanisms including mutation, overproduction or impairment of its degradation; however, these mechanisms are not fully understood [138]. Recently DeBosch and coworkers [139] studied the effects of trehalose on hepatic lipid accumulation and discovered that trehalose increases autophagic flux by inducing a starvation-like state, decoupled from food intake.

Indeed, they observed that trehalose can inhibit the activity of glucose transporters at the plasma membrane. The receptors manly affected by trehalose inhibition are GLUT1, GLUT2, GLUT3, GLUT4, andGLUT8, and their inhibition result in the activation of adenosine monophosphate kinase (AMPK) and the phosphorylation of ULK1 (the autophagy inducer kinase) [140]. The first treatment with trehalose in neurodegenerative disease was conducted in a mouse model of Huntington's disease, characterized by aggregates of the mutant huntingtin protein. Trehalose treatment was able to reduce the symptoms and reduce inclusion formation. As a consequence there was also an increase of mouse motor coordination and survival [141]. A similar therapeutic outcome was observed in a mouse model of amyotrophic lateral sclerosis (ALS), in which trehalose administration enhanced autophagic clearance of aggregates of mutant superoxide dismutase 1 (SOD1). Likewise, trehalose induced autophagy and had protective effects in a mouse model of tauopathy, one of the hallmarks of Alzheimer's disease [142].

Moreover, more detailed in vitro studies suggest that trehalose may induce aggregate degradation enhancing autophagy through a mechanism that is independent of the autophagy regulating activity of the kinase mammalian target of rapamycin (mTOR) [137]. Trehalose mediated increase in autophagy was associated with higher expression of key autophagy related genes and activation of the transcription factor FoxO1, a regulator of autophagy in neurons [143]. These examples illustrate the beneficial effects of trehalose in a disease context and point to an alternative route of autophagy induction, which could circumvent the side effects of mTOR inhibition [144].

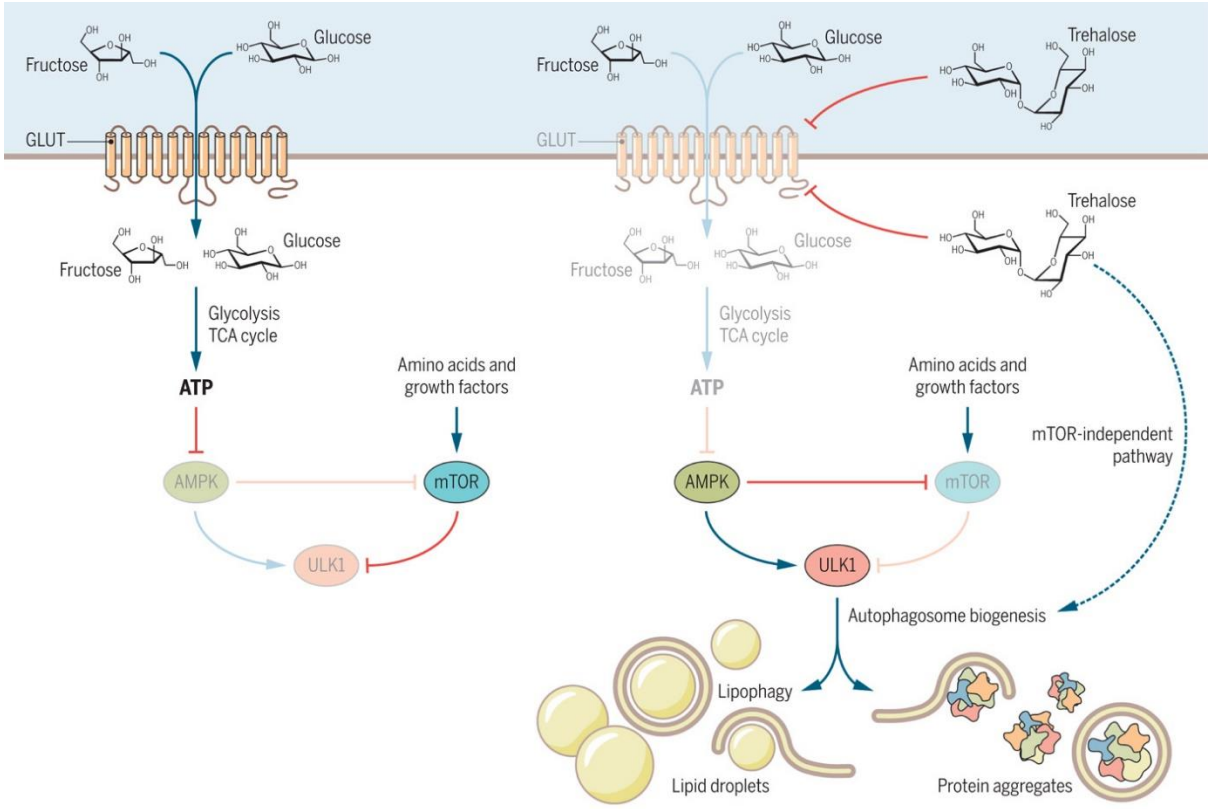

Figure 4 -Trehalose inhibits cellular import of glucose and fructose through SLC2A (GLUT) transporters, generating a starvation-like (low adenosine triphosphate) state that stimulates autophagy through AMPK and activation of ULK1. This pathway triggers autophagosome biogenesis and autophagic flux, which favors the clearance of pathological protein aggregates and lipid stores. Conversely, autophagy is inhibited by mTOR, a sensor of nutrient availability and recipient of growth factor signaling. AMPK activation may interfere with mTOR-mediated inactivation of ULK1. Trehalose may induce autophagy through additional unidentified mTOR-independent mechanisms (Mardones 2016).

In the context of NAFLD (nonalcoholic fatty liver disease), study by DeBosch and coworkers brings new insights into the biological activity of trehalose. Primary in the hepatocytes, an also in other cells type, trehalose can inhibit the action of SLC2A family transporters, which are necessary for hexose import. This inhibition, leads to a reduction in glucose availability and then to a phosphorylation and activation of AMPK and a concomitant increase in ULK1 phosphorylation and activation, which induced autophagy. Although canonical mTOR targets were not evaluated directly, the dephosphorylation of ULK1 in the site regulated by mTOR (Ser757) suggests a potential connection between both autophagy regulating pathways. Now there are no information about how and if trehalose compromises glucose transport into neurons through GLUT3. If so, this mechanism of enhancing neuronal autophagy through the AMPK pathway may explain some of the broad neuroprotective effects of trehalose. A general consideration of the study highlights the potential influence of trehalose on global carbohydrate and energy metabolism, depending on its administration route. The inhibition of GLUT transporters predicts additional metabolic consequences in vivo because GLUT2 is also involved in facilitating trans epithelial hexose transport in the gut, whereas GLUT8 facilitates fructose import into hepatocytes, and GLUT4 mediates the regulated transport of glucose into adipocytes [140].

Trehalose has been already tested in many disease models resulting a promising treatment, including neuronal and non-neuronal ones, both in-vivo and in-vitro [98]. In ALS and FTD autophagy induced by trehalose seems to an amelioration of symptoms and to a delay in disease progression in vivo or vitro

test. Unfortunately, now more of this trial are restricted to only in vitro models. Definitively, clinical trials are needed to demonstrate a role of trehalose in controlling the development of neurodegenerative diseases and cancer.

Huntington's disease (HD) is a hereditary disorder cause by a progressive degeneration of nerve cells in brain. Neuron degeneration is due by CAG trinucleotide elongation, causing an abnormal long polyglutamine (polyQ) tract in the N terminal of the huntingtin protein leading to a misfolded protein. This mechanism lead to a formation of amyloid fibrils [145,146]. The toxicity is exerted by deficient RNA synthesis or ubiquitin proteasome system inefficiency, generating cellular deposits and at the end, cell death [147].

The first protective effect of trehalose is its binding to expanded polyQ and stabilization of the toxic mutant protein, and to an enhanced clearance of soluble mutant huntingtin. Another activity of trehalose is the triggering of autophagy, through a mTOR-independent mechanism, protecting cells from the subsequent mitochondria-dependent pro-apoptotic damage [137]. In addition, trehalose-induced solubilization of 103Q-htt protein results in the overexpression of the heat shock protein, Hsp104, which, finally, decreases the oxidative stress, the cell death and rescues endocytosis process [148]. In a study to discover the epoxomicin and trehalose co-treatment effects on skin fibroblasts HD patients, it was found that trehalose have some desirable effects including reverting the effects of epoxomicin, protecting against huntingtin and polyubiquitinated protein deposits as well as pro-apoptotic pathways induced by caspase-3 in HD human skin fibroblasts, rising the number of skin proliferative cells and decreasing reactive oxygen species [149]. Additionally, it is reported that co-treatment with trehalose and europium hydroxide nanorods enhances autophagy through different pathways [149].

Huntingtin inclusions were also found in non-neuronal cells in brain[147]. For instance in glial cells which are important for their support in neuronal functions and survival[150]. Inclusions were observed also in astrocytes and microglia leading to their function alteration and to a detriment of neurons.

Therefore, HD glial cultures are more prone to stress oxidative injury, particularly through HDAC6 activation, to activate protective chaperones as well as formation of aggregations, and are less responsive than WT glial cultures to hydrogen-peroxide- induced toxicity [151]. Indeed, trehalose treatment can reduce microglia activity, the HDAC6 expression an also decrease the inflammatory activation usually induced by epoxomicin in both HD and healthy astrocyte. Moreover, it is observed an increase of mitochondrial numbers and size and an and enhancement in the number of gliofibrillar acidic protein (GFAP+). It is also detected an increase in the synthesis of neurotrophic factor in astrocyte, leading to an increase of stimuli for dopaminergic neurons survival. Trehalose, through its capacity to induce autophagy, also prevents p62/SQSTM1 aggregation and enhances the degradation of cytoplasmic accumulations from mHTT and α-synuclein proteins [151].

Prion disease are categorized as neurodegenerative disorders resulted from misfolded forms of the prion protein, which are proteinaceous infectious particles, and are reported among humans and many type of animal species [152]. The peculiarities of prion disease are the conversions of the healthy prion protein (PrP^{C}) in to an infectious isoform (PrP^{sc}), able to aggregate in the patient brain and, finally, lead it to death. Trehalose effect are also tested in this condition, and can induce the autophagy flux and reduce the amount of PrP^{sc} in a time and dose dependent manner[153]. Moreover, the treatment can also induce the clearance of PrP^{sc} in infected cells. With the help of some autophagy

inducers like trehalose, rapamycin and imatinib, it is suggested that autophagy might have a role in physiological breakdown of cellular PrP^{sc} [154]

Amyotrophic lateral sclerosis (ALS) is a fatal neurological disorder which influences motoneurons responsible for controlling voluntary muscle movement. Sporadic forms of ALS are 90% of the cases, and mutation in TARDBP, FUS, or SOD1 are associated with this disorder [155]. Mutation in the same gene are reported for familiar forms of the disease[156]. Misfolding of SOD1 is the most studied mutation , an anomalous [CuZn] superoxide dismutase found in tissues of ALS patients, is toxic for cells as it induces many organelles' dysfunction and accounts for one-fifth of familial ALS [118].
It was proved that mutant SOD1 aggregation could be reduced by trehalose treatment in cells. Other studies suggest that trehalose are also able to extend longevity and to postpone the progression of disease[157]. The mechanism is still unknow, but some result suggests an autophagy activation followed by FOXO1 induction. This may prevents the cell- nonautonomous effects of glia over primary motor neurons, protects mitochondria and ameliorate the transcription of autophagy-regulatory genes[143].

Parkinson's disease (PD) is a common progressive neurological disorder that affects movement and is characterized by a massive loss of nigrostriatal dopaminergic neurons. The main cause of the disease is the formation of Lewy body, intraneuronal aggregates usually of α-synuclein (α-Syn), present in both familiar and sporadic PD [158]. Therefore, usually PD is characterized by high level expression of inflammatory cytokines from glial cells. The disease is due by a mutation in Park-2 gene coding for parkin, a protein with ubiquitin ligase function[159]. In preliminary experiments, autophagy inducers such as rapamycin help the elimination of α-Syn [160], whilst autophagy inhibitors augment its accumulation [161].
Also the effects of trehalose was assessed in vitro model of PD, showing that trehalose treatment is able to enhance the clearance of mutant form of α-Syn[158].
Moreover, trehalose not only enhance macroautophagy flux, but also increases the autophagosomes and decreases cell viability; however, the latter effect is not specifically due to trehalose, but it is common among disaccharides, indicating that changes in osmolality might account for reduced cell viability. Interestingly, trehalose can also delay aging, a process attributed to PD pathogenesis, and extend longevity [162]. Trehalose treatment in PD it is also clear in rodent model. Indeed, autophagy improve leading to a reduction of α-synuclein deposition in substantia nigra, with the subsequent effect of enhance dopamine neuronal survival [163].

Amyloid pathology (Alzheimer's disease AD) is the most prevalent type of dementia, which induces memory loss and leads to problems with thinking and behavior. Small anesthetics, both in vitro and in vivo, show pro-amyloidogenic properties [164], which increase the behavioral anomalies and brain lesions in patients with Alzheimer's disease. The sequential proteolytic process of β- and ϒ-secretase on amyloid precursor protein lead to Aβ-amyloid generation. The interaction between the Aβ-amyloid (Aβ) and the lipid bilayer membranes triggers molecular mechanisms crucial for the progress of AD[165]. [165]. Trehalose treatment seems to reduce Aβ-amyloid generation and secretion[166], reducing also amyloidogenesis[167] and β-amyloid accumulation in vitro model[168].
To investigate the role of trehalose in amyloid pathology Induced by isoflurane anesthesia, research into APPs mice, which expresses the human mutation of the amyloid precursor protein, treated with isoflurane has been carried out. Also, in this case trehalose can help to counteract the effect of

isoflurane, such as prevent increase of pro-apoptotic proteins and apoptosis in the hippocampus. Furthermore, isoflurane leads to increased expression of GFAP reducing hippocampal tau expression and trehalose again reverts these effects. As a preventive agent, trehalose enhances autophagic markers and chaperones, thereby inhibiting accumulation of β- amyloid [168].
Additional research suggests that trehalose damages the metabolism of amyloid precursor protein (APP) and vesicular transport but does not prevent ϒ-secretase activity. This selective inhibition is reported to be m-TOR-dependent. It also results in high deposition of the autophagic marker proteins LC3-II and p62, and decreased processing of Cat D, an abundant aspartic endopeptidase in lysosomes. However, it should be taken into consideration that proteasome pathway, in parallel with autophagy is needed to decrease aggregated proteins [129].

Tauopathy are a big family of neurodegenerative disease due by an accumulation of tau protein in neurofibrillary or gliofibrillary tangles in human brains [68]. Some of them depend of post-translational changes of tau, usually caused by a different mutations of the Tau gene [169]. Tau deposit is a common pathologic finding of AD [168] as knockdown of tau expression removes Aβ-induced neurodegeneration in different species [170].
As result of trehalose treatment in mouse showing parkinsonism symptoms, it is found increase of dopamine neurons and the increase of dopamine-related protein levels in the striatum. Also, an increase of aberrant protein clearance is observed through augmentation of autophagy[168]. Furthermore, trehalose enhances motor and cognitive behavior of this species and reduces tau abnormalities, astrogliosis and the number of murine β-amyloid plaques. On the other hand, a long-term enhancement of autophagy may result in neurodegeneration. An additional role of trehalose is to help the degradation of mutant tau through chemical chaperone activity. To compare proteasome with autophagy, on the other hand, it is declared that not only proteasome does not have a considerable role in tau breakdown in primary neurons [171], but also its inhibition activates some yet unknown pathways which decrease the level of endogenous tau; however, this depends on the cell type according to some investigations performed on non-neuronal cell lines [172]. Another important topic in this regard is to examine the effect of phosphorylation on the autophagic degeneration, which results in the minor interaction between them [171].

Hereditary ataxias (HA) is a neurological disorder often characterized by slow progressive degeneration of cerebellum. A lot of gene seem to be involved in HA. One of this is CHIP, a ubiquitin ligase which act as a bridge between proteasome system and chaperones[173]. Moreover, it is known that CHIP is a key factor for the ubiquitination and degradation of proteins like tau and α-synuclein and therefore, it plays a vital role in other neurological diseases. In several studies was observed that mutation in STUB-1 gene lead to low autophagy activity and variation in CHIP and HSP70 levels [174]..
Trehalose was tested in vitro, fibroblasts of a patient with ataxia with mutation in CHIP. Cells were treated with both epoxomicin and trehalose in vitro. Treatment with epoxomicin induced proteasome inhibition, pathophysiological age-related alteration, protein ubiquitination and reduction in cell viability. Treatment with trehalose reduced epoxomicin effect, and an increase of CHIP and HSP70 was evident. Moreover, trehalose treatment reduce caspase-3 and free radical expression and enhancing mitochondrial morphology in both untreated and CHIP-mutant fibroblasts. Moreover, markers of autophagy were increased during this process, indicating the activation of autophagy, the most beneficial effect of this disorder, in both mentioned groups

Frontotemporal degeneration (FTD) and fronto-temporal lobar degeneration (FTLD), is a disease process that results in progressive damage to the temporal and/or frontal lobes of the brain. FTD is due by low expression of progranulin, a pleiotropic factor essential for neuron survival[175]. Low levels of progranulin may induce neurodegeneration leading to loss of function by reducing GRN mRNA and PGRN protein by at least 50% via haplo-insufficiency [90]. PGRN partially regulates lysosome homeostasis, which itself is associated with regulation of GRN expression [176]. The main strategy to counteract FTD is to increase levels of PGRN, and trehalose and mTOR inhibitors have been found to increase PGRN expression and to induce autophagy.
Although, they all augment both intracellular and secreted PGRN, mTOR inhibitors fail to increase PGRN in human and mouse neuroblastoma cell lines, whilst trehalose is shown to have this ability, too. Therefore, mTOR-inhibition and PGRN upregulation are shown to be independent pathways. Trehalose mainly acts by enhancing GRN gene transcription, although transcription factor EB (TFEB), which is strongly regulated by mTOR phosphorylation, does not affect it [177].

Spinal and bulbar muscular atrophy and trehalose

Data obtained in our laboratory and published by Giorgetti [87], examine trehalose effects on SBMA suggests that trehalose decreases ARpolyQ insoluble forms in vitro and stimulates HSPB8, which enhances solubility and elimination of ARpolyQ via both autophagy and ubiquitin proteasome system. Furthermore, cotreatment with anti-androgen Bicalutamide attenuates AR activation and nuclear translocation, and increases the efficiency of this treatment, even in the presence of testosterone. This combination, also, removes insoluble species of AR with a very long polyQ (Q112) tract. Now for this disease in vivo analysis are not available.

Mouse models of Kennedy disease

Transgenic mice overexpressing ubiquitously an androgen receptor characterized by 97Q were obtained by random insertion of a cassette composed of the cytomegalovirus immediate early enhancer, the chicken beta-actin promoter and AR97Q [14].Transgenic mice with ubiquitous overexpression of poly-glutamine-expanded AR were generated by random insertion of a cassette composed of the cytomegalovirus immediate early enhancer, the chicken beta-actin promoter and AR97Q [14]. AR97Q-expressing male mice show progressive motor impairment, body weight loss, short life span (50 % mortality at 5 months of age), reduced cage activity, and severe muscle atrophy starting from 2 months of age in males and 4 months of age in females. Pathological phenotype of AR 97Q transgenic mice is androgen dependent, since all symptom can be attenuated by chemical or surgical castration[14]. This mouse model shows several symptoms also present in human patient. Androgen receptor transgene can be detected in the spinal cord, cerebellum, heart, muscle, pancreas, and other tissues, and in most of them inclusion formation or nuclear staining for AR can be detected. Muscle pathology is characterized by grouped, small angulated fibers, and reduced fiber size [14], together with very large fibers with central nuclei [41]. No significant reduction in the number of spinal motor neurons has been detected. Interestingly, the diameter of large myelinated fibers is reduced, and no defects in the cerebellum, cerebrum, and dorsal root ganglia have been detected.

A second mouse model of the disease is represented by transgenic SBMA mice with selective expression of poly-glutamine expanded AR in neurons, generated by random insertion of a cassette in

which the expression of AR112Q transgenes was driven by the prion promoter [74]. Male mice of this model are not smaller, and they didn't show lower survival than their wild type littermates. In this model only, male show symptoms of slowly progressing motor dysfunction. Indeed, male AR112Q present clasping starting to 6 weeks an age, rotarod deficits at 4 months of age, and gait abnormality around 7 months of age, open field activity shows reduced vertical and horizontal activity by 7 months of age, and grip strength is reduced by 10 months of age. AR112Q transgenic mice show androgen receptor inclusions in neuronal tissue. Also, in this case, all symptoms are androgen dependent since all symptom can be attenuated by chemical or surgical castration. Because these mice express the transgene in the central nervous system but not in skeletal muscle or other peripheral tissues, this model allows for investigation of cell-autonomous mechanisms of degeneration in neurons and non-cell-autonomous degeneration of peripheral organs.

By homologous recombination, it is possible to generate mice expressing a mutant gene by replacing the wild type counterpart, the knock-in technology. This strategy allows to avoid the possible problem of overexpressed gene since the mutant gene is finely regulated by the endogenous promoter and regulatory sequences, such as enhancers. Knock-in SBMA mice have been generated by replacing the mouse exon 1 of AR, located on the X chromosome, with the human exon 1 113 glutamine residues [178]. AR113Q-expressing mice recapitulate several features of human disease. AR113Q-expressing mice show a phenotype characterized by premature death at approximately 3–5 months of age [75]. Premature death is associated with dysfunction of the urinary tract and atrophy of the levator ani/ bulbocavernosus muscles. Male AR113Q-expressing mice develop muscle atrophy, body weight loss, and motor dysfunction. AR113Q-expressing male mice also show partial androgen insensitivity, reduced fertility, and atrophic testes, although serum testosterone levels are like control mice. In these mice, muscle pathology is characterized by the presence of both neurogenic and myogenic signs, with upregulation of several denervation markers. Because expression of poly-glutamine-expanded AR in this model is physiologically regulated, this model allows for in vivo analysis of pathogenic mechanisms in a context in which poly-glutamine-expanded AR is not overexpressed.

Aim

Aim

In previous in vitro studies conducted in our laboratories it was evaluated whether a combined pharmacological treatment, aimed both to reduce the nuclear toxicity exerted by mutant AR and to enhance its autophagic clearance, may be a novel therapeutic approach for SBMA.
These experiments suggest that a co-treatment with bicalutamide, known to lead to a reduction in nuclear translocation of androgen receptor, and trehalose can induce an increase in AR nuclear inclusions in vitro in presence of testosterone. This study was focused on motoneuronal cells; remain to be determined whether the therapeutic approach here postulated may have beneficial effects also in muscle, in which the toxicity exerted by ARpolyQ may be due to different causes.
Interestingly both single treatment and the combined treatment seems to don't affect the amount of soluble ARpolyQ, both in presence or absence of testosterone. Indeed, the degradative induction promoted by the two compounds, involves only ARpolyQ misfolded protein, in a synergic manner. Therefore, the combined treatment can limit the formation of aggregate and inclusions in immortalized motor neurons. These in vitro data suggest that, at least in their earlier formation stages, aggregates may protect against ARpolyQ toxicity by confining neurotoxic species into a physically defined subcellular compartment.
However, they become toxic at later stages by altering essential neuronal processes. Moreover, aggregate and inclusion may be an important hallmark through observe misfolding protein behavior, and its amount reduction usually represent a positive effect of the treatment and in our tests, trehalose and bicalutamide combined were more efficiently in aggregate reduction than when the same compounds were used separately.
Therefore, the longer ARpolyQ cytoplasmic retention by bicalutamide facilitates a better cytoplasmic autophagic recognition of the misfolded species prior to its migration into the nucleus; at the same time, the enhanced autophagy by trehalose improves the capability of this proteolytic system to clear the excess of misfolded ARpolyQ released from accessory chaperones after ligand interaction, also preventing any possible autophagic flux blockage.
This goal can be reached by trehalose treatment, able to induce HSPB8, which is a known autophagy facilitator. Indeed, many heat shock proteins are involved in the cells response to protein misfolding.
For instance, HSPB8 dramatically increases solubility and clearance of ARpolyQ (and other misfolded proteins), decreasing their aggregation rate. HSPB8 can induce clearance by both the UPS and autophagy; when autophagy is involved, HSPB8 lead to formation of a complex with BAG3/HSC70/CHIP, in which CHIP ubiquitinates HSPB8-associated substrates, permit to SQSTM1/p62 to recognize specific signal in autophagosome. With this mechanism, HSPB8 facilitates ARpolyQ autophagic clearance and relieves the blockage of autophagic flux.
Several advantages may arise from the use of these two active compounds in SBMA. First, the antiandrogen bicalutamide is an FDA-approved and commercially available drug, already widely used in prostate cancer therapy. It can be administered for chronic treatment and it is relatively well tolerated by patients. Secondly, trehalose is not considered a drug, but a nutrient supplement, with no restriction for its oral intake.
Even if trehalose has been found active in cellular models of SBMA, no studies have been conducted in mouse models of SBMA. Similarly, several studies performed in cellular models of SBMA have demonstrated that bicalutamide alone counteracts ARpolyQ aggregation possibly facilitating the autophagic removal of ARpolyQ misfolded species, thus preventing their neurotoxicity. Even in this case, no data are yet available in mouse models of SBMA. We have also tested the combinatory use

of bicalutamide and trehalose on cell models of SBMA, demonstrating a synergistic effect of the two compounds on ARpolyQ removal. The slowed kinetics of ARpolyQ nuclear translocation induced by bicalutamide allows for an increased clearance of misfolded ARpolyQ species via the cytoplasmic autophagic machinery, made more efficient and active by trehalose treatment. It is worth noting that the autophagic process is induced by trehalose but not influenced by bicalutamide, as shown by the two well-known autophagic markers, SQSTM1/p62 and LC3-II. Collectively, the data published by Giorgetti et al. in 2015 lay the foundation for preclinical trials in SBMA mouse models to test the therapeutic potential of bicalutamide and trehalose in single or combined administration. We choose the “Knock-in SBMA mouse” as model. It is characterized by 113 polyQ. The non-transgenic littermates were used as control.

Results

Results

Model characterization

First, to verify the reliability of the animal model selected for this study, we characterized the mouse colony with a set of preliminary tests and analyses.
Mice with a targeted insertion of 113 CAG repeats into exon 1 of the AR gene (see "Materials and Methods" section) were examined for evidence of an androgen dependent neuromuscular phenotype.
We found that AR113Q males show a significantly lower body mass than NTg males at all ages examined starting from 20 weeks of age (Figure 5A).
Analysis of survival revealed that AR113Q males die at young age. As shown in Figure 5B, approximately 39% of AR113Q males survive at 52 weeks. We observed that the KI AR113Q mice death occurs between 16 and 36 weeks, while no NTg mice died in this same period.
The seminal vesicle weight analysis is a further sign of AR loss of function or alteration, and we found that seminal vesicle weight of KI mice at the age of sacrifice, 52 weeks, were smaller than that of NTg littermates at the same age (Figure 5C).

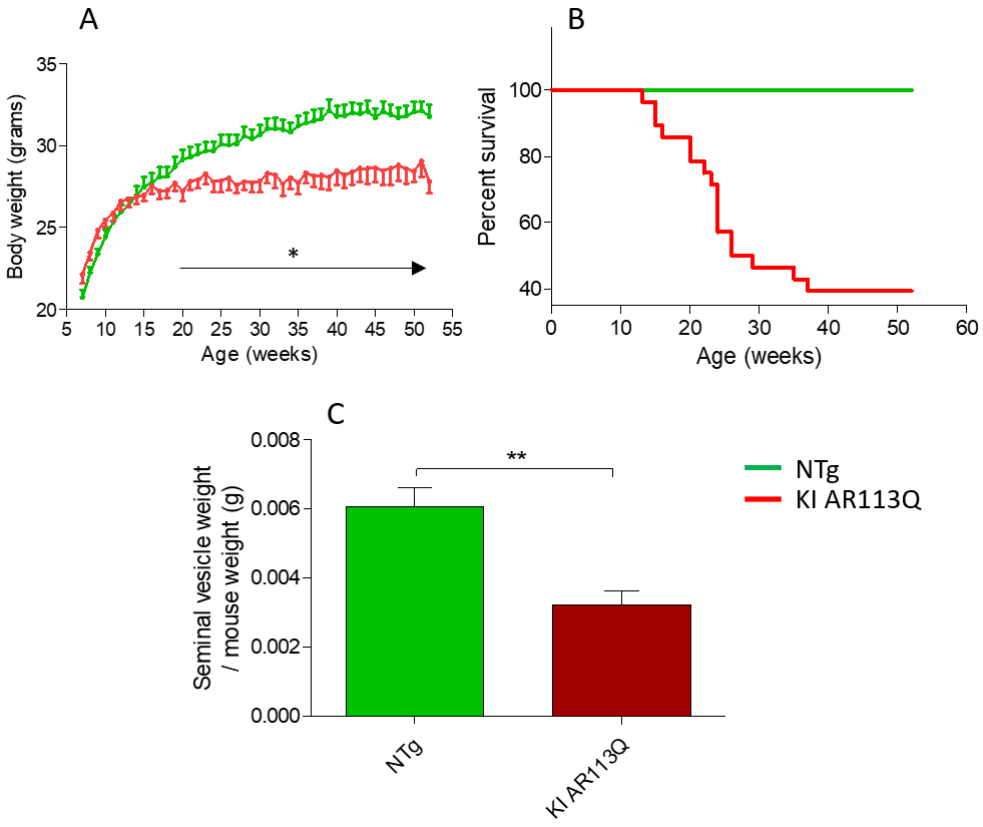

*Figure 5 – Preliminary characterization of SBMA mouse model – (A) Body mass (mean ± SEM) reported by age of NTg mice (green line, n=14), KI AR113Q (red line, n=17). (B) Kaplan-Mayer survival curve of NTg mice (green line, n=14), and KI AR113Q (red line, n=17). (C) seminal vesicle weight of NTg mice (green n=11) and KI AR113Q (red n=9) at 24 weeks of age (**p<0.01 by unpaired Student's t test) normalized to the mouse weight.*

We performed forelimb grip strength analysis on NTg and AR113Q mice, that is a simple test allowing evaluation of the muscular strength of animals. We find that SBMA male mice have a significantly decreased forelimb strength compared with wild type mice (Figure 6B). This deficit appeared in adults as early as 20 weeks of age, correlating with the decrease in the body mass (Figure 5A). At the same time AR113Q mice show also a worse performance than non-transgenic mice on rotarod, suggesting a reduction of motor coordination (Figure 6A).

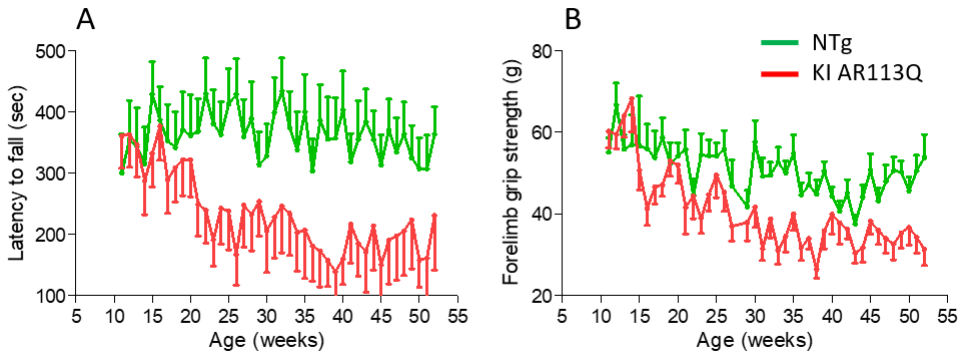

Figure 6 - Behavior analysis - (A) Rotarod test (mean ± SEM) of NTg mice (green line, n=14), KI AR113Q (red line, n=17) evaluated weekly beginning at 10 weeks age until the age of sacrifice (52 weeks). (B) Forelimb grip strength (mean ± SEM) of NTg mice (green line, n=14), KI AR113Q (red line, n=17) evaluated weekly beginning at 10 weeks until the age of sacrifice (52 weeks)

The functional deficit of motor behavior of AR113Q males was accompanied by morphological changes in skeletal muscle indicative of both neurogenic and myopathic effects, like the features described in muscle biopsies of Kennedy disease patient[27]. The skeletal muscle of AR113Q male mice (24 weeks) analyzed (gastrocnemius) contained groups of angulated, mild atrophic fibers suggestive of neurogenic atrophy (Figure 7D, 7E). Histological analyses revealed also the presence in Tg mouse muscle of fibers smaller than that of Ntg (Figure 7A, 7B). On the contrary, we did not find an increase of internal nuclei, usually indicative of a myopathic process (Figure 7C).

To determine whether changes in the gene expression reflect muscle health and denervation, we performed real-time RT-PCR to measure the levels of mRNAs coding for myogenin, acetylcholine receptor α-subunit and myogenic differentiation antigen also known as MyoD. Usually, the expression of these markers is induced following denervation [179].

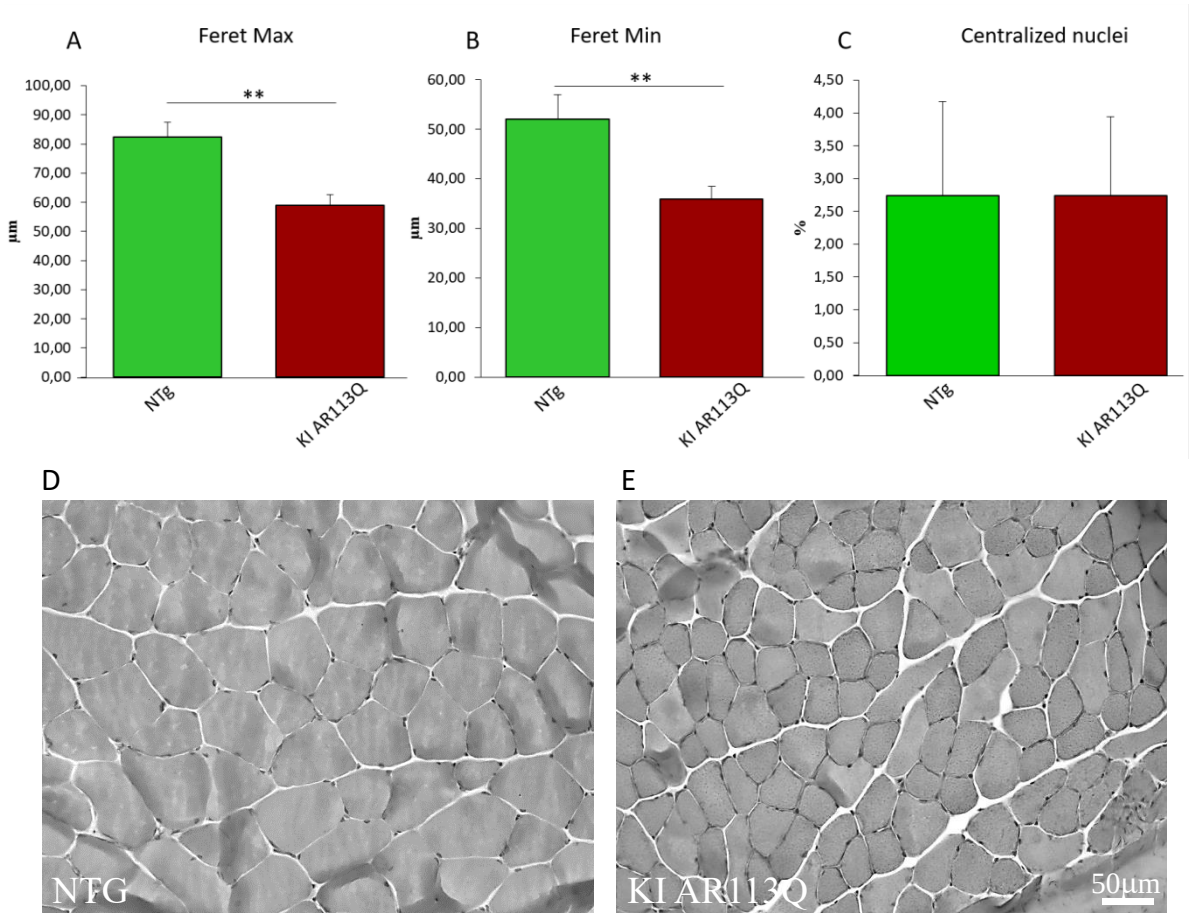

*Figure 7- Gastrocnemius morphology - A, B) Analysis of gastrocnemius muscles fiber size (A, maximum Feret diameter; B, minimum Feret diameter) from NTg (green) and KI AR113Q (red) mice at 24 weeks of age (symptomatic stage). Neurolucida analysis on a section of 40 µm. Each bar represents the mean ± sem of four independent replicates (**p<0.01). Statistical analysis has been performed through Student's t test. C) Analysis of gastrocnemius muscles centralized nuclei from NTg (green) and KI AR113Q (red) mice. Neurolucida analysis on a section of 40 µm. Each bar represents the mean ± sem of four independent replicates (**p<0.01). Statistical analysis has been performed through Student's t test. (D, E) The morphology of the muscles (gastrocnemius) is highlighted by hematoxylin/eosin staining. Scale bar = 50 µm*

AR113Q gastrocnemius muscle expressed 5-fold higher levels of acetylcholine receptor α-subunit at symptomatic stage, 24 weeks of age, and 7-fold higher levels at end stage, 52 weeks of age, both compared with NTg littermates (Figure 8A). Expression of MyoD and MyoG mRNA did not show significant changes (Figure 8B, 8C). We also analyzed the mRNA expression of Pax7, a characteristic marker of muscle satellite cells, staminal cells able to differentiate to skeletal muscle cells, and to give rise to other satellite cells. Pax7 expression is a clue of regenerative attempt in muscle. In our mice gastrocnemius samples, we found 2-fold higher levels of Pax7 at symptomatic (24 weeks), and end stage (52 weeks) (Figure 8D).

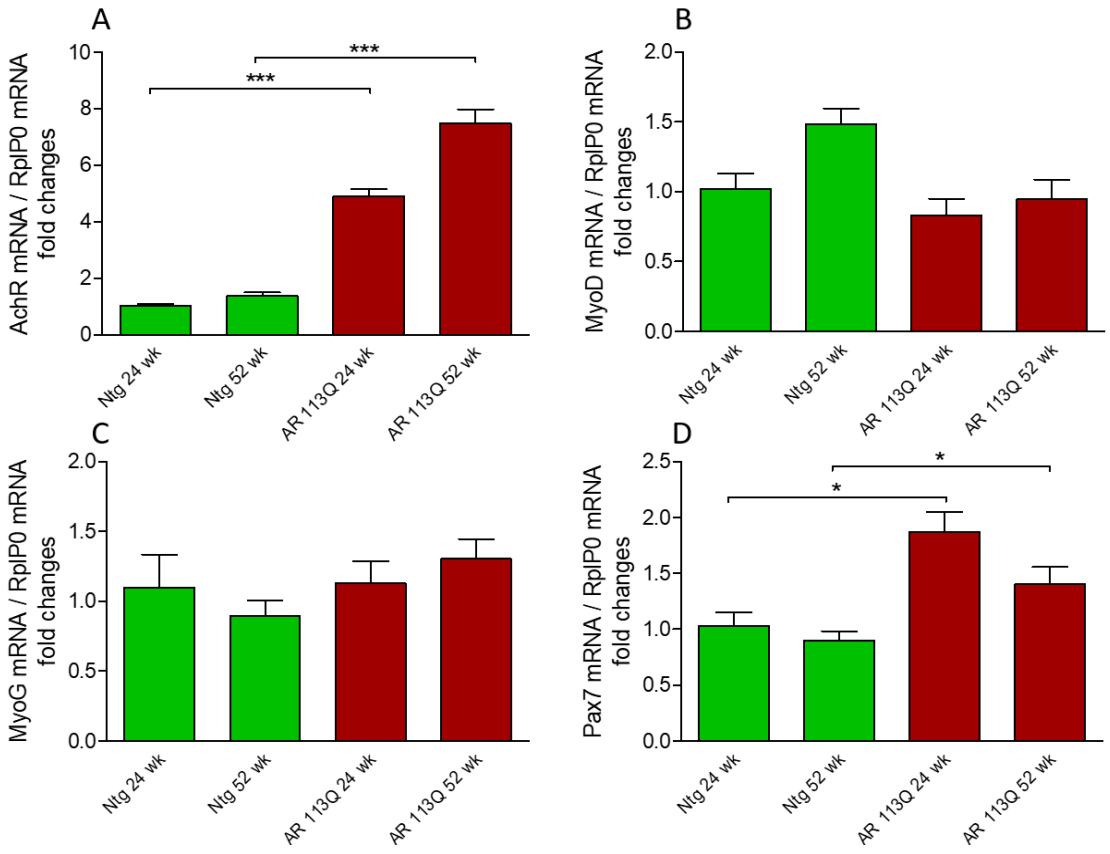

*Figure 8 – Expression of muscular markers- RT-qPCR analyses of the mRNA levels of AchR (A), MyoD (B), MyoG (C), Pax7(D) performed on total RNA extracted from gastrocnemius of male NTg mice (green) and KI AR113Q (red) at 24 (symptomatic stage) or 52 (end stage) weeks of age. Data have been normalized to Rplp0 mRNA, expressed relative to the levels determined in NTg mice at 24 weeks of age, which are taken as internal reference, and expressed as fold changes. Each bar represents the mean ±s.e.m. of five independent replicates (*p<0.05, ***p<0.001). Statistical analysis has been performed through two-way ANOVA for group comparisons followed by Bonferroni post-hoc test.*

Treatment validation

The dose of trehalose used in this study was selected on the basis of previous reports for other neurodegenerative disease, such as Parkinson's and Huntington's diseases [163], while the dose of bicalutamide was selected on the basis of that classically adopted in human therapy [180], since this drug is widely used in clinics against prostate cancer, and its pharmacokinetics is very well known.
Preliminary studies were performed to validate both the doses and the route of administration. These studies were done by treating 5 NTg mice with trehalose and 5 NTg mice with bicalutamide. Trehalose was administered orally in drinking water at 2% ad libitum, while bicalutamide was administered by subcutaneous injection (2mg/Kg) twice a week, both starting from 6 weeks of age until the age of sacrifice (20 weeks).

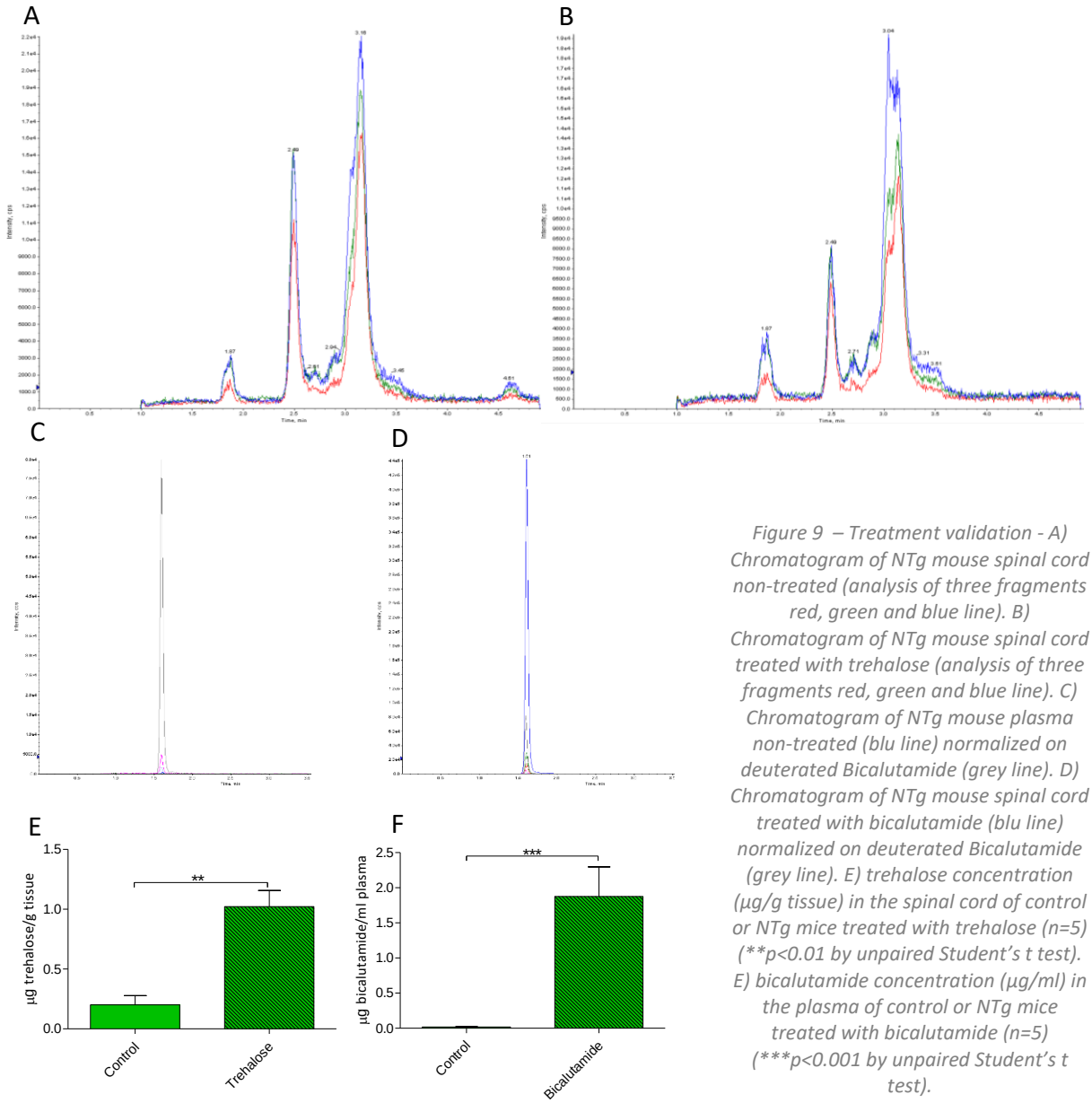

*Figure 9 – Treatment validation - A) Chromatogram of NTg mouse spinal cord non-treated (analysis of three fragments red, green and blue line). B) Chromatogram of NTg mouse spinal cord treated with trehalose (analysis of three fragments red, green and blue line). C) Chromatogram of NTg mouse plasma non-treated (blu line) normalized on deuterated Bicalutamide (grey line). D) Chromatogram of NTg mouse spinal cord treated with bicalutamide (blu line) normalized on deuterated Bicalutamide (grey line). E) trehalose concentration (µg/g tissue) in the spinal cord of control or NTg mice treated with trehalose (n=5) (**p<0.01 by unpaired Student's t test). E) bicalutamide concentration (µg/ml) in the plasma of control or NTg mice treated with bicalutamide (n=5) (***p<0.001 by unpaired Student's t test).*

The mass spectrometry analysis allowed us to detect the presence of trehalose in the spinal cord of treated mice, confirming us that trehalose is not completely metabolized by trehalase in the gut and is able to pass the blood-brain barrier. Figure 9A shows the chromatogram of the spinal cord extract of control mice, with the peak of trehalose (at 3,15'); peaks of glucose (1,87'), sucrose (2,49'), maltose (3,04') that partially hide the trehalose signal are also visible. After the treatment (Figure 9B), the concentration of trehalose increases but again, in the chromatogram, the trehalose peak is partially hide by maltose. Figure 9E shows that trehalose levels are tripled in the spinal cord of treated mice.
The presence of trehalose in a central nervous system tissue, protected by the blood brain barrier, assure us that the compound reaches their target.
The analysis of bicalutamide resulted to be simpler than that of trehalose. Indeed, using plasma collected from mice treated with bicalutamide, we can clearly detect the presence of the drug (Figure 9C, 9D). The quantification of the bicalutamide levels is reported in Figure 9F.
Moreover, we also measured blood sugar levels of mice at sacrifice to be sure that continuous high levels of the disaccharide trehalose does not cause alteration of glucose metabolism in mice, since in the SBMA patient metabolism problems and diabetes are often present (Figure 10).

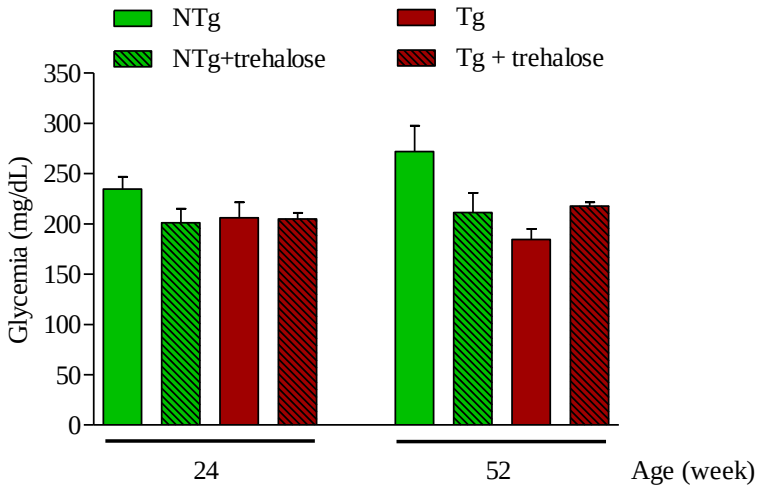

Figure 10 – Glycemia (mg/dL) of NTg mice (n=4), NTg mice treated with trehalose (n=5), KI AR113Q mice (n=7), KI AR113Q mice treated with trehalose at 24 weeks of age, and NTg mice (n=5), NTg mice treated with trehalose (n=6), KI AR113Q mice (n=4), KI AR113Q (n=4) mice treated with trehalose at 52 weeks of age. Statistical analysis has been performed through two-way ANOVA analysis for group comparisons followed by Bonferroni post-hoc test.

Effect of trehalose or/and bicalutamide treatments on SBMA mice

In the first set of experiment performed, we compared the effect of single treatments with trehalose or bicalutamide and of the combined treatment with the two drugs on KI AR113Q mice and their NTg littermates. Trehalose was administered orally in drinking water at 2% ad libitum, while bicalutamide was administered by subcutaneous injection (2mg/Kg) twice a week, both starting from 6 weeks of age until the age of sacrifice (52 weeks).
As we did during mouse characterization, we analyzed the body mass of treated and non-treated mice. We did not find any variation in NTg or KI AR113Q treated mice (Figure 11A, 11B).
Regarding the survival analysis, we observed that the treatment with trehalose or bicalutamide alone can increase the survival of KI AR113Q mice (Figure 11C); the survival increased from 39% to 56% with trehalose treatment, and to 58% with bicalutamide administration. The combined treatment increased the survival to 61%, and partially delayed disease progression, even if this result is not statistically significant.

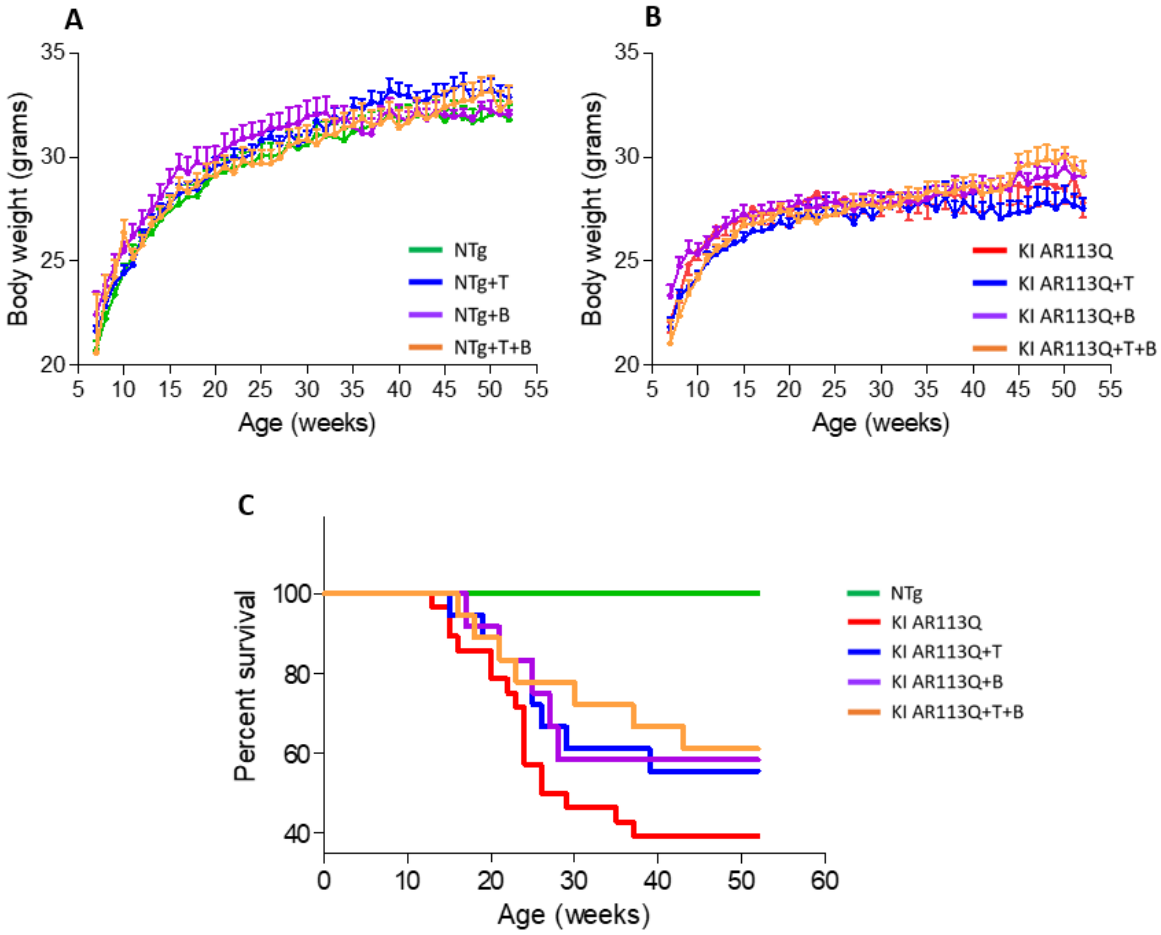

Figure 11 – Effects of trehalose and/or bicalutamide treatment - A) Body mass (mean ± SEM) reported by age of NTg mice (green line, n=14), NTg mice treated with trehalose (blue line, n=15), NTg mice treated with bicalutamide (purple line, n=8), NTg mice treated with trehalose and bicalutamide (orange line, n=12); B) Body mass (mean ± SEM) reported by age of KI AR113Q mice (red line, n=17), KI AR113Q mice treated with trehalose (blue line, n=18), KI AR113Q mice treated with bicalutamide (purple line, n=18), KI AR113Q mice treated with trehalose and bicalutamide (orange line, n=17); C) Kaplan-Mayer survival curve of NTg mice (green line, n=14), KI AR113Q mice (red line, n=17), KI AR113Q mice treated with trehalose (blue line, n=18), KI AR113Q mice treated with bicalutamide (purple line, n=18), KI AR113Q mice treated with trehalose and bicalutamide (orange line, n=17) until 52 weeks of age.

Then, we measured: a) the forelimb skeletal muscle strength performing grip strength analysis, and b) motor coordination taking advantage of rotarod test, on NTg and AR113Q mice during the treatments. Mice were trained for test execution starting at 8 weeks of age. We weekly collected behavioral data starting from 10 weeks of age, until the age of sacrifice. Regarding the grip strength test, we did not observe any positive effect after our treatments, both alone or combined, in KI AR113Q mice (Figure 12C). Nevertheless, we noticed a faster decline of performance in mice treated with bicalutamide alone or combined with trehalose both in NTg and SBMA mice (Figure 12A, 12C). Probably, this unexpected effect depends on the anti-anabolic effect of bicalutamide. Indeed, we administrated the anti-androgenic compound, that has also anti-anabolic side effects, starting from 6 weeks of age. At this age, mice are post-pubertal, perfectly able to reproduce, but their muscle development is not fully completed.

About motor coordination, measured by rotarod, we did not observe the negative effect of bicalutamide find in grip strength test in NTg mice (Figure 12D), strengthening the theory of the detrimental anti-anabolic action on muscle; indeed, rotarod test can give information not only on the muscle health but also on the integrity of the sensory nervous system. Rotarod test analysis, indicated a great increase of AR113Q mice performance after trehalose treatment alone: the performance of these mice was comparable to that of NTg mice (Figure 12D).

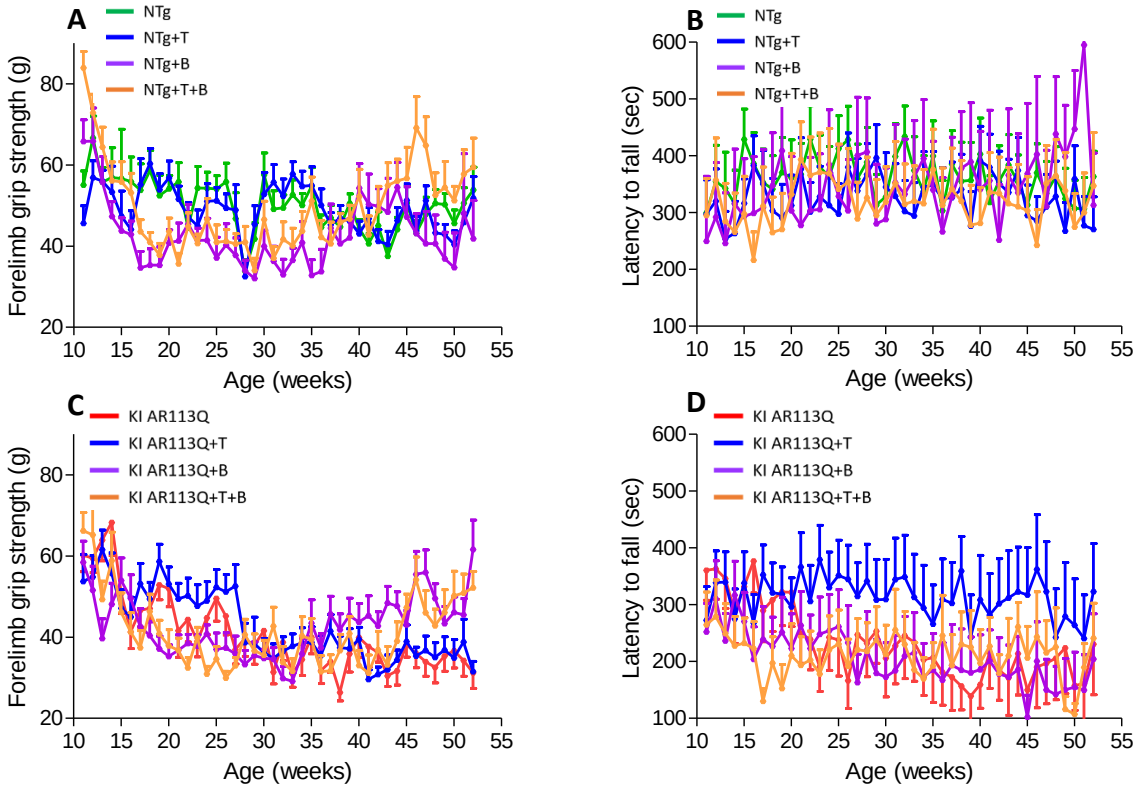

Figure 12 – Motor behavioral effects of KI ARQ113 mouse treatments - A) Forelimb grip strength (mean ± SEM) by age of NTg mice (green line, n=14), NTg mice treated with trehalose (blue line, n=15), NTg mice treated with bicalutamide (purple line, n=8), NTg mice treated with trehalose and bicalutamide (orange line, n=12) evaluated weekly beginning at 10 weeks of age until the age of sacrifice (52 weeks). B) Rotarod test (mean ± SEM) by age of NTg mice (green line, n=14), NTg mice treated with trehalose (blue line, n=15), NTg mice treated with bicalutamide (purple line, n=8), NTg mice treated with trehalose and bicalutamide (orange line, n=12) evaluated weekly beginning at 10 weeks of age until the age of sacrifice (52 weeks) C) Forelimb grip strength (mean ± SEM) by age of KI AR113Q mice (red line, n=17), KI AR113Q mice treated with trehalose (blue line, n=18), KI AR113Q mice treated with bicalutamide (purple line, n=18), KI AR113Q mice treated with trehalose and bicalutamide (orange line, n=17) evaluated weekly beginning at 10 weeks of age until the age of sacrifice (52 weeks). D) Rotarod test (mean ± SEM) by age of KI AR113Q mice (red line, n=17), KI AR113Q mice treated with trehalose (blue line, n=18), KI AR113Q mice treated with bicalutamide (purple line, n=18), KI AR113Q mice treated with trehalose and bicalutamide (orange line, n=17) evaluated weekly beginning at 10 weeks of age until the age of sacrifice (52 weeks).

To better clarify the possible role of our treatments, in particular with bicalutamide alone or with trehalose, on the loss of muscle strength, we decided to create a second group of mice and to treat them starting from 10 weeks of age instead of 6, trying to avoid the anti-anabolic effect of antiandrogen compound. We observed that all NTg treated mice preserve their strength and motor coordination (Figure 13A, 13B). The strength of KI AR113Q mice resulted to be higher after the treatment with bicalutamide alone or with trehalose. Also, the performance at the rotarod test showed an increase in all groups of treated mice respect to untreated KI AR113Q mice (Figure 13C, 13D).

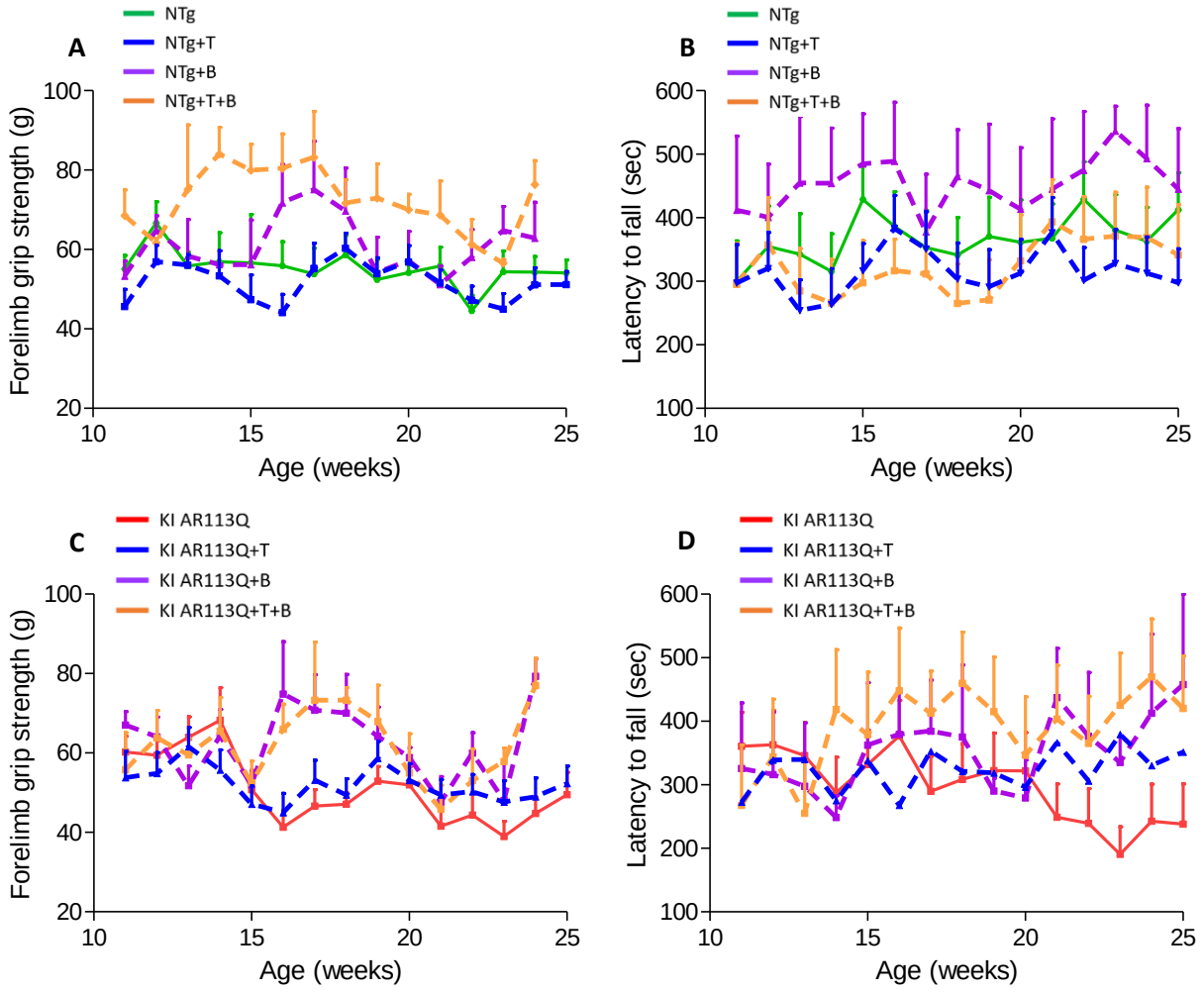

Figure 13 – Effects of delayed bicalutamed treatment on mouse motor behavior - A) Forelimb grip strength (mean ± SEM) by age of NTg mice (green line, n=14), NTg mice treated with trehalose (blue line, n=5), or bicalutamide (purple line, n=5), or trehalose and bicalutamide (orange line, n=5) evaluated weekly beginning at 10 weeks until 24 weeks. B) Rotarod test (mean ± SEM) by age of NTg mice (green line, n=14), NTg mice treated with trehalose (blue line, n=5), or bicalutamide (purple line, n=5), or trehalose and bicalutamide (orange line, n=5) evaluated weekly beginning at 10 weeks until 24 weeks. C) Forelimb grip strength (mean ± SEM) by age of KI AR113Q mice (red line, n=17), KI AR113Q mice treated with trehalose (blue line, n=5), or bicalutamide (purple line, n=5), or trehalose and Bicalutamide (orange line, n=5) evaluated weekly beginning at 10 weeks until 24 weeks. D) Rotarod test (mean ± SEM) by age of KI AR113Q mice (red line, n=17), KI AR113Q mice treated with trehalose (blue line, n=5), or bicalutamide (purple line, n=5), or trehalose and bicalutamide (orange line, n=5) evaluated weekly beginning at 10 weeks until 24 weeks. Bicalutamide was administered from 10 weeks of age, while trehalose from 6 weeks of age.

Morphological and biochemical analysis of skeletal muscle

To elucidate whether the treatments with trehalose and bicalutamide have an impact on the morphological and biochemical markers, we decided first to focus our attention on muscle of our mice. This part of the studies was performed in collaboration with the group of Prof. Vercelli of the University of Turin

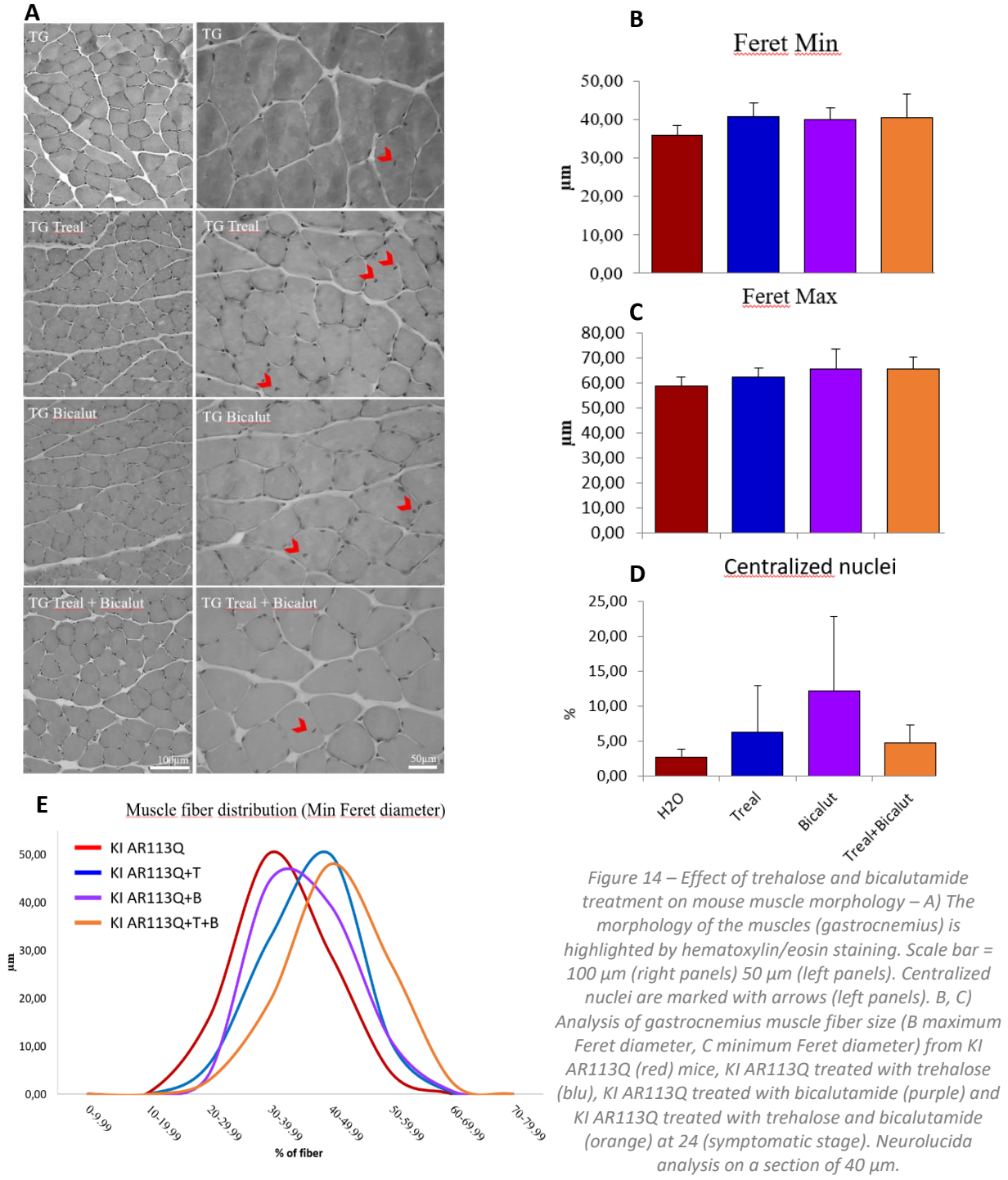

Figure 14 – Effect of trehalose and bicalutamide treatment on mouse muscle morphology – A) The morphology of the muscles (gastrocnemius) is highlighted by hematoxylin/eosin staining. Scale bar = 100 µm (right panels) 50 µm (left panels). Centralized nuclei are marked with arrows (left panels). B, C) Analysis of gastrocnemius muscle fiber size (B maximum Feret diameter, C minimum Feret diameter) from KI AR113Q (red) mice, KI AR113Q treated with trehalose (blu), KI AR113Q treated with bicalutamide (purple) and KI AR113Q treated with trehalose and bicalutamide (orange) at 24 (symptomatic stage). Neurolucida analysis on a section of 40 µm. Statistical analysis has been performed through two-way ANOVA for group comparisons followed by Bonferroni post-hoc test. D) Analysis of gastrocnemius muscles centralized nuclei from KI AR113Q (red) mice, KI AR113Q treated with trehalose (blu), KI AR113Q treated with bicalutamide (purple) and KI AR113Q treated with trehalose and bicalutamide (orange) at 24 (symptomatic stage). Neurolucida analysis on a section of 40 µm. Each bar represents the mean ± SEM of four independent replicates. Statistical analysis has been performed through tow-way ANOVA for group comparisons followed by Bonferroni post-hoc test. (E) Muscle fiber size distribution analysis by percentage of fiber from gastrocnemius KI AR113Q (red) mice, KI AR113Q treated with trehalose (blu), KI AR113Q treated with bicalutamide (purple) and KI AR113Q treated with trehalose and bicalutamide (orange) at 24 (symptomatic stage).

The treatment with trehalose induced an increase of the muscle fiber size, not appreciable analyzing only maximum or minimum Feret diameter (Figure 14B, 14C), but observing muscle fiber distribution graphic (Figure 14E), where the percentage of big fiber resulted to be higher in the muscle of mice treated with trehalose than that in untreated mice. This increase of fiber size was greater when the double treatment with trehalose and bicalutamide was administrated to SBMA mice. We did not find variation counting the number of centralized nuclei, usually associated to muscle regeneration (Figure 14A, 14D).

To determine whether changes in gene expression, a quantitative real-time RT-PCR was used to measure levels of myogenin, acetylcholine receptor α-subunit, myogenic differentiation antigen also known as MyoD and Pax7. Surprising none of these markers showed variation after any treatment both at symptomatic stage (24 weeks) and end stage (52 weeks) (Figure 15).

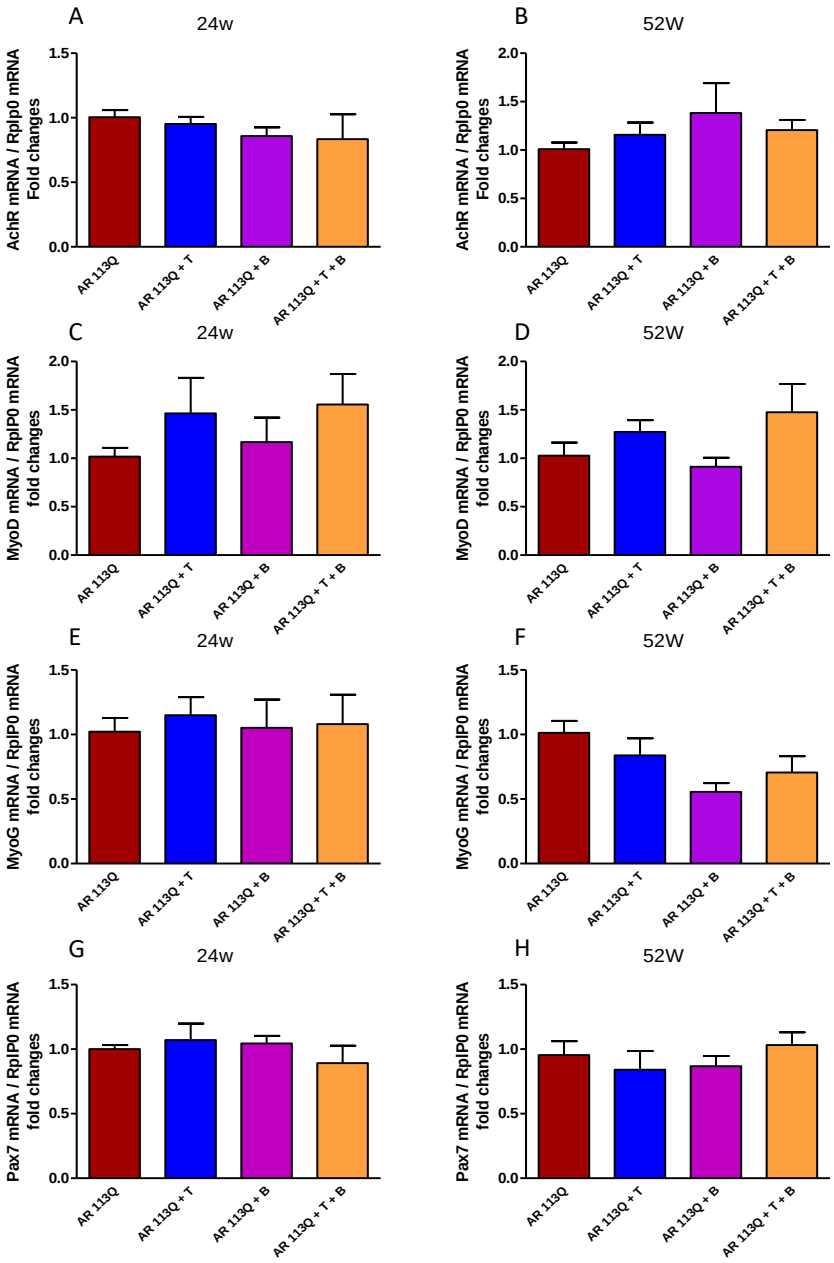

Figure 15 – Expression of muscle marker doesn't change - RT-qPCR analyses of the mRNA levels of AchR (A, B), MyoD (C, D), MyoG (E, F), Pax7(G, H) performed on total RNA extracted from gastrocnemius of male KI AR113Q (red), KI AR113Q treated with trehalose (blu), or bicalutamide (purple) or trehalose and bicalutamide (orange) at 24 (symptomatic stage) or 52 (end stage) weeks of age.

Data have been normalized to RpLP0 mRNA, expressed relative to the levels determined in NTg mice at 24 weeks of age, which are taken as internal reference, and expressed as fold changes. Each bar represents the mean ± s.e.m. of five independent replicates.

Statistical analysis has been performed through two-way ANOVA for group comparisons followed by Bonferroni post-hoc test.

Therefore, we analyzed several markers with the aim to find variation which could correlate with the positive data obtained with rotarod test and with survival analysis. One of these markers is Pgc1α, a key factor for mitochondria biogenesis. We found that its mRNA expression is increased 2-3 times after mice treatment with both trehalose and bicalutamide, at the end-stage of the disease (52 weeks) (Figure 16B).

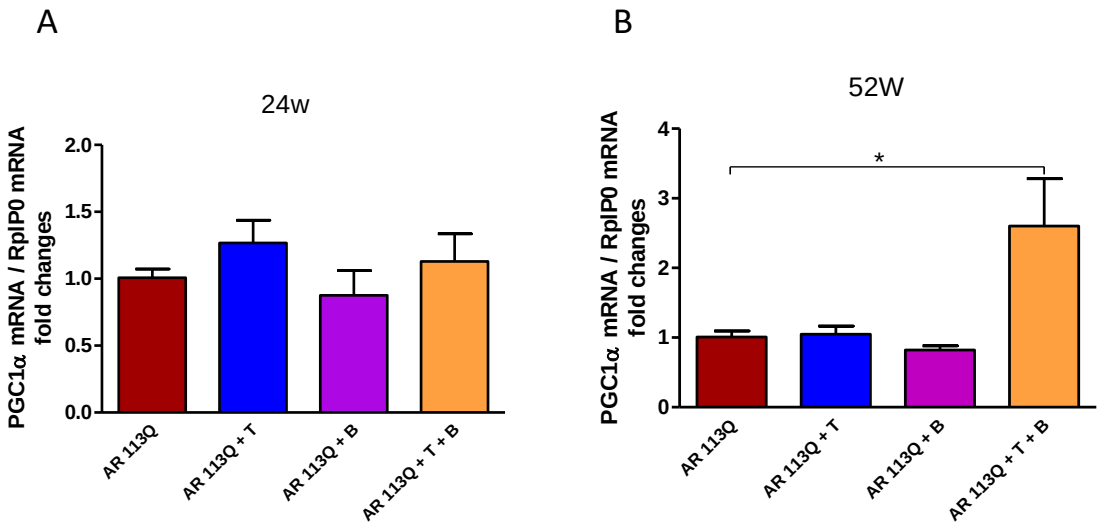

*Figure 16 - PGC1α mRNA is induced by the combined treatment with trehalose and bicalutamide - RT-qPCR analyses of the mRNA levels of PGC1α (A, B) performed on total RNA extracted from gastrocnemius of male KI AR113Q (red), or trehalose (blu), or bicalutamide (purple), or trehalose and bicalutamide (orange) at 24 (symptomatic stage) or 52 (end stage) weeks of age. Data have been normalized to RpLP0 mRNA, expressed relative to the levels determined in NTg mice at 24 weeks of age, which are taken as internal reference, and expressed as fold changes. Each bar represents the mean ± sem of five independent replicates (*p<0.05). Statistical analysis has been performed through two-way ANOVA for group comparisons followed by Bonferroni post-hoc test.*

Analysis of the autophagic pathway in KI AR113Q mice

Since our goal was to induce and take advantage of autophagy with trehalose and bicalutamide we decided to measure changes in the expression of autophagic markers, in skeletal muscle of symptomatic and end stage AR113Q male mice. It has already been reported [181] that the autophagy master regulator gene product TFEB is up-regulated in these mice when symptoms appear, and TFEB controls the expression of a series of genes whose protein products are involved in the autophagy and lysosome dynamics.

Here, we analyzed the expression of some genes encoding proteins which are essential for autophagy initiation and are critical markers for the autophagic process. Beclin-1 (the ATG6 ortholog, which regulates and associates to Vps34 to induce autophagy) is critical for autophagosome assembly, p62/SQSTM1 (which recognizes ubiquitinated protein for their insertion into autophagosomes) is a TFEB regulated autophagy marker, HSPB8, that we already demonstrated is one of the key protein involved in the autophagic removal of misfolded proteins [182], and his co-chaperone BAG3 (Figure 17). Beclin-1 mRNA expression is the only one that changed, showing a reduction after the treatment with bicalutamide alone or with trehalose at symptomatic stage (24 weeks) (Figure 17E).

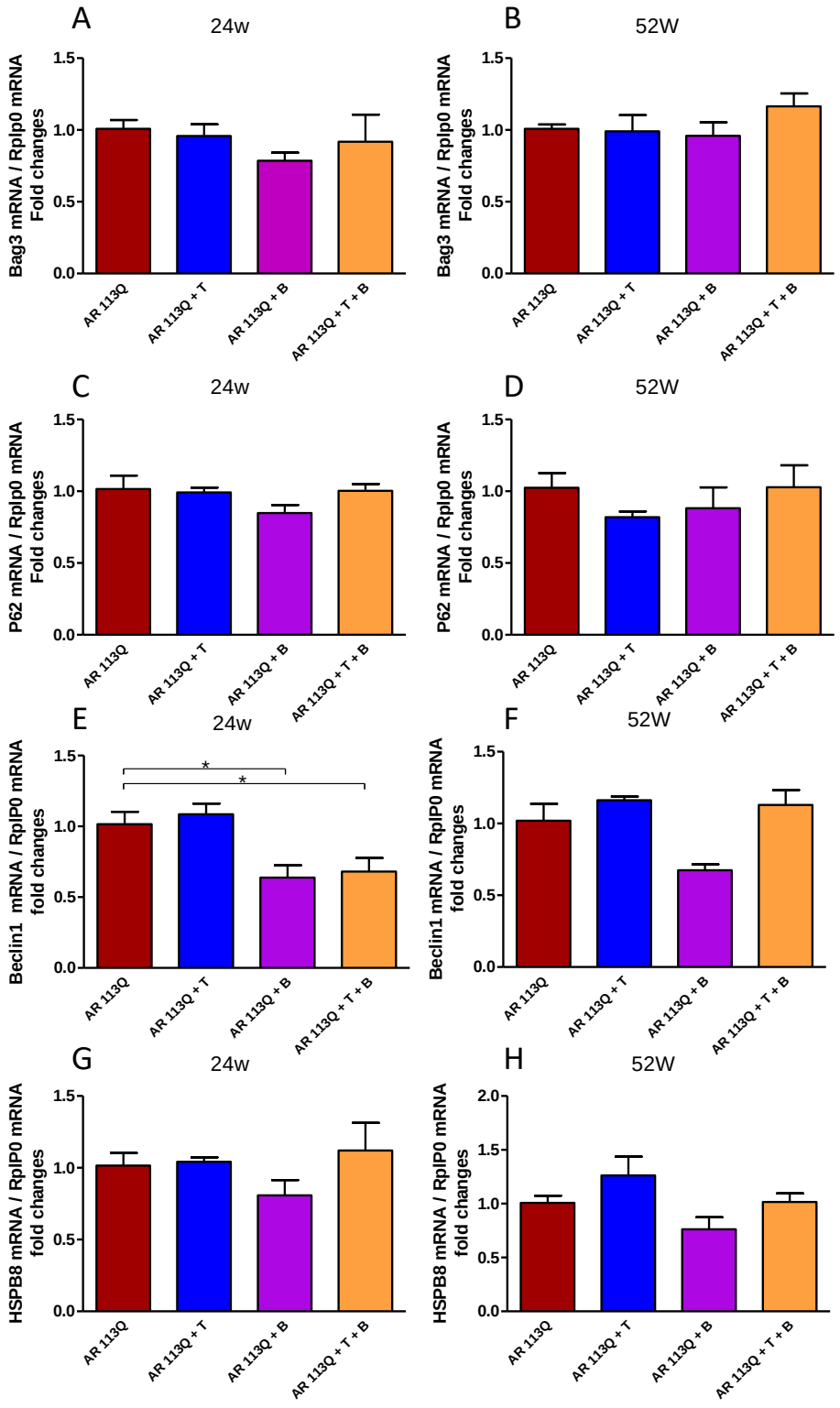

Figure 17- Expression of autophagic markers in muscle of trehalose and/or bicalutamide treated mice.- RT-qPCR analyses of the mRNA levels of BAG3 (A, B), p62/SQSTM1 (C, D), Beclin1 (E, F), HSPB8 (G, H) performed on total RNA extracted from gastrocnemius of male KI AR113Q (red), KI AR113Q treated with trehalose (blu), or bicalutamide (purple), or trehalose and bicalutamide (orange) at 24 (symptomatic stage) or 52 (end stage) weeks of age.

*Data have been normalized to Rplp0 mRNA, expressed relative to the levels determined in NTg mice at 24 weeks of age, which are taken as internal reference, and expressed as fold changes. Each bar represents the mean ± s.e.m. of five independent replicates (*p<0.05).*

Statistical analysis has been performed through two-way ANOVA for group comparisons followed by Bonferroni post-hoc test.

Discussion

Discussion

Spinal and bulbar muscular atrophy (SBMA) or Kennedy's disease is an X-linked motor neuron disease characterized by lower motor neuron degeneration in anterior horns of the spinal cord and in brainstem [6] , involving also dorsal root ganglia neurons causing motor and sensory disturbances [10]. The loss of motor neurons results in atrophy of bulbar, limb and facial muscle [7].

Recent evidence seems to suggest that muscle atrophy is not only a simple consequence of denervation induced by loss of motor neuron and their trophic effects, but also depends on direct damage occurring in muscle cells [183]. Kennedy's disease is linked to an expanded CAG triplet-repeat sequence in the androgen receptor gene. Consequently, the gene is translated into an elongated poly-glutamine tract in the androgen receptor protein, found longer than 38 glutamine in patients [6].

The study of SBMA presents two important advantages; first, the profound knowledge of androgen receptor structure, mechanisms and function, and, second, the mutated AR toxicity become evident only after the interaction between androgen receptor and testosterone. Indeed, Kennedy's disease occurs only in men and surgical or chemical castration ameliorates the phenotype in SBMA mice models [38,74].

The absence of testosterone lead ARpolyQ to localize in the cytoplasm where it forms a multi-heteromeric complex with chaperones preventing AR to exert its toxic effect in the nucleus. This aggregation process, initially may result to be protective, but at later stages lead to sequester also other proteins altering the physiological function of neurons and becoming toxic [42,184]. Based on this evidence, the key strategies to treat SBMA may be the prevention of the interaction between AR and testosterone, and the enhancement of the androgen receptor aggregates degradation.

To reach this goal we have already tested in vitro two different compounds obtaining promising results, therefore we decided to start a trial on a mouse model of the pathology.

We choose a knock-in mouse expressing a humanized AR in which the coding region of mouse exon 1 is exchanged for human sequence. Expression of the AR gene is under the control of the endogenous mouse regulatory machinery, resulting in expression levels similar to WT allele [75], to better mimic the real progression.

Our first analyses have been focused on the characterization of the animal model. We found symptoms of muscular atrophy, as already demonstrated by Yu in 2012[75]. Our analysis showed a mouse smaller than non-transgenic littermates, weaker and mainly with lower motor performance. Indeed, it is known that AR aggregates are present also in dorsal root ganglion neurons compromising the sensory pathways. In fact, it is also known that patients complain an alteration of their sensory performance[5]. In accordance with this alteration we reported a lower performance of SBMA mice at the rotarod test that is known to reflect the coordination between motor with sensory inputs.

PolyQ AR is sequestered into aggregates and the great part of the receptor can't reach the nucleus and interact with the target genes. This gives rise to a second category of symptoms in SBMA patient characterized by endocrine alterations leading to gynecomastia, infertility and hypogonadism [65]. In KI AR113Q models we founded a huge reduction of the weight of seminal vesicles suggesting a low AR activity, as in SBMA patients.

Kennedy's disease, unlike other neurodegenerative disease, is a pathology with a very slow rate of progression, leading at the end to the death of patients. Our model represents also this feature of the pathology, with a mortality of 61% of the animals before one year of life. The cause of death of the animals that die earlier is a block of urinary system. Urinary system alterations and deficits are also present in patients, leading to the need for catheterization.

We analyzed the mRNA expression of muscle atrophy markers; unfortunately, we were not able to find any variation in MyoG (myogenin) or MyoD gene expression, two proteins usually associated with

muscle differentiation; the expression of Pax7 was found to be increased both at 24 and 52 weeks old mice respect to NTg mice. Interestingly, an elevated Pax7 mRNA expression is indicative of an attempt to regenerate after muscle injury. Together with the observation of elevated levels of AchR, these data confirm alteration in muscle and possibly an association to denervation in skeletal muscle of AR113Q mice. To strengthen this evidence, in histological analysis we also observed that functional and molecular alterations are accompanied by morphological changes such as groups of angulated fiber, mild atrophic fibers which are once again indicative of muscle damage. All this evidence and the data reported in literature on KI AR113Q [75,184] mice confirm its reliability as disease model.

The second step of our experiment was to analyze the effects of the treatment with trehalose or bicalutamide alone or in combination.

Regarding the treatment with trehalose, it is known that enterocytes express the enzyme trehalase which is able to metabolize trehalose into glucose[139]. For this reason, we tried to measure the levels of trehalose into the blood. Furthermore, trying to demonstrate that the absorbed trehalose can pass the brain blood barrier we evaluated the levels of trehalose into the spinal cord through mass spectrometry analysis. The set-up of plasma analysis has been very difficult because trehalose is a disaccharide which may be confused with other sugars such as maltose or sucrose which are obvious "contaminants" in the plasma of mice. The analysis was easier in the spinal cord. In this tissue, we found higher trehalose concentration in treated mice than in untreated mice, confirming that the oral administration of trehalose we performed (2% in drinking water ad libitum) is effective to overcome the degradation by intestinal trehalase and the blood brain barrier. Also, the treatment with bicalutamide was effective since its blood concentration reached pharmacological active levels. Furthermore, we also collected glycemia data from all trehalose treated mice to confirm the absence of metabolism alteration since it is known from literature that patients are also characterized by metabolism alteration, diabetes and metabolic syndrome like symptoms. We did not find any alteration in glycemia levels at 24 weeks of age.

After having characterized KIAR113Q mouse model and controlled the efficacy of the route of administration, we start to treat and analyze mice observing their behavior. Surprisingly trehalose alone proved to drastically increase the performance on rotarod of SBMA mice, while the treatment with bicalutamide alone or combined with trehalose worsened mice motor performance and muscle strength, also of wild type mice. Therefore, suspecting an anti-anabolic effect of the antiandrogen bicalutamide on muscle of mice not completely developed, we decided to treat a second group of mice starting at 10 weeks of age instead of 6. In the first set of experiment, we started to treat animals with bicalutamide at 6 weeks of age. At this age, mice can reproduce but they are still in the middle of their development. The new age of beginning of treatment clearly showed better result than that obtained with the first group of treated mice. Indeed, while results obtained with grip strength meter were highly variable, data obtained with rotarod test indicated that bicalutamide treatment (alone or in combination) can ameliorates KI ARQ113 mouse motor performance to comparable levels of NTg mice.

The result previously obtained in vitro [87] showed a huge effect of the combined treatment, suggesting a synergic effect of bicalutamide and trehalose administered together. We cannot observe any synergic effect at rotarod test, because trehalose or bicalutamide single treated mice already reached the performance of untreated wild type mice. However, analyzing survival data, we found an increase of survival for all treated group, comparable between both single and combined treatments. Furthermore, the group treated with both trehalose and bicalutamide showed also a delay of disease progression, suggesting, as in vitro, a synergic effect.

At the moment, we focused our attention and analysis on gastrocnemius muscle, to find a possible molecular mechanism changed by treatments. The histological analyses did not show any significant

difference in maximum and minimum fiber diameter, but the fiber size distribution analysis suggested a greater increase of fiber size in mice treated with both compound than single treatments.
Unfortunately, we did not find any variation in mRNA expression of markers of muscle regeneration, differentiation or degeneration. About autophagy, we found a reduction in beclin1 mRNA expression at 24 weeks of age in presence of bicalutamide alone or combined with trehalose. This variation may suggest a reduction of autophagy induction, probably because of lower quantity of aggregate to degrade, since trehalose induced clearance has already reduced the AR aggregates. This is only an explanation that we must prove since at 52 week of age we don't observe again this reduction.
We also analyzed several markers of muscle metabolism and, interestingly, we found an increase of Pgc1α mRNA expression, which regulates energy metabolism and mitochondria biogenesis and function. Also, in this case we observed an increase only after the combined treatment.
In the future, we want to focus our attention on mitochondria analysis to confirm this data and clarify if and how an increase of Pgc1α may lead to an amelioration of the motor behavior.
Moreover, in the future we want to analyze dorsal root ganglia trying to find molecular changes involved in the enhancement of motor coordination after mice treatment.
Another key step will be the analysis of androgen receptor expression, aggregation, and distribution in different tissue, from muscle to spinal cord, to better understand the AR behavior after trehalose, bicalutamide and their combined treatment.

Chapter 2

Introduction

Introduction

Amyotrophic lateral sclerosis

Amyotrophic lateral sclerosis (ALS) is a neurodegenerative disorder that affects motor neurons in the brain, brainstem and spinal cord, resulting in progressive weakness and atrophy of voluntary skeletal muscles [185].

The onset age of familiar forms (fALS) is a decade earlier than the onset age of sporadic forms (sALS), which have an age-dependent incidence. The incidence of sALS is 1.89 people per 100,000/year and the prevalence is 5.2 people per 100,000. The median age of onset is approximately 60 years. The median survival ranges between 3 and 5 years from symptom onset, which varies between 55 and 65 years with a median age of 64 years [186]. Onset before age 30, called juvenile sporadic onset, is only found in 5% of cases. The life-time risk of sALS by the age of 70 has been accurately estimated to be 1 in 400. Another important consideration is that many studies have demonstrated that a slight excess of males are affected with sALS compared to females, with a male/female ratio of approximately 1.5: 1 [123].

Interestingly, despite ALS cases are widespread, in the Western Pacific ALS prevalence is 50–100 times higher than elsewhere in the world. The population of the Chamorro people of Guam and Marianas is very well known. One of the first studies performed in this population in 1957 described a genetic origin of ALS associated with Parkinsonism and dementia independent of environmental changes [187].

ALS is a complex disease characterized by several different symptoms and phenotypic heterogeneity. New theory ad results suggest that ALS phenotype could be depend from different disorder that lead to comparable end stage symptoms[188]. More than half of the ALS patients also present cognitive disorder, and some of them show characteristic features, such as progressive social, behavioral and/or language dysfunction, of frontotemporal dementia or frontotemporal lobar degeneration.

The majority of ALS is sporadic with unknown etiology, while 10% is familial with dominant inheritance. Sporadic and familial ALS are clinically indistinguishable and share several pathogenic pathways [189]. Several ALS-related genes are known; however, genetic mutations do not explain the existence of the large number of idiopathic cases. Interestingly, sporadic ALS has been linked to many environmental factors, including heavy metal toxicity and exposure to pesticides and fertilizers.

A simple view would predict that genetic variation and environmental exposure contribute to ALS, yet it is also likely that environmental exposures influence epigenetic mechanisms, influencing gene expression, to promote the onset and progression of ALS [190].

Pathogenesis

ALS is considered a multifactorial disease, therefore caused by several alterations. Indeed, modification in RNA processing, apoptosis, mitochondrial dysfunction, fragmentation of the Golgi apparatus, and metal imbalances, alterations to the motor neuron microenvironment, including accumulation of protein aggregates and glutamate excitotoxicity are observed in patients[191,192].

One of the first event observed is a molecular alteration in the neuro muscular junction, before that neurodegeneration begin. In both ALS and FTD are present alterations in neurotransmitter release. Moreover, often ALS neurons are characterized by the presence of inclusions and ubiquitinated protein aggregates[193]. Furthermore, RNA processing disruptions is also a feature of ALS, inducing alteration in RNA maturation, regulation and also in exon splicing. Despite 90% of ALS cases are

sporadic, in the past years attention was focused on familiar forms of disease, to find a common mechanism. Were found some mutation in gene, usually involved in RNA maturation. The most diffuse mutation include 20% of SOD1 gene mutation and approximately 5% have mutations in the TARDBP gene (TAR DNA binding-protein, TDP-43) [194,195].

Other genes, such as fusion in malignant liposarcoma/translocated in liposarcoma (FUS/TLS), angiogenin (ANG), the vesicle associated membrane protein-associated protein B (VAPB), senataxin (SETX), dynactin, and the most recently discovered gene, a hexanucleotide repeat expansion in C9ORF72, have been identified in ALS patients [196]. C9ORF72 gene has been defined as the most common mutation in SALS and FALS, representing up to 6% and up to 40% respectively. Other candidate genes that have been described in ALS genome association studies, such as neurofilament, peripherin, vascular endothelial growth factor (VEGF), angiogenin, survival motor neuron (SMN), and hemochromatosis (HFE) [197].

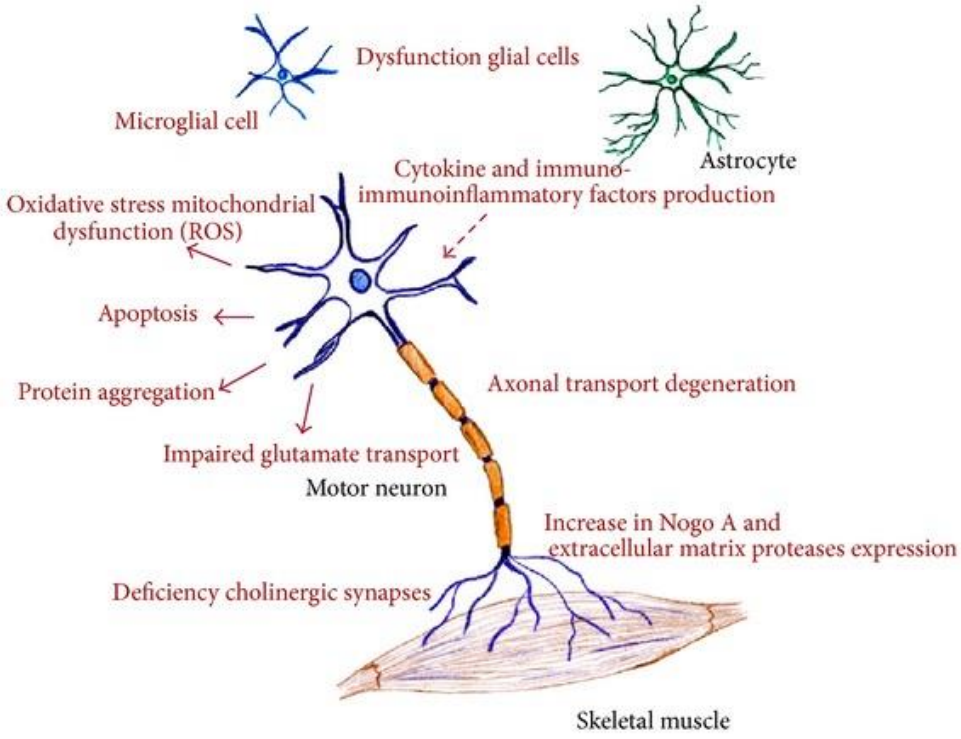

Figure 18 -Schematic representation of the different molecular pathways altered in amyotrophic lateral sclerosis. Although the trigger for neurodegeneration remains unknown, all these deregulated mechanisms prompt motor neuron death (Calvo 2014).

The first mutation discovered to be involved in ALS is a mutation in the superoxide dismutase 1 (SOD1) gene are present in 20% of fALS cases. For this reason SOD1 mutant form are widely use to generate in vivo and in vitro model and study disease features[198]. SOD1 in a physiological condition can be found in the intermembrane of mitochondria. It's an antioxidant protein with the role of converts superoxide radicals to hydrogen peroxide. More than 170 mutation were found on SOD1 gene, and the majority lead to an unknown gain of toxic function[199]. Toxicity of mutant SOD1 may also depend on a loss of function. Indeed, low level of active SOD1 can't degrade all superoxide radicals. Accumulation of

radicals lead to an oxidative stress that induce neurodegeneration[200]. Moreover mutant forms of SOD1 seems to has prion-like properties and sequester in aggregate also native forms of the protein, and also induce wild type SOD1 to misfolding[201]. Additionally, mutations in SOD1 cause misfolding of the nascent SOD1 polypeptide, promoting also the formation of aggregates, especially during oxidative stress [202].

TAR DNA-binding protein 43 (TDP-43) and RNA binding protein FUS are members of the heterogeneous nuclear ribonucleoprotein (hnRNP) family. FUS and TDP-43 are both involved in RNA maturation and transport. They are also involved in transcription, splicing and are considered a shuttle between cytoplasm and nucleus[193]. Were found more than 40 mutations in the gene coding for TDP-43 involved in ALS[203]. In the inclusion observed in ALS and FTD patient often is detectable the C-terminal region of TDP-43, the same region where almost all mutation TDP-43 are described[204]. ALS-associated mutations in FUS occur within a linkage region on chromosome 16 and affect the protein C-terminus. FUS mutations account for 5% of familial ALS [205], and most patients with FUS associated ALS have FUS-immunoreactivity cytoplasmic inclusions but the typical phosphorylated TDP-43 positive inclusions are absent [206]. FUS mutation can be linked TDP-43 alteration or share the pathway, inducing axonal defects , neurodegeneration sequestering in inclusions also the survival of motor neuron protein (SMN) [207]. This protein is necessary for the formation of spliceosome. Low level of SMN in children induce muscular atrophy and ALS like symptoms. In present of mutation, FUS and TDP-43 can't interact with their target, and they also can't regulate RNA metabolism. Therefore, in this pathological condition both FUS and TDP-43 association with RNA may lead to an abnormal phosphorylation, ubiquitination and aggregation of proteins, as well as aberrant cellular functions, and formation of stress granules [208]. Stress granules are composed of repressed translation complexes, where mRNA-binding proteins consolidate stalled mRNA. Notably, in most patients with familial ALS, TARDBP is not mutated, yet TDP-43 aggregates may be present (except in cases caused by SOD1 or FUS mutations), disrupting RNA processing and could be one trigger of degeneration [209].

The most common genetic cause of ALS and FTD is linked to chromosome 9p21, where a founder haplotype occurs in the so-called ALS–FTD locus, including the chromosome 9 open reading frame 72 (C9orf72) gene, and is associated with autosomal dominant inheritance [210]. In the affected haplotype, expansions in a large non-coding hexanucleotide (GGGGCC) repeat in the first intron of C9orf72 can reach hundreds of copies in patients presenting an FTD/ALS [211]. The exact mechanism by which the C9orf72 repeat expansion triggers disease is unclear, and several possible explanations currently exist [212]. The main mechanism suggest that the repeat expansion could potentially alter the expression of the mutant allele since the mRNA expression of C9orf72 has been observed reduced in ALS patients suggesting a kind of loss of function [196].

Despite it is known that a genetical predisposition could be crucial for ALS development other pathogenic factors are likely to be environmentally determined [213]. Moreover, seems that sporadic form of ALS may depend also on inflammatory cytokines, diet, toxic exposures and other factors that together could induce the neurodegeneration, usually interfering or inducing epigenetic changes [214]. Accumulation of mercury, a neurotoxin that inhibits SOD1 activity, in motor neurons damages the cytoskeletal components and impairs axonal transport, causing phenotypes similar to ALS[215]. Also, high level of aluminum corelate with motor neuron disease like symptoms. For instance, high level of aluminum is present in the drinking water in western Pacific region, where are reported many case of sALS. Nevertheless, it is known than high metal levels alone can't induce ALS pathogenesis[216]. ALS risk has also been linked with exposure to fertilizers, insecticides and herbicides. Occupational and home

exposure to pesticides and fertilizers tend to be higher in patients with ALS than in controls and these exposures are also associated with increased risk for developing Parkinson disease (PD) [217]. Many studies suggest also cigarette smoking contribution in ALS development, and in a faster disease progression. Moreover, also head injuries or physical trauma seems to correlate with higher risk of ALS [218].

Epigenetics, defined as structural adaptation of chromosomal regions to register signal, or perpetuate altered activity states, represents a potential convergence between genetic predisposition and environmental exposures [219]. Epigenetic is important for neuronal adaptation, plasticity and development and respond to stimuli beyond the inherited genetic outline. The possibility to switch on or switch off epigenetic mechanism, make it a possible target for ALS therapy. Epigenetic mechanisms include DNA methylation, histone remodeling, RNA editing, and expression of noncoding RNAs such as microRNAs (miRNAs) [220].

DNA methylation involves the post-transcriptional covalent addition of a methyl group to cytosine residues in DNA, leading to 5-methylcytosine formation. This modification can induce variation in the interaction between DNA and the chromatin protein and also change the transcription rates of the target gene [221]. Usually DNA I methylated in its regulatory region, for example element CpG dinucleotides, which are clustered in CpG islands or CpG island shores [222]. Methylation of DNA may be a power candidate for a possible therapy because of its nature of stable and reversible bind. Supporting a role for reversible DNA methylation in ALS, DNMT3A, the DNA-(cytosine-5)-methyltransferase (DNMT) enzyme 3A, is present in the brain and spinal cord of patients with ALS, and its overexpression prompts cell death in motor-neuron-like cells in vitro [223]. Moreover, genome wide methylation arrays have revealed hypomethylation of the ALS-related gene.

DNA methylation may also be a promising approach in ALS form characterized by C9orf72 mutation, since the hexanucleotide repeat expansion usually depend on a CpG islands hypermethylation[220]. Indeed, in some studies hypermethylation of CpG islands near C9orf72 gene is associated with the presence of the repeat expansion in tissue samples from patients with ALS. Modification in DNA methylomes, isn't a feature only of ALS, but is show also in many other neurodegenerative disease, especially if involving nucleotide repeat expansion, including spinocerebellar ataxia type 1, Friedreich ataxia, fragile X syndrome, myotonic dystrophy, PD and Alzheimer disease (AD). Together, these findings support the hypothesis that altered DNA methylation contributes to neurodegeneration in patients with ALS [224].A second epigenetic mechanism is represented by post-translational modifications of H3 and H4 histone tails via acetylation and methylation allowing chromatin to dynamically change from a highly packaged, transcriptionally inactive, conformation (heterochromatin) to a transcriptionally active state (euchromatin) [225]. The histone acetyltransferases promote acetylation of histone tails and so also transcription, while histone deacetylases remove acetylation, silencing the gene. The methyltransferases promote histone methylation. It is reported in literature that overexpression of histone deacetylases may have a detrimental role in nervous system, indeed low levels of histone acetylation are often observed in neurodegenerative disease models[226]. For instance, high level of histone deacetylases 3 causes degeneration of rat neurons and cultured HT22 hippocampal cells and a post mortem analysis reported an increase in histone deacetylases 2 mRNA and a reduction in HDAC11 mRNA in spinal cord and brain tissue from patients with ALS [227]. Thus, DNA methylation and histone modifications might be important therapeutic targets.

Several patients present also modification in RNA editing, another epigenetic mechanism. This system occur to change the some RNA nucleotide sequence, obtaining a sequence different from the original DNA[228]. The most common change in patients with ALS is the deamination of adenosine to inosine.

This modification might underlie the excitotoxic effects of variants of the AMPA (alpha-amino-3-hydroxy- 5-methyl-4-isoxazolepropionate) receptor in ALS, linked to excitotoxity theory of glutamate [229].

Also, miRNA may have an important part in ALS development, since in several disease differences in miRNA expression have been observed between normal and pathological cells or tissue, and miRNA expression seems to change during the pathogenetic progression. miRNAs are small, more or less 22 nucleotides, noncoding RNA highly conserved. miRNA are involved in regulation of several hundred targets via RNA-dependent posttranscriptional silencing mechanisms and mRNAs, and their expression can be regulated by other miRNAs[230]. miRNAs undergo a detailed maturation process that occurs in the nucleus and cytoplasm [231]. Thus, the miRNA-mediated alteration of biological pathways could partially explain complexity of ALS and other diseases [232]. In neurodegenerative pathologies, the implications of miRNA dysregulation have not been fully elucidated, and it is crucial to determine whether dysregulation occurs via transcriptional or post-transcriptional mechanisms, or both.

Alteration in miRNA biogenesis may have some important consequence and development of different diseases symptoms. For example, it is known that a loss of function in the protein Dicer1, an extremely important factor in miRNAs maturation, in rodent motor neurons lead to a SMA like phenotype[233]. Likewise, low activity of TDP-43 its lower interaction with Drosha-containing protein complexes, another main character in the miRNA maturation, lead to alteration in miRNA processing[234].

Since miRNA have an important role in many pathway, recently several studies focus their attention on miRNA expression. Interestingly data about alteration in miRNAs levels was obtained from patient biopsy. For instance, miR-663a and miR-9-5p were exclusively downregulated in patients with FUS mutations and let-7b was altered in both FUS and C9orf72 mutation carriers. Overall, the prevalence of mostly downregulated TDP-43-binding miRNAs suggests that a general defect in RNA metabolism may be present in patients with ALS. Also decreases in miR-124a are seen in the spinal cord of mutant SOD1 mice, suggesting that dysregulated glutamate transport pathways probably contribute to the exacerbation of ALS pathology [235].

Also, observation from skeletal muscle samples of patients are source of important information. Indeed, expression of miR-23a, miR-29b, miR-206, and miR-455 has been observed. miR-23a suppresses the activity of the peroxisome proliferator-activated receptor-γ co-activator (PGC)-1α, a protein involved in mitochondrial biogenesis and function, which might indicate that specific miRNAs represent therapeutic targets [236]. Similarly, miR-206 is increased in skeletal muscles of patients with ALS and in symptomatic mutant SOD1 mice, possibly owing to the effects of denervation. The loss of miR-206 accelerates disease progression in mice, probably because of its involvement in skeletal muscle development, synaptic plasticity, neuromuscular junction regeneration, and nerve to muscle communication [236].

Phenotype and symptoms

Familiar and sporadic ALS patients are characterized by motor neurons degeneration, both upper, in the cerebral cortex, and lower in the anterior horn in the spinal cord. The mains clinical features are muscle weakness, usually until death because of respiratory failure [237].

Median survival ranges from months to decades but is 19 months from diagnosis and 4/5 years from onset. The variability and overall rapid progression make it difficult to predict survival time or the timing of interventions [238].

ALS could have a limb-onset, characterized by younger patients, and usually milder symptoms of muscle dysfunction, higher breathing capacity, longer interval between symptom onset and diagnosis and longer survival than other classes of ALS[239]. In all ALS type loss of lower motor neurons lead to cramps, muscle atrophy, fasciculation and muscle weakness. Usually for the patient weakness result the most disabling features. Other symptoms are spasticity, hyperreflexia. ALS is clinically heterogeneous even among family members harboring the same gene mutation; a single etiology can lead to numerous clinical syndromes. In addition to variable progression rate, primary and secondary motor neurons are differentially affected, onset occurs in different body regions, and cognitive as well as behavioral disturbances could be mutable.

In the most of case, two-third of patients, the first symptoms occur in the limbs and usually only one arm or leg. Early features usually are weakness when lifting the arms, foot drop or difficult to walk. Bulbar- onset ALS, is characteristic of older patient than limb-onset. Often occur in women and carries a worse prognosis[197]. Primary symptoms are dysphagia, dysarthria and an atrophied fasciculating tongue, which usually lead to malnutrition and anarthria. Axial weakness can cause dropped head and kyphosis, which are associated with pain and poor balance. Eye movements are preserved in all type of ALS, until advanced stages [240].

Frontotemporal dementia (FTD) occurs in approximately 15% of people with ALS. Primary progressive aphasia, semantic dementia and the behavioral variant are subtypes of FTD that affect executive function, language, judgment, personality, and behavior [240].

It is reported that patient that present both ALS and FTD have a shorter survival[241]. Moreover, symptoms like as anxiety, depression could impair patient quality of life through poor sleep and appetite, while usually ALS patient are characterized by a rational approach the disease, and rates of depression seem to be lower than expected[242].. Pain can occasionally result from involvement of sensory neurons, and frequently from contractures, immobility, inability to turn in bed, or bedsores. As the disease advances, shortness of breath occurs during simple tasks such as dressing and eating, and eventually at rest [243].

Transforming growth factor β

Transforming growth factor β (TGF β) isoforms (TGF β1, 2, and 3) are pleiotropic factors with important roles during embryonal development and in the regulation of tissue homeostasis [244]. Overactivity of TGF β has been connected to diseases such as fibrotic conditions and malignancies [245].TGF β isoforms exert their cellular effects by binding to heterotetrameric complexes of type I and type II serine/ threonine kinase receptors. Upon formation of the receptor complexes, the constitutively active type II receptor phosphorylates and activates the type I receptor [246]. The main pathway through TGF β exert its function, involved Smad family protein. Indeed, the primary substrate of TGFβ type I receptor for the phosphorylation are Smad2 and Smad3, although non-Smad pathways are also possible. Phosphorylated Smad2/3 can interact with the common partner Smad4, which are a sort of importin and can translocate in to the nucleus. Here, the complex Smad2/3 and Smad4 can cooperate with many transcription factors and regulate their target gene transcription among the genes that are induced by TGFβ stimulation is the inhibitory (I-) Smad7, which is involved in a negative feedback mechanism to inhibit TGFβ signaling [247].

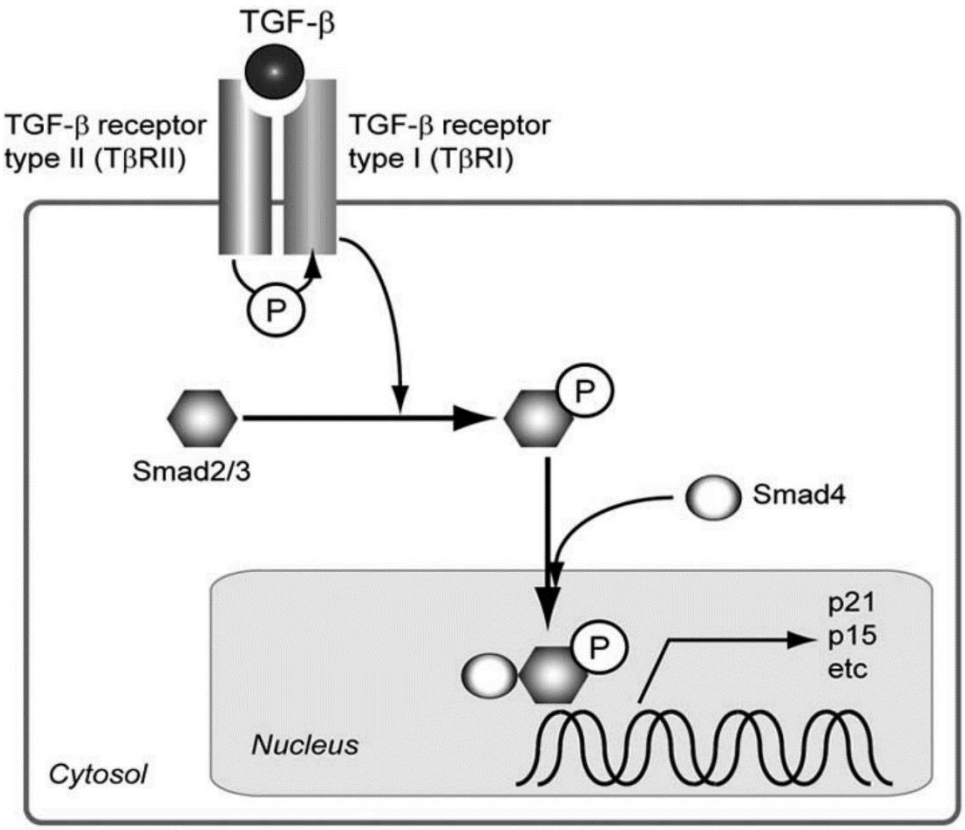

Figure 19 - TGFβ binds to type I (TGFβRI) and type II (TGFβ RII) receptors. Ligand binding induces the formation of heteromeric complexes in which TGFβRII phosphorylates TGFβRI. Phosphorylated TGFβ RI then activates the receptor-regulated Smad proteins (Smad2 and 3). Phosphorylated Smad2/3 (pSmad2/3) translocate into the nucleus, together with a common-partner Smad (Smad4), and regulate the transcription of target genes such as p21 and p15 (Katsuno 2011)

TGFβ in motor neuron and muscle

The three TGFβ isoforms are usually expressed by both neurons and glial cells, while TGFβ receptors can be find in all the central nervous system. The isoforms 2 and 3 is expressed mainly in astrocytes, whereas TGFβ 1 is present only in the choroid plexus and meninges. Moreover, immunohistochemical analysis have detected high present of TGFβ also in pyramidal neurons in the cortex and motor neurons in the brainstem and spinal cord. It is already known that TGFβ and its pathway have an important role in the survival of adult neurons[248].

For example, TGFβ 1 increased the survival and augmented choline acetyltransferase (ChAT) activity of rat primary motor neurons cultured on monolayers of cortical astrocytes. It is important to note that TGFβ has only a weak neurotrophic effect by itself, but strongly promotes motor neuron survival when administered with other growth factors such as fibroblast growth factor-2 [8]. TGFβ show also to play an important role in the growth of synapsis, release of neurotransmitter and neuron maintenance. In Aplysia, TGFβ 1 modulates synaptic functions via the induction of phosphorylation and the redistribution of the presynaptic protein synapsin and mediates long-term neuronal plasticity [249]. Taking advantage of TGFβ knockout mouse the role of TGFβ signals in central nervous system was exhaustively analyzed. In these mice, various part of the brain shows microgliosis, reduced synaptic density and at the end neuronal death. Moreover the brain shows an increased vulnerability to kainic acid toxicity[250]. Anyway, at the moment no information are available about motor neuron system in absence of TGFβ signaling[251].

TGFβ signaling is also known to regulate the functions of the neuromuscular junction (NMJ). The motor nerve terminals at the NMJ contain TGFβ receptors, and TGFβ 2 increases the postsynaptic response through the regulation of presynaptic quantal size [252]. Schwann cells express TGFβ 1, which is both sufficient and necessary to promote synaptogenesis at the NMJ.
The TGFβ-Smad2/3 pathway functions virtually in all cell types, including muscle. TGFβ -signaling has negative effects on muscle growth [253]. Myostatin, a member of the TGFβ superfamily, has gained attention as a potential therapeutic target for myopathies because genetic deletion of this factor results in increased muscle volume [254].

TGFβ in SBMA

In SBMA patient pathogenic AR interacts with the expression of TGFβRII, reducing the expression of TGFβRII in spinal motor neurons of SBMA transgenic mice (AR 97Q) before the onset of the neuromuscular symptoms[255]. Moreover, also the activity of pSmad2/3 is inhibited in the motor neurons of SBMA mice. It is known, that pSmad2/3 is particularly decreased in the motor neurons showing nuclear accumulation of pathogenic AR in SBMA models and in autopsied patient. In vitro experiments show that low level of TGFβRII, induced by siRNA, decreased the levels of nuclear pSmad2/3 while overexpression of TGFβRII seem to inhibit the cell death induced by mutant AR[255].
These results suggest that the alteration induced by mutant androgen receptor lead to cytotoxic effects on neuronal cells associated with polyglutamine-mediated cellular damage[10].
Smads protein are retrogradely transported in axons by dynein-dynactin complex, usually altered by pathogenic AR. This alteration may enhance TGFβ signal disruption in SBMA. Moreover, the muscle-specific expression of IGF-1 ameliorates motor neuron degeneration in a mouse model of SBMA. This result also supports the idea that TGFβ and Smad signaling plays a protective role in the pathogenesis of motor neuron damage in SBMA, given the cross-talk between the IGF-1 and TGFβ pathways[41].

TGFβ in amyotrophic lateral sclerosis

In ALS patients, TGFβ isoforms and their receptors are highly expressed in motor neurons, and it is observed in animal model that injection of TGFβ can reduce the motor neuron induced by axotomy. This evidence suggest that TGFβ may regulate motor neuron survival[256]. Moreover, sever analysis have detected high levels of TGFβ in plasma and serum of ALS patient, nevertheless the mechanisms that induce this increase are unclear[257]. Also the markers of TGFβ pathway, such as Smad2/3 and Smad 4, are increased in the spinal cord of ALS patient, analyzed post mortem[258]. All this evidence suggests that TGFβ may play and important role in disease pathogenesis but is not still clear if is causative or protective in motor neuron degeneration. Some study seem to suggest a detrimental role of Smads signal induced by TGFβ in ALS[259]. Indeed, active form of SMAD2 and 3 are find in Round hyaline inclusions (RHIs) in sALS motor neurons. Moreover, Smads protein colocalized with TDP-43, suggesting a sort of interference TGFβ-Smad2/3 signaling in the motor neurons of ALS cases [260]. On the other hand, neither Bunina bodies in sporadic ALS nor Lewy body like hyaline inclusions in familial ALS cases with an SOD1 mutation show immunoreactivity for pSmad2/3. TGFβ was also shown to protect neurons from glutamate-mediated excitotoxicity, a putative molecular mechanism underlying the pathogenesis of a variety of neurodegenerative disorders including motor neuron diseases.
Based on this hypothesis, the possible neuroprotection induced by TGFβ was tested as a trial therapies for ALS. For instance, in mice characterized by the expression of mutant SOD1 protein, intraperitoneal injection of TGF β2 lead to an increase of mice motor activity[261]. A deep analysis shows also an increase

of motor neuron nuclei size and axons. These evidences suggest that TGFβ, through Smads signaling, may lead to a restoration of neuro muscular activity, and increase the motor neuron survival. However, neither the lifespan nor the numbers of motor neurons in the mutant SOD1 mice are improved by TGFβ2 administration. This study seems to indicate that systemic treatment with TGFβ may protect motor neurons from toxic protein insults in the short term, although the long-term effects of TGFβ on motor neuron degeneration has yet to be determined [262].

Aim

Aim

Despite the apparent selectivity for motor neurons, multiple lines of evidence indicate that nonneuronal cell types contribute to pathogenesis and disease progression in SOD1-mediated neurodegeneration. Mutant SOD1 expression in motor neurons directs the onset and development of early disease but does not influence its progression [198]. In contrast, mutant SOD1 expression in microglia or astrocytes accelerates disease progression without affecting its onset. Expression of a dismutase-active mutant SOD1 specifically in Schwann cells was found to slow disease progression, but the role of a dismutase-inactive mutant in these cells has not been tested [198]. In the mutSOD1 mouse model, the reduction of mutant protein in skeletal muscles has no effect on disease progression [263], but the selective expression of mutSOD1 in skeletal muscle results in progressive muscle atrophy, although some reports suggest that muscle might be a direct target of mutant SOD1 toxicity. Lastly, the vasculature is damaged very early in disease, leading to loss of tight junctions between endothelial cells and microhemorrhages, but whether any of this is from mutant SOD1 within pericytes, the terminal astrocyte, or coming from cells outside the vasculature is not established [264].

Thus, toxicity to motor neurons might also derive from their target muscular cells. Furthermore, muscle dysfunction and neuromuscular junction degeneration occur long before disease onset and motoneuronal death. Indeed, there are evidence of several alterations in gene expression and regenerative potential of skeletal muscles because of the expression of mutSOD1 in muscle [265,266]. Among the genes identified as dysregulated in ALS muscle there is TGFβ 1.

There is increasing evidence that TGFβ 1 promotes neuronal survival, maintains neuronal function, and protects neurons from various types of insults such as glutamate and amyloid β. Several studies suggest that the disruption of TGFβ 1 signaling is likely to be associated with the pathogenesis of motor neuron diseases. Given that the genes regulated by TGFβ 1 are implicated in a variety of molecular events including the cell cycle, it is of importance to elucidate the precise molecular mechanisms by which impaired TGFβ 1 Smad pathway induces neuronal dysfunction and cell death [267]. The far-reaching biological effects of TGFβ 1, however, may also include the induction of neuroinflammation and the suppression of muscle regeneration. These insights suggest the necessity for the successful manipulation of the neuroprotective and neurotoxic properties of TGFβ 1 for the development of therapies for motor neuron diseases.

Unfortunately, there are no information available on TGF β 1 and its signaling pathway in ALS muscle. TGF β 1 functions are mediated by type I and type II transmembrane receptors forming a serine/threonine kinase complex. TGF β 1 binds to a homodimer of type II receptor which recruits and phosphorylates the type I receptor, which then phosphorylates Smad 2 and 3 (the receptor-regulated Smad proteins). These proteins after binding to the common Smad 4 translocate into the nucleus and act as transcription factors for target genes [268]. It is reported that in ALS patient concentration of TGF β 1 in the serum is increased, and that it is significantly higher in the cerebrospinal fluid of the patients with a long duration of illness, suggesting a neuroprotective activity of this growth factor against toxic agents, such as free radicals, or glutamate excitotoxicity [269]. Furthermore, in SOD1 mice the treatment with TGF β 2 produces an acute improvement in the motor performance, even if without preventing motor neurons loss. TGF β 1 is known to be implicated in different neurodegenerative diseases, like for example Alzheimer disease [270], and SBMA [255], both reporting an altered subcellular location of phosphorylated Smads (pSmads). An aberrant nucleocytoplasmic transport with an accumulation of cytoplasmic pSmad2/3 immunoreactivity has also been reported in ALS [259]. A dysregulation of TGF β

type II receptor (TGF β -RII) levels is present in G93A spinal cords with a TGF β-RII immunoreactivity more intense predominantly in motor neurons of the ventral horns of G93A lumbar spinal cords [271].
In this study, we decided to analyze the gene expression of TGF β 1 and of the related signaling molecules (TGF β -RII, Smad 2,3, and 4) both in the spinal cord and in the muscle of mutant human SOD1-G93A mice. We performed the analyses at pre-symptomatic and symptomatic stage, taking also in consideration mouse gender. Furthermore, we evaluated the expression of TGF β 1 also in a cohort of ALS patient. The results demonstrate that the expression of this growth factor is increased in tissues affected by ALS, both in mice and humans. The adverse effects of a TGF β 1 pathway dysregulation can reflect both on motor neurons (lack of neuroprotection) and muscle (fibrosis, deficient regeneration, cytoskeletal structure impairment).

Results

Results

TGFβ 1 gene expression

We previously showed that in skeletal muscle of presymptomatic male G93A-SOD1 mice TGFβ1 expression is upregulated compared to control male mice [266]. In addition, we found that the administration of nandrolone, an androgenic - anabolic steroid, can enhances TGFβ 1 expression in these mice [266]. For these reasons, we now evaluated whether gender influences TGFβ1 expression in the same ALS model. The study has been performed on 8 (presymptomatic, PS) and 16 (symptomatic, S) week-old G93A-SOD1 mice, compared to age-matched non-transgenic (NTg) mice, and to Tg mice expressing the human wt SOD1 (wt-SOD1). Each set of animals was divided into male and female groups, and the analyses performed on total RNA extracted from spinal cords and quadriceps muscles. In samples derived from spinal cord at the PS stage, TGFβ1 mRNA levels were reduced in G93A-SOD1 mice in both sexes, when compared to age-matched control animals (Figure 20A). The decreased TGFβ1 mRNA expression was reverted at the S stage; in fact, TGFβ1 mRNA levels were found to be increased of about 50% when compared to the levels detected at PS stage of G93A-SOD1 mice in both sexes (Figure 20A). TGFβ1 gene expression in NTg and in wt-SOD1 mice remained unchanged in all examined conditions.

On the other hand, in samples derived from the quadriceps muscles at the S stage, TGFβ1 mRNA levels were found to be greatly increased in G93A-SOD1 mice compared to the same animal at PS stage and to age-matched control mice in both sexes (Figure 20B). At the PS stage TGFβ1 mRNA levels were significantly upregulated only in male G93A-SOD1 animals (Figure 20B). Combined with our previous data, this observation corroborates the idea that at the muscular level male androgens exert a detrimental role in ALS, since they exacerbate some of the alterations induced by G93A-SOD1 [266].

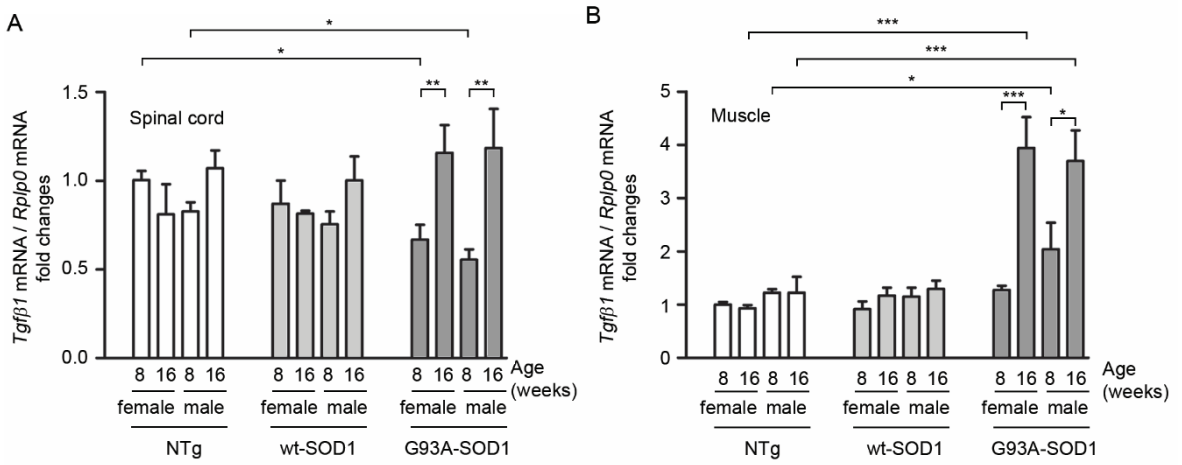

*Figure 20 - Tgfβ1 expression levels in G93A-SOD1 mice - RT-qPCR analyses of Tgfβ1 mRNA performed on total RNA extracted from spinal cord (A) or quadriceps muscles (B) of female and male mice NTg, Tg expressing either the wild type human SOD1 transgene (wt-SOD1) or the G93A mutant form of human SOD1 (G93A-SOD1)], at 8 and 16 weeks of age. Data have been normalized to Rplp0 mRNA, expressed relative to the levels determined in female NTg mice at 8 weeks of age, which are taken as internal reference, and expressed as fold changes. Each bar represents the mean ± s.e.m. of four independent replicates. *p<0.05; **p<0.01; ***p<0.001. Statistical analysis has been performed through two-way ANOVA for group comparisons followed by Bonferroni post-hoc test.*

Since data from wt-SOD1 mice did not differ from those obtained from NTg animals, we decided to use the latter model as control for subsequent analyses.
Next, we analyzed TGFβ1 protein expression (Figure 21). Western blot (WB) analysis of spinal cord lysates showed that, at S stage, TGFβ1 levels were increased when compared to PS stage both in male and female mice, even if this difference was not statistically significant (Figure 21A). In muscle at PS stage TGFβ1 levels were increased specifically in male G93A-SOD1 mice as compared to NTg mice. At the S stage, TGFβ 1 levels were increased in female and male G93A-SOD1 mice, as compared to NTg mice (Figure 21B).

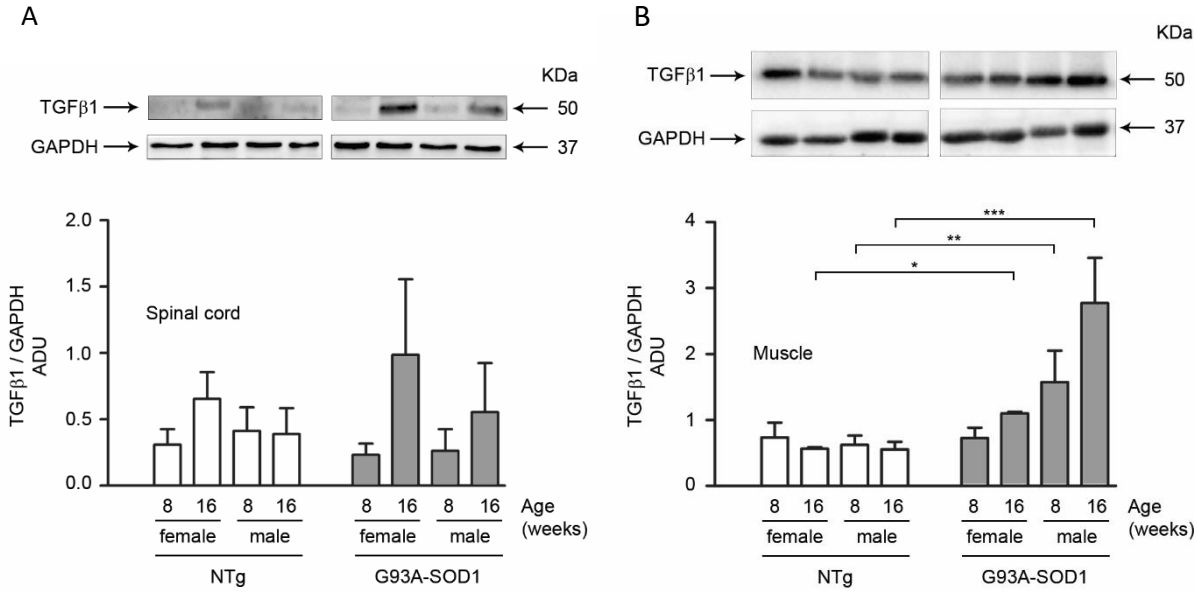

*Figure 21 - Tgfβ1 protein levels in G93A-SOD1 mice - Representative immunoblot and densitometric analysis of Tgfβ1 and GAPDH proteins extracted from spinal cords (A n=3) and quadriceps muscles (B n=4) of female and male mice NTg, Tg expressing either the wild type human SOD1 transgene (wt-SOD1) or the G93A mutant form of human SOD1 (G93A-SOD1)], at 8 and 16 weeks of age. GAPDH was used to normalize protein loading. *p<0.05, **p<0.01, ***p<0.001. Statistical analysis has been performed through two-way ANOVA for group comparisons followed by Bonferroni post-hoc test.*

We next wanted to investigate whether these differences in TGFβ1 expression observed in G93A-SOD1 mice were also present in muscle biopsies derived from a cohort of ALS patients. Demographical and clinical data of ALS patients have been reported in Table 1. The results overlapped in muscle derived from rodent and human. In fact, as reported in Figure 22 the expression of TGFβ1 mRNA was increased in sALS patients (disease effect p=0.0003), and a statistically significant gender effect (p=0.0196) was observed, with TGFβ1 mRNA levels increased by 73% in female (from 1±0.15 to 1.73±0.43), and by 106% in male (from 0.63±0.06 to 1.30±0.16). Thus, modifications of TGFβ1 levels could be related to the male higher risk of developing ALS as well as it may represent a marker of some specific alterations occurring in muscle of ALS patients.

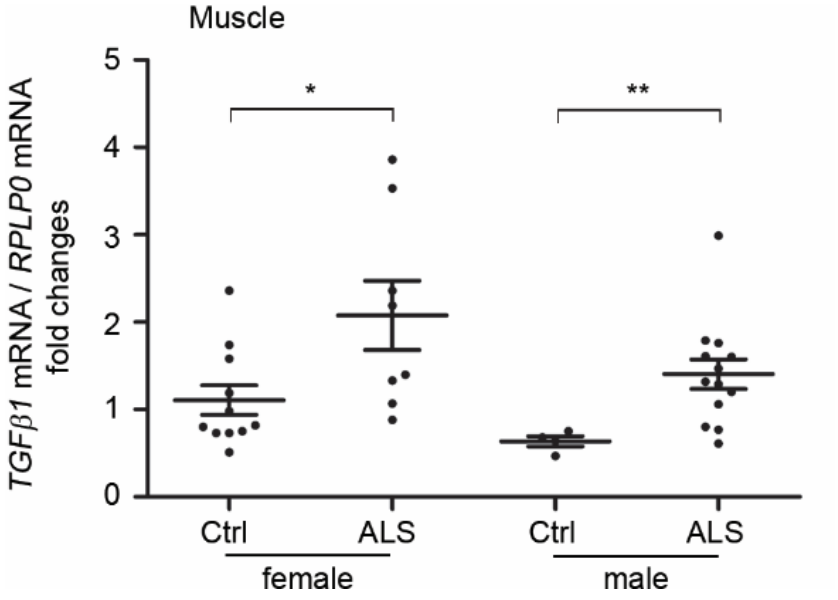

*Figure 72 - Tgfβ1 levels in patients -RT-qPCR analyses of Tgfβ1 mRNA levels from muscles biopsies of male and female human controls and ALS patients. Disease effect p=0.0003; gender effect p=0.0196; *p<0.05; **p<0.01. Statistical analysis has been performed through two-way ANOVA for group comparisons followed by Bonferroni post-hoc test.*

Table 1 - Tgfβ1 signaling is altered in the spinal cord and muscle of amyotrophic lateral sclerosis mice and patients. Abbreviations: y=years; m=months; VL=vastus lateralis; CAN=chronic neurogenic atrophy; NA=not available

Patient	**Sex**	**Age at biopsy (y)**	**Time onset (m)**	**Site of biopsy**	**Clinical diagnosis**
1	F	76	24	VL	CNA
2	F	68	6	VL	CNA
3	F	73	NA	VL	CNA
4	F	67	12	VL	Early neurogenic atrophy
5	F	71	12	VL	CNA
6	F	67	10	VL	CNA
7	F	47	36	VL	CNA
8	F	50	24	VL	CNA
9	F	56	2	Biceps brachii	CNA
10	F	58	8	VL	CNA
11	M	77	4	VL	CNA
12	M	32	12	VL	CNA
13	M	61	36	VL	Early neurogenic atrophy
14	M	61	12	VL	CNA
15	M	58	36	VL	CNA
16	M	42	12	VL	CNA
17	M	61	8	VL	CNA
18	M	53	24	VL	CNA
19	M	69	6	VL	CNA
20	M	56	2	VL	CNA
21	M	83	24	VL	CNA
22	M	62	4	Triceps	CNA
23	M	79	5	Biceps brachii	CNA
Control	**Sex**	**Age at biopsy (y)**		**Site of biopsy**	**Clinical diagnosis/source**
1	F	47		VL	Mild non-specific myopathy
2	F	73		VL	Mild non-specific myopathy
3	F	40		Gluteus	Orthopedic surgery
4	F	70		NA	Orthopedic surgery
5	F	64		VL	Within normal limits
6	F	49		Biceps brachii	Within normal limits
7	F	63		VL	Within normal limits
8	F	41		Biceps brachii	Mild non-specific myopathy
9	F	65		VL	Mild non-specific myopathy
10	M	45		VL	Mild non-specific myopathy
11	M	45		VL	Mild non-specific myopathy
12	M	50		VL	Mild non-specific myopathy
13	M	70		VL	Prevalence of type I fiber
14	M	19		VL	Within normal limits

TGFβ1 signaling

Not only TGFβ1 levels, but also its signaling pathway is dysregulated in different neurodegenerative diseases [271]. Thus, we evaluated possible variations of the mRNA levels of TGFβRII, the membrane receptor engaged by TGFβ1, both in the spinal cord and in the quadriceps muscle of PS, and S G93A-SOD1 and age-matched NTg mice. In spinal cord samples, TGFβRII expression was found increased in G93A-SOD1 at S stage in both sexes (Figure 23A). On the contrary, in quadriceps muscles, TGFβRII expression remained unchanged in all samples considered (Figure 23B).

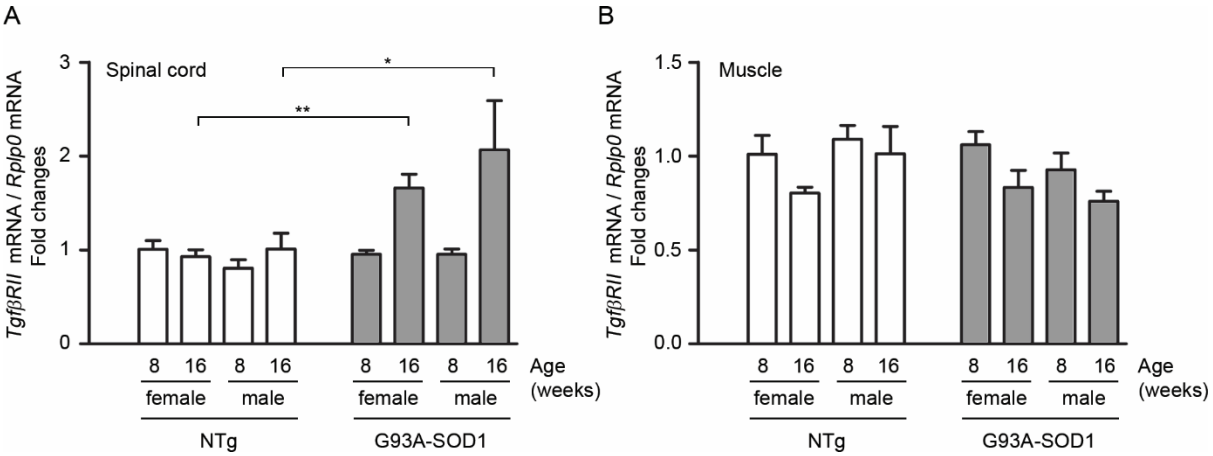

*Figure 23 - TgfβRII levels - RT-qPCR analyses of TgfβRII mRNA performed on total RNA extracted from spinal cord (A) and quadriceps muscle (B) of female and male mice [NTg (non-transgenic), and Tg mice expressing the G93A mutant form of human SOD1 (G93A-SOD1)], at 8 (presymptomatic stage) and 16 (symptomatic stage) weeks of age. Data have been normalized to Rplp0 mRNA, expressed relative to the levels determined in female NTg mice at 8 weeks of age, which are taken as internal reference and expressed as fold changes. Each bar represents the mean ± s.e.m. of four independent replicates. **p<0.01, ***p<0.001. Statistical analysis has been performed through two-way ANOVA for group comparisons followed by Bonferroni post-hoc test.*

Then, we evaluated the expression of Smads, which are the canonical intracellular mediators of TGFβ1 signaling pathway. In spinal cord samples, we found that mRNA expression of Smad2 and 3 are differently regulated; Smad2 expression diminished during disease progression (Figure 24A), while Smad3 expression remained unchanged (Figure 24B). In quadriceps muscles, the Smad2 mRNA levels diminished during disease progression (Figure 24C), showing a pattern like that found in the spinal cord. On the contrary, Smad3 mRNA levels were up-regulated at S compared to PS stage in both sexes (Figure 24D).

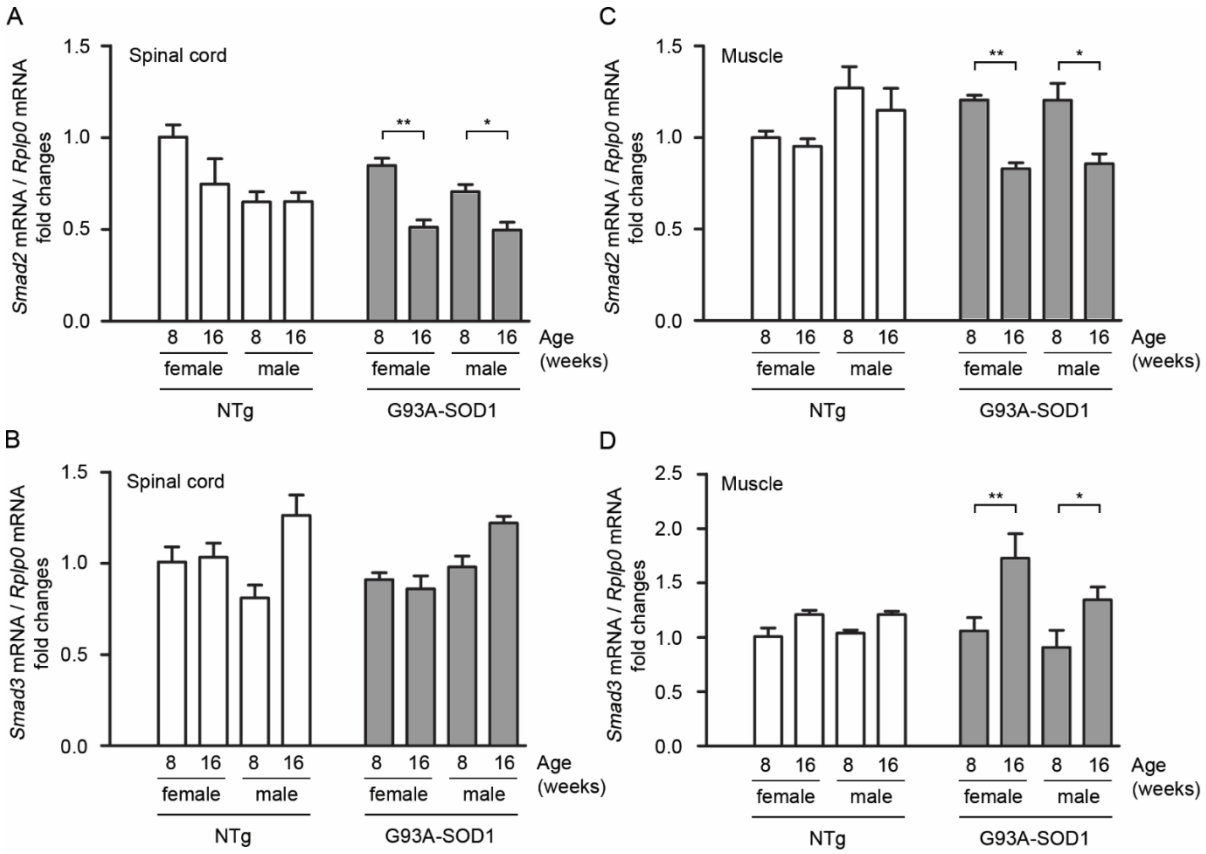

*Figure 84 – SMADs expression in ALS tissues are dysregulated - RT-qPCR analyses of the mRNA levels of Smads2 and 3 performed on total RNA extracted from spinal cord (A,B) or quadriceps muscles (C,D) of female and male mice [NTg (non-transgenic), Tg expressing the G93A mutant form of human SOD1 (G93A-SOD1)], at 8 (presymptomatic stage) or 16 (symptomatic stage) weeks of age. Data have been normalized to Rplp0 mRNA, expressed relative to the levels determined in female NTg mice at 8 weeks of age, which are taken as internal reference, and expressed as fold changes. Each bar represents the mean ± s.e.m. of four independent replicates (*p<0.05, **p<0.01). Statistical analysis has been performed through two-way ANOVA for group comparisons followed by Bonferroni post-hoc test.*

By WB assay of quadriceps muscles, we found that Smad2 and 3 protein levels are both upregulated at S stage in both sexes (Figure 25). At the PS stage, Smad2 and 3 levels were not changed in G93A-SOD1 mice respect to NTg mice, even if their levels tend to be higher in male than in female mice, in line with the variations found for TGFβ 1 expression.

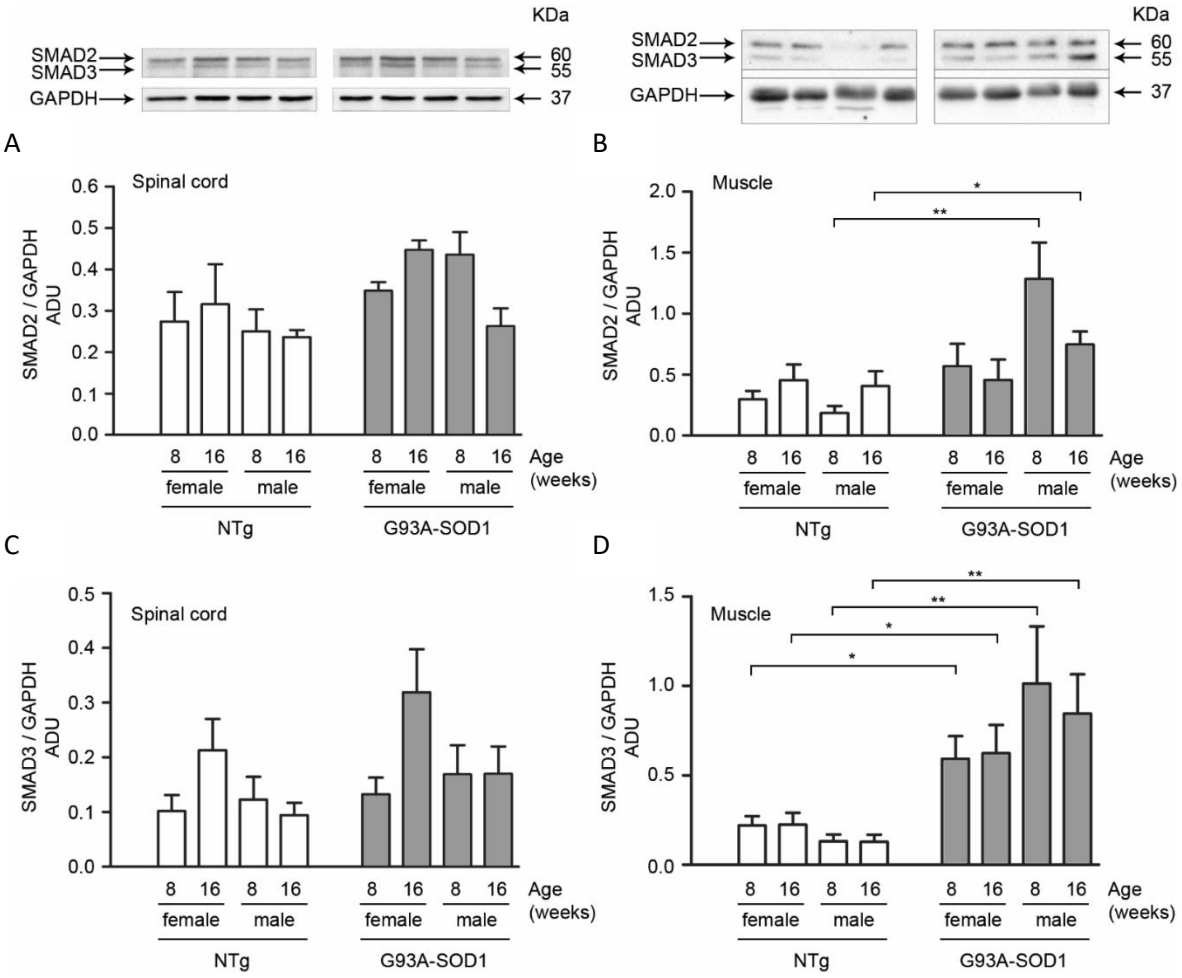

*Figure 95 – SMAD's protein levels are dysregulated -Representative immunoblot and densitometric analyses of SMAD2 and 3 extracted from spinal cords (n=3) or quadriceps muscles (n=4) of female and male NTg, and G93A-SOD1mice, at 8 or 16 weeks of age. GAPDH was used to normalize protein loading. Images have been cropped from different parts of the same gel, and full-length blots are included in the Supplementary Figure 1. *p<0.05; **p<0.01. Statistical analysis has been performed through two-way ANOVA for group comparisons followed by Bonferroni post-hoc test.*

We also evaluated variations of Smad 4, the common Smad shared among different members of the TGFβ superfamily (TGFβ s, BMPs, activins, etc.), and found that in spinal cord of G93A-SOD1 mice Smad 4 mRNA levels are gender related, being reduced during disease progression in female, but not in male samples (Figure 26A). In quadriceps, Smad 4 mRNA levels were reduced at the S stage compared to PS stage in G93A-SOD1 mice in both sexes (Figure 26B).

These data indicate that changes in Smad levels, both in muscle and spinal cord, reflect TGFβ 1 changes, and that the gene expression of the two receptors regulated Smads is differently controlled. Furthermore, also the tissue specific modulation of the TGFβ RII expression could mediate different roles of TGFβ 1 in muscle and spinal cord.

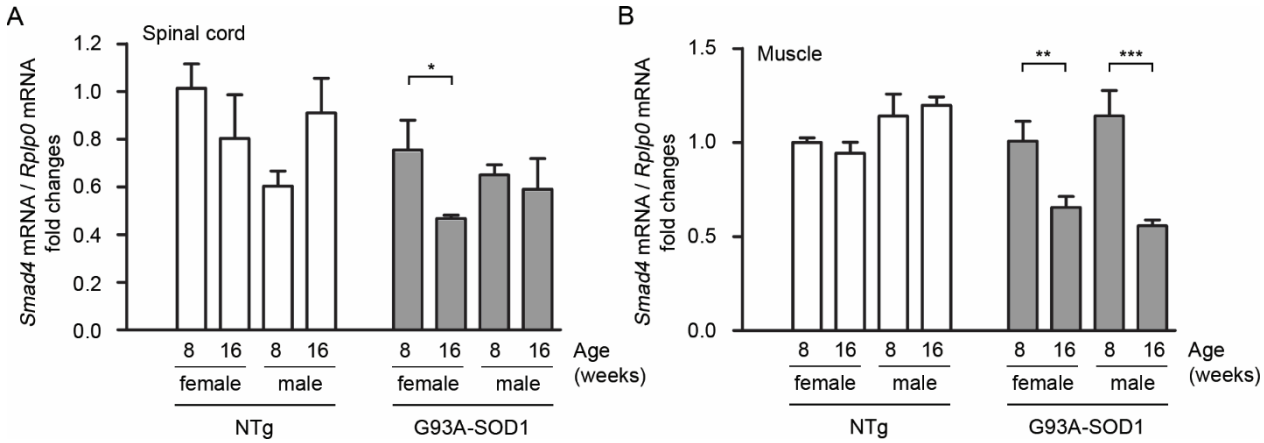

*Figure 106 – SMAD4 dysregulation in G93A mice -RT-qPCR analyses of Smad4 mRNA performed on total RNA extracted from spinal cord (A) or quadriceps muscles (B) of female and male mice [NTg (non-transgenic), and Tg expressing the G93A mutant form of human SOD1 (G93A-SOD1)], at 8 (presymptomatic stage) or 16 (symptomatic stage) weeks of age. Data have been normalized to Rplp0 mRNA, expressed relative to the levels determined in female NTg mice at 8 weeks of age, which are taken as internal reference, and expressed as fold changes. Each bar represents the mean ± s.e.m. of four independent replicates. * p<0.05, **p<0.01, ***p<0.001. Statistical analysis has been performed through two-way ANOVA for group comparisons followed by Bonferroni post-hoc test.*

TGFβ 1 in ALS muscle

To understand the impact of the upregulation of TGFβ 1 in ALS muscle, we analyzed different pathways known to mediate the effect of TGFβ1 on muscle development, and functions. It is known that TGFβ1 could suppress muscle differentiation by inhibiting the expression of muscle specific genes [266], and hamper muscle regeneration in muscular diseases, likely by inhibiting satellite cell proliferation and myofiber fusion. The normal functions of satellite cells during myogenesis are mainly regulated by the transcription factor Pax7, which in turn is known to be modulated by TGFβ. Thus, we analyzed whether Pax7 expression is altered in G93A-SOD1 mouse muscles. The results (Figure 27A) show that Pax7 mRNA levels are reduced in G93A-SOD1 mice at S stage compared to PS stage and to NTg mice and no gender effect was present. To evaluate whether this effect could be generally ascribed to myofiber denervation, we measured Pax7 expression in two other conditions characterized by motor neuron loss: i) muscles derived from acutely axotomized NTg mice; ii) muscles from a mouse model of SBMA (spinal bulbar muscular atrophy, or Kennedy's disease), which represent another type of motor neuron disease sharing some features with ALS. In our analysis we found that denervation due to axotomy (7 days) did not lead to modification of Pax7 expression, while an increased Pax7 expression was detected in muscle of SBMA mice at S stage (24 weeks) compared to age-matched control NTg mice (Figure 27B, 27C). Therefore, the reduction of Pax7 in the ALS muscle could be due to a specific action of G93A-SOD1 and could lead to an impairment of muscle regeneration.

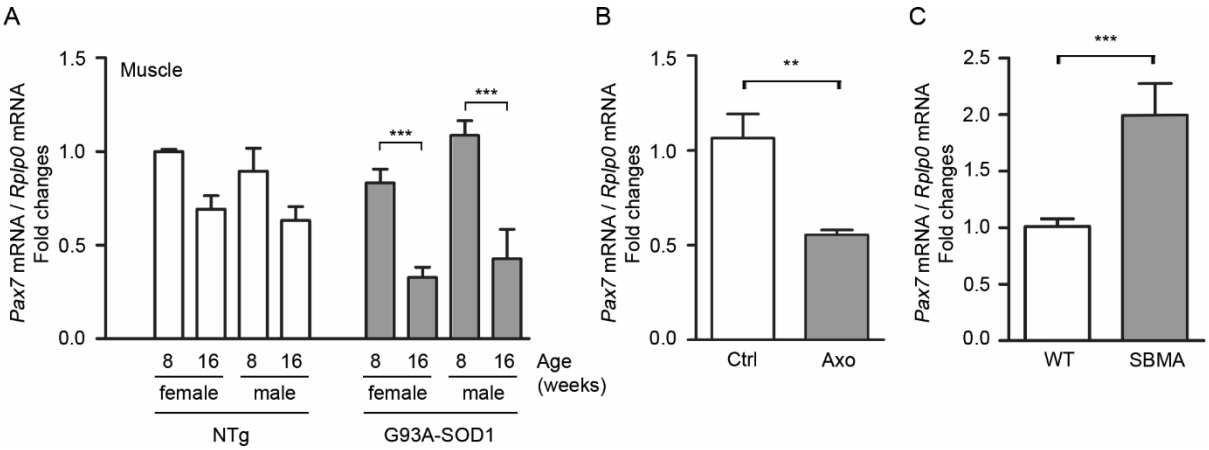

*Figure 117 – Pax7 expression in denervated muscle - RT-qPCR analyses of the Pax7 mRNA levels performed on total RNA extracted from: (A) quadriceps muscles of female and male mice [NTg (non-transgenic), and transgenic expressing the G93A mutant form of human SOD1 (G93A-SOD1)], at 8 (presymptomatic stage) or 16 (symptomatic stage) weeks of age. Data have been normalized to of Rplp0 mRNA, expressed relative to the levels determined in female NTg mice at 8 weeks of age, which are taken as internal reference, and expressed as fold changes. Each bar represents the mean ± s.e.m. of four independent replicates. ***p<0.001. (B) gastrocnemius muscles of left axotomized non-transgenic mice (Axo). Right gastrocnemius muscles of the same animals were used as controls (Ctrl). Data have been normalized to the amount of Rplp0 mRNA, expressed relative to the levels determined in control muscles, which are taken as internal reference, and expressed as fold changes. (C) quadriceps muscles of male non-transgenic (WT) mice, and of Knock In AR113Q (SBMA) mice at 24 weeks of age (corresponding to symptomatic stage). Animals were age-matched. Data have been normalized to the amount of Rplp0 mRNA, expressed relative to the levels determined in WT mice taken as internal reference, and expressed as fold changes. **p<0.01, ***p<0.001. Statistical analysis has been performed through two-way ANOVA for group comparisons followed by Bonferroni post-hoc test.*

Since in different muscle disorders, TGFβ1 promotes an aberrant differentiation of myogenic cells to myofibroblasts inducing fibrosis, and muscular fibrosis is a major pathological feature of ALS, we analyzed in G93A-SOD1 mice the mRNA expression of two extracellular matrix protein, widely considered as hallmark of fibrosis: collagen 1alpha1 (Col1α1), and fibronectin (FN). Surprisingly, we found that in muscle tissues of both G93A-SOD1 and control mice the expression of Col1α1 is massively reduced at 16 weeks of age (corresponding to S stage in G93A-SOD1) as compared to mice at 8 weeks of age (corresponding to PS stage in G93A-SOD1) (Figure 28A). The FN expression was also greatly reduced in muscle tissue from G93A-SOD1 at S stage as compared to PS stage and to age matched controls, while no differences were present in control NTg mice at the two ages considered (Figure 28B). To determine whether the effect on Col1α1 and FN gene expression is due to G93A-SOD1 or to denervation, we measured their expression in axotomized mouse muscle. Figure 28C and 28D indicates that denervation due to acute axotomy caused a dramatic increase in Col1α1 and FN expression, strongly suggesting that the reduction in the expression of these two genes in muscle of G93A-SOD1 is not due to motor neuron loss and muscle denervation, but probably is due to the presence of the G93A-SOD1 protein.

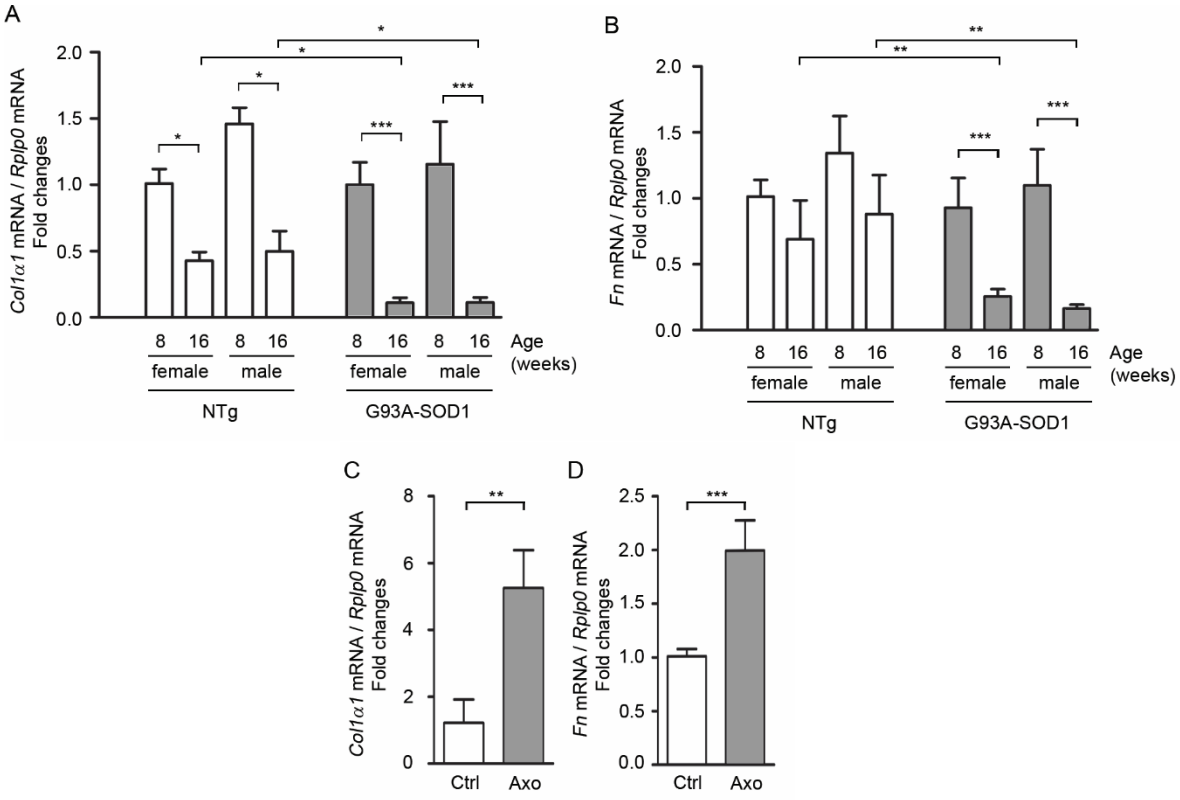

*Figure 128 – Change in Collagen 1α1 and Fibronectin -(A,B) RT-qPCR analyses of Collagen (Col) 1α1 and Fibronectin (Fn) mRNA levels performed on total RNA extracted from quadriceps muscles of female and male mice [NTg (non-transgenic), and transgenic expressing the G93A mutant form of human SOD1 (G93A-SOD1)], at 8 (presymptomatic stage) or 16 (symptomatic stage) weeks of age. Data have been normalized to the amount of Rplp0 mRNA, expressed relative to the levels determined in female NTg mice at 8 weeks of age, which are taken as internal reference, and expressed as fold changes. Each bar represents the mean ± s.e.m. of four independent replicates. *p<0.05, **p<0.01, ***p<0.001. (C, D) RT-qPCR analyses of Col1α1 and Fn mRNA levels performed on total RNA extracted from gastrocnemius muscles of left axotomized NTg mice (Axo). Right gastrocnemius muscles of the same animals were used as controls (Ctrl). Data have been normalized to the amount of Rplp0 mRNA, expressed relative to the levels determined in control muscles, which are taken as internal reference, and expressed as fold changes. **p<0.01, ***p<0.001. Statistical analysis has been performed through two-way ANOVA for group comparisons followed by Bonferroni post-hoc test.*

To validate this hypothesis, we analysed the expression of Col1α1 and FN in an in vitro model of ALS muscle, based on C2C12 cells transiently transfected with G93A-SOD1 [266]. Accordingly, with our previous results, we found that TGFβ1 expression is increased in C2C12 expressing G93A-SOD1 as compared to control C2C12 cells (pcDNA3) (Figure 29A); indeed, in the same experimental conditions the presence of G93A-SOD1 protein reduced Col1α1 and FN mRNA levels (Figure 29B, 29C). No effect was detected in cells transfected with the wt-SOD1 (Figure 29).

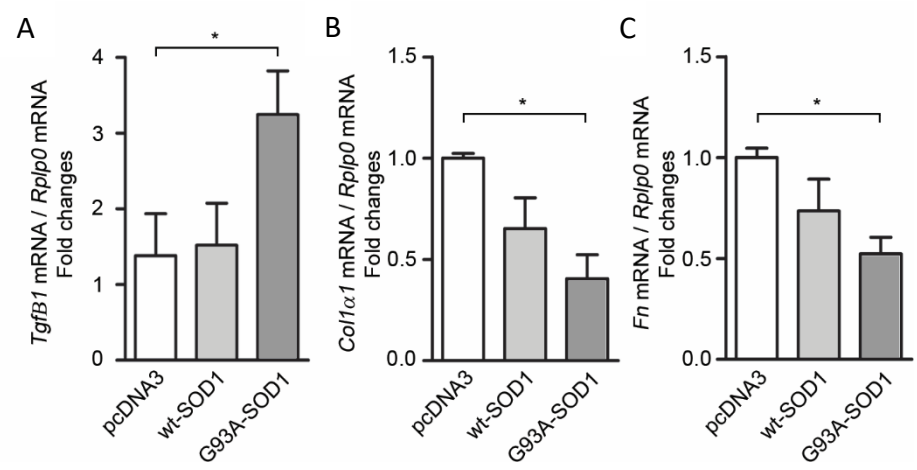

*Figure 29 - Tgfβ1, Col1α1 and Fn dysregulation in C2C12 - RT-qPCR analyses of Tgfβ1, Col1α1 and Fn mRNAs, performed on total RNA extracted from C2C12 cells transfected with wild type human SOD1 (wt-SOD1) or G93A mutant form of human SOD1 (G93A-SOD1). Data have been normalized to the amount of Rplp0 mRNA, expressed relative to the levels determined in control cells (mock transfected, pcDNA3), which are taken as internal reference, and expressed as fold changes. Each bar represents the mean ± s.e.m. of four independent replicates. *p<0.05. Statistical analysis has been performed through two-way ANOVA for group comparisons followed by Bonferroni post-hoc test.*

Discussion

Discussion

In the last few years it has become clear that ALS is not a cell autonomous disease of motor neuron, but other cell types are involved and modulate ALS onset and progression. Based on other and our previous works, muscle cells could also be a primary target of G93A-SOD1 mediated toxicity [266]. Our data confirm and expand those previously obtained on the expression of TGFβ 1 in ALS affected tissues. Since gender is a risk factor for developing ALS, here we differentially analyzed and compared female and male tissues. The results indicate that TGFβ 1 is highly expressed in muscle at the S stage both in female and male mice, and that the increase of TGFβ 1 mRNA levels takes place much earlier in male than in female (at the PS stage). Since TGFβ 1 is an androgen responsive gene, it is possible to hypothesize that the increased risk of ALS in males is linked to the higher serum levels of male sex steroids. This hypothesis is corroborated by the fact that TGFβ 1 gene expression resulted to be increased in muscle biopsies of ALS patients and that, also in this case, the increase is greater in male than in female. Other Authors have studied the involvement of TGFβ 1 in ALS disorder. High TGFβ 1 plasma levels have been detected in ALS patients, with a significant positive correlation with disease duration [257], while other results reported that expression levels of endogenous TGFβ 1 mRNA at the end stage negatively correlates with the survival time of G93A-SOD1 mice. All these results indicate that TGFβ 1 might be a potential biomarker of ALS progression in males and females, might predict disease onset in fALS males.

With regards the specific role of TGFβ 1 in ALS, it must be recalled that in the nervous system TGFβ 1 is neuroprotective [272]; indeed, a reduced neuronal TGFβ signaling is implicated in age-dependent neurodegeneration [273]. Conversely, in muscle an excessive presence of TGFβ 1 is considered a harmful factor. Gene expression analysis in the spinal cord of mice expressing G93A-SOD1 showed decreased TGFβ 1 levels at the PS stage, possibly indicating a lack of neuroprotective effects in the early stages of disease leading to the death of motor neurons at later stages. In ALS mouse spinal cord, TGFβ 1 mRNA levels have a huge increase with disease progression that can be explained with the development of reactive astrogliosis [271]. Indeed, astrocyte-derived TGFβ 1 accelerates ALS progression, while the same parameter is counteracted by the administration of a TGFβ signaling inhibitor [36]. Furthermore, the effects of TGFβ 1 are also mediated by the inhibition of microglial activation with the consequent reduction of neuroprotective properties of microglial cells [10].

The first step of TGFβ 1 signaling pathway is the binding to the type II receptor. Our study indicated that the TGF β-RII mRNA levels are increased in the spinal cord at the S stage but remained unchanged in the muscle. These results agree with previous studies showing a high TGFβ-RII immunoreactivity in spinal cord motor neurons of mice expressing G93A-SOD1 which correlates with reactive astrogliosis and disease progression [271]. The higher TGFβ-RII expression might also correlate with dysregulation of the intracellular pathway mediating TGFβ effects. In fact, we found a diminished Smad2 expression in the spinal cord of ALS mice. The regulation of Smad2 and 3 in the muscle seems to be more complex. In fact, while Smad2 and 3 proteins are both increased at the S stage, data on their gene expression are divergent being Smad2 mRNA reduced, and Smad3 mRNA increased. Although Smad2 and 3 are usually grouped together as receptor-activated Smads, Smad2 is unable to bind DNA directly as Smad3. Furthermore, in some systems Smad2 and Smad3 are antagonists, suggesting that their relative levels determine different biological response (Labbe, 1998). Additionally, it has been reported a decrease of Smad2, accompanied by an activation of Smad3, in culture of hepatic cells becoming fibrogenic. Thus, Smad2 and Smad3 could mediate different cellular responses, and this is also supported by data showing that Smad2 knockout is lethal at the embryonic stage, whereas Smad3

knockout mice survive to adulthood. Additionally, to be imported into the nucleus the phosphorylated Smad3 associates with importin-beta in the cytoplasm, whereas the phosphorylated Smad2 is autonomously imported into the nucleus. Seems that a disturbed Smad nuclear translocation may impair the neuroprotective TGFβ signaling, leading to neurodegeneration. The common Smad 4 is the protein that shuttles receptor regulated Smads into the nucleus, even if Smad4 independent effects of TGFβ have been described. We found a decreased Smad 4 expression both in spinal cord and muscle, suggesting a further site of dysregulation of TGFβ intracellular signaling.

TGFβ profoundly influences the differentiation of myoblasts inhibiting the induction of muscle-specific gene expression and myotube formation [246]; this suggests that it targets one or more master regulators of myogenesis, such as Pax7. Indeed, an impaired regenerative capacity concomitant with a progressive loss in satellite cell number has been reported in Pax7-null mice [214]. Notably, we found that Pax7 expression is decreased in muscle of ALS mice at the S stage, and this may suggest that the myogenic potential and the ability for tissue repair of ALS muscle is impaired. This hypothesis agrees with a previous work on G93A-SOD1 mice and has been recently confirmed in patient biopsies showing a reduction in mRNA levels of satellite cells and early myogenic markers. The effect on Pax7 gene is a specific feature of ALS disease, since denervation induced by axotomy does not alter Pax7 mRNA levels. In agreement, Pax7 gene expression is increased in muscle of the mouse model of SBMA, another disease characterized by progressive death of motor neuron and denervation.

TGF β 1 can promote an aberrant differentiation of myogenic cells to myofibroblasts inducing fibrosis [118], which is a pathological feature of ALS. Col1α1 gene expression is age dependent in NTg mice, in line with the normal age-related rearrangement of skeletal muscle fibers and of the connective tissue network. Surprisingly, in ALS mice we found that Col1α1, and FN mRNA levels were much lower at S than at PS stage. This effect is not due to denervation, since in axotomized muscle the expression of these two extracellular matrix proteins is highly increased. On the other hand, Col1α1, and FN mRNA reduction could be due to the decline in the ability to move of mice during disease progression, since poor mobility downregulates total muscular collagen synthesis [274]. Furthermore, in the ALS muscle cellular model the expression of the G93A-SOD1 lead to decreased levels of Col1α1, and FN mRNA, indicating that mutant SOD1 could be directly responsible of the Col1α1, and FN gene expression modulation. It is possible that the decrease in collagen expression is an attempt to prevent collagen accumulation that leads to fibrosis; a similar mechanism has been proposed in hepatic cells. It has been demonstrated that TGFβ is able to promote Col1α1 transcription through specific responsive sequence, therefore it remains to understand why the levels of Col1α1 mRNA, and of FN, are reduced in the presence of high levels of TGFβ 1. A possible explanation comes from a work demonstrating that high doses of TGFβ potently suppress Col1α1 transcription via the transcription factor CUX1 [275].

In conclusion, data in this second chapter indicate that TGFβ 1 and its signaling pathway are altered in ALS affected tissues even at PS stage of disease. In spinal cord, the reduction of TGFβ 1 expression could reflect a lack of its neuroprotective effect. In muscle, the higher levels of TGFβ 1 could contribute to muscular atrophy since this correlates with an altered differentiation of satellite cells, and changes in extracellular matrix production. Androgen sensitivity of TGFβ 1 and its higher levels in males could also be a possible explanation of their higher risk of developing ALS. All together these data increase the possibilities of new and complementary therapies to treat the disease or, at least, to delay muscle wasting. Furthermore, TGF β 1 could also be proposed as a biomarker of ALS disease.

Materials and methods

Materials and methods

ANIMAL MODELS

Mice were maintained according to the institutional guidelines, that follow national (D.L. 26/2014) and European laws and policies (2010/63/UE). All the experimental procedures were approved by the Italian Ministry of Health. All the animals were kept under controlled temperature and humidity conditions, with dark/light cycles of 12 h. Food and water were supplied ad libitum.

ALS model

BL6JLTg(SOD1)2Gur/J (Stock number 002297, The Jackson Laboratory) male mice or BL6JL-Tg (SOD1-G93A)2Gur/J (Stock number 002726, The Jackson Laboratory) male mice were crossed with wild type female mice purchased (Stock number 100012, Charles River) or obtained in house by crossing C57Bl/6J female and SJL male mice. All the experiments were performed in mice coming from the F1 generation of the cross described above. Non-transgenic (NTg) littermates were used as controls. The genotyping of the litters was conducted by PCR on tail biopsy DNA as previously described[182,266]. To evaluate disease stages, starting from the 8th week of age and twice a week, mice were tested for the deficits by rotarod, and hanging wire by the same operator as previously described (Aggarwal et al., 2014). Body weight loss was also monitored. Disease onset was set as the time at which the mouse permanently starts to lose body weight. Four mice per group were anesthetized with isoflurane and sacrificed at 8 or 16 weeks of age, corresponding to presymptomatic (PS) or symptomatic (S) stage of disease. Spinal cord and quadriceps muscles were rapidly collected after the sacrifice, snap frozen on dry ice, and conserved at -80°C until extraction.

SBMA model

Generation and genotyping of mice containing the exon 1 of the human *androgen receptor* gene with 113 CAG repeats (AR113Q mice) has been previously described [75,184]. Mice genetic background was C57Bl/6J. Females carrying one copy of AR113Q in the X chromosome were crossed with C57Bl/6J mice to maintain the colony. Genotypes were verified by PCR on tail DNA. Symptomatic mice of 24 weeks of age were anesthetized with isoflurane and sacrificed; quadriceps muscles collected, snap frozen, and maintained at –80°C.

Denervation model

Three-months-old NTg male mice were anaesthetized with ketamine and xylazine. An incision was made through the skin and the upper region of the left gluteal muscle to expose the sciatic nerve, which was then cut 1–2 mm distal to the sciatic notch. The proximal portion of the nerve was sutured to prevent errant re-innervation of the gastrocnemius muscle. Right sciatic nerve was exposed and utilized as sham internal control in each animal. Mice were sacrificed 7 days later, and gastrocnemius muscles collected, snap frozen and conserved at -80°C.

Human samples

All evaluations involving anonymized controls and patients and experiments involving muscle tissue samples were performed in accordance with relevant guidelines and regulations and were approved by the University of Padova Ethics Committee for Clinical Experimentation. Written informed consent to study procedures was obtained from each patient, or his legal guardians. Confidentiality was guaranteed by assigning a study code to each patient. Bioptic samples were conserved in a genetic biobank supported by Telethon, Italy, fully complying with highest quality standards, according to rigorous ethical principles complying with Italian laws and International Recommendations. All patients were clinically affected with the definite ALS diagnosis, according to the revised El Escorial criteria[276] and were followed at Neuromuscular Clinic of the University of Padova. Supplementary table 1 reports demographic and clinical data of twenty-three ALS patients enrolled (ten females and

thirteen males). Control bioptic samples were obtained from healthy aged-matched subjects (nine females and five males), who had undergone hip arthroprosthesis. Muscle biopsies were obtained using an open biopsy procedure and 100–200 mg of muscle tissue was collected. All biopsies were immediately frozen in liquid nitrogen for histopathology and biochemical analyses and stored at −80°C until analyzed. Total RNA was isolated from frozen muscle biopsies using TRIzol Reagent (Sigma-Aldrich), according to the manufacturer's instructions.

Cell cultures

The myoblast C2C12 cell line was originally obtained from the American Type Culture Collection (Rockville, MD, USA). The cell line was routinely maintained in high glucose (4500 mg/L) Dulbecco's modified Eagle's medium (Biochrom KG, Berlin, Germany) supplemented with 4 mM glutamine, 1 mM sodium pyruvate, 100 U/mL penicillin, 100 µg/mL streptomycin, and 10% fetal bovine serum (Thermo Fisher Scientific, Monza, Italy) at 37°C with 5% CO_2. The plasmids pcDNA3-wtSOD1, pcDNA3-G93ASOD1[266], were transiently transfected into C2C12 using Lipofectamine 2000™ (Thermo Fisher Scientific) following Manufacturers' instructions. Briefly, 60,000 cells/ml were plated in 12-well dishes, and transfected with 1,6 µg of DNA, and 4 µL of Lipofectamine/well. Controls were mock transfected. Cells were harvested for RNA isolation at 48 h after transfection.

WESTERNBLOTTING ASSAY

Vivo

Total proteins from muscles were extracted in 1% SDS using the standard TRI Reagent protocol, in accordance with the manufacturer's protocol (Sigma-Aldrich). Protein concentration was determined with the bicinchoninic acid method (BCA assay, EuroClone, Pero, Milan, Italy). Western immunoblot analysis was performed on 12% sodium dodecyl sulfatepolyacrylamide gel electrophoresis loading 15 µg of total proteins. Samples were then electrotransferred to nitrocellulose membranes (Trans-blot, Bio-Rad Laboratories, Hercules, CA, USA) using a semi-dry transfer apparatus (Trans-Blot® Turbo™ Transfer System, Bio-Rad). Nitrocellulose membranes were treated with a blocking solution containing 5% non-fat dry milk in TBS-T overnight and then incubated with the primary antibodies overnight at 4 °C:

rabbit polyclonal anti-phospho-Smad2 (Calbiochem, dilution 1:1000)
rabbit polyclonal anti-phospho-Smad3 (Merck Millipore, diluition 1:1000)
mouse monoclonal anti-TGFβ1 (R&D, diluition 1:1000)
rabbit polyclonal anti-GAPDH (Santa Cruz Biotechnology, dilution 1:1000).

Immunoreactivity was detected using the following secondary peroxidase-conjugated antibodies:
goat anti-rabbit (Santa Cruz Biotechnology diluition 1:5000) was used to identify anti-phospho-Smad2, anti-phospho-Smad3 and anti-GAPDH; goat anti-mouse (Santa Cruz Biotechnology diluition 1:5000) was used to identify the anti-TGFβ1 antibody.
The immunoreactive regions were then visualized using the enhanced chemiluminescence detection kit reagents (ECL; GE Healthcare). A ChemiDoc XRS System (Bio-Rad) was used for the image acquisition. Optical intensity of samples assayed was detected and analyzed using the Image Lab software (Bio-Rad).

Vitro

For western blot assays, C2C12 cells were plated in 12-well multiwells at 65 000 cells/mL density. Transient transfections were performed transfecting 1 µg of pCDNA3, wt or G93A-SOD1 plasmids transfected 4 µL of Lipofectamine 2000.
After 48 h from transfection, cells were harvested and centrifuged 5 min at 100 *g* at 4°C; the pellets of cells were resuspended in PBS (added of a protease inhibitors cocktail, Sigma Aldrich) and

homogenized using slight sonication. Total proteins were determined with the bicinchoninic acid method (BCA assay, Pierce, Rockford, IL, USA). Western immunoblot analysis was performed on 12% sodium dodecyl sulfatepolyacrylamide gel electrophoresis loading 15 µg of total proteins. Samples were then electrotransferred to nitrocellulose membranes (Trans-blot, Bio-Rad Laboratories, Hercules, CA, USA) using a semi-dry transfer apparatus (Trans-Blot® Turbo™ Transfer System, Bio-Rad). Nitrocellulose membranes were treated with a blocking solution containing 5% non-fat dry milk in TBS-T overnight and then incubated with the primary antibodies overnight at 4 °C:

rabbit polyclonal anti-phospho-Smad2 (Calbiochem, dilution 1:1000)
rabbit polyclonal anti-phospho-Smad3 (Merck Millipore, diluition 1:1000)
mouse monoclonal anti-TGFβ1 (R&D, diluition 1:1000)
rabbit polyclonal anti-GAPDH (Santa Cruz Biotechnology, dilution 1:1000).

Immunoreactivity was detected using the following secondary peroxidase-conjugated antibodies:
goat anti-rabbit (Santa Cruz Biotechnology diluition 1:5000) was used to identify anti-phospho-Smad2, anti-phospho-Smad3 and anti-GAPDH; goat anti-mouse (Santa Cruz Biotechnology diluition 1:5000) was used to identify the anti-TGFβ1 antibody.
The immunoreactive regions were then visualized using the enhanced chemiluminescence detection kit reagents (ECL; GE Healthcare). A ChemiDoc XRS System (Bio-Rad) was used for the image acquisition. Optical intensity of samples assayed was detected and analyzed using the Image Lab software (Bio-Rad).

mRNA EXTRACTION

Tissues (ALS)

Total RNA from frozen spinal cords or muscles was extracted using the standard TRI Reagent protocol based on the method developed by Chomczynski and Sacchi (Chomczynskiand Sacchi, 1987).
RNA was subsequently extracted in accordance to manufacturer's protocol (Sigma-Aldrich). The precipitated RNA was dissolved in RNase-free water. Total RNA (1µg) was treated for 15min at room temperature with 1U of DNaseI (SigmaAldrich). Samples were reverse-transcribed using the HighCapacity cDNA Reverse Transcription Kit (Life Technologies Corporation, Carlsbad, CA, USA) according to the manufacturer's instructions.

Tissues (SBMA)

Total RNA from frozen spinal cords or muscles was extracted using the standard TRI Reagent protocol based on the method developed by Chomczynskiand Sacchi (Chomczynskiand Sacchi, 1987) and purified using Direct-zol RNA miniprep Plus kit (ZYMO RESEARCH) according to the manufacturer's instructions.
RNA was subsequently extracted following manufacturer's protocol (Sigma-Aldrich). The precipitated RNA was dissolved in RNase-free water. Samples were reverse-transcribed using the HighCapacity cDNA Reverse Transcription Kit (Life Technologies Corporation, Carlsbad, CA, USA) according to the manufacturer's instructions.

Cell cultures

C2C12 were plated in 6-well multiwells at 65 000 cells/mL density. After 24 h, cells have been transfected with 2 µg of plasmids coding for pCDNA3, wt or G93A-SOD1 with addition of 8 µL of Lipofectamine 2000 for each sample. After 24 h, cells were harvested and centrifuged 5 min at 100 *g* at 4°C; the pellets were resuspended in 300 µl of TRI Reagent (Sigma-Aldrich) and RNA isolated according to manufacturer's instruction. RNA quantification was carried out by absorbance at 260 nm. Total RNA (1 µg) was treated with DNAse (Sigma-Aldrich), and reverse transcribed into cDNA using the

High-Capacity cDNA Archive Kit (Life Technologies Corporation) according to the manufacturer's protocol

mRNA EXPRESSION ANALYSIS

Primers for selected genes were designed using the program Primer 3 and purchased from Eurofins MWG Operon (Ebersberg, Germany) with the following sequence:

mRplP0: 5'-GGT GCC ACA CTC CAT CA-3' (forward), 5'-AGG CCT TGA CCT TTT CAG TAA GT-3' (reverse)

AchR: 5'-GTG CTG GGC TCT TTC ATC TC -3' (forward), 5' -TTC TGT GCG CGT TCT CAT AC -3' (reverse)

MyoD: 5' -GGC TAC GAC ACC GCC TAC TA -3' (forward), 5' -GTG GAG ATG CGC TCC ACT AT -3' (reverse)

Myogenin: 5' -GGG CAA TGC ACT GGA GTT -3' (forward), 5' -CAC GAT GGA CGT AAG GGA GT -3' (reverse)

mPax7: 5'-GTA TGG CCA AAC TGC TGT TGA T-3' (forward), 5'-GGA GTG TTC CCC AAG CTT CA-3' (reverse)

PGC1-α: 5' -GGA ATG CAC CGT AAA TCT GC -3' (forward), 5' -TTC TCA AGA GCA GCG AAA GC-3' (reverse)

BAG3: 5' -ATG GAC CTG AGC GAT CTC A -3' (forward), 5' -CAC GGG GAT GGG GAT GTA -3' (reverse)

p62/ SQSTM-1: 5' -AGG GAA CAC AGC AAG CT -3' (forward), 5' -GCC AAA GTG TCC ATG TTT CA -3' (reverse)

Beclin1: 5' -TGA AAT CAA TGC CTG GG-3' (for- ward), 5' -CCA GAA CAG TAT AAC GGC AAC TCC -3' (reverse)

HSPB8: 5' -ATA CGT GGA AGT TTC AGG CA -3' (forward), 5' -TCC TTT GAC CTA ACG CAA CC -3' (reverse)

mTGFβ1: 5'-GAA GGA CCT GGG TTG GAA GT-3' (forward), 5'-CGG GTT GTG TTG GTT GTAGA-3' (reverse)

mTGFβRII: 5'-AGT CGT TCA AGC AGA CGG AT-3' (forward), 5'-CCT TCA CTT CTC CCA CAG CAT T-3' (reverse)

mSmad 2: 5'-GTA AGA TCC CAC CAG GCT GTA A-3' (forward), 5'- CTC CCC AGC CCT TCA CAA AA -3' (reverse)

mSmad 3: 5'-CGG TCA AGA GCT TGG TGA AGA A-3' (forward), 5'-TCC AGT GAC CTG GGG ATG GTA A-3' (reverse)

mSmad 4: 5'-CAA GTC AGC CGG CCA GTA TT-3' (forward), 5'-CCA GGT AGT GCT GTT ATG-3' (reverse)

mCollagen 1α1: 5'-CGG CTC CTG CTC TTA G-3' (forward), 5'-GGT TTC CAC GTC TCA CCA TT-3' (reverse)

mFibronectin: 5'-GAC CAC TCC CAA AAA TG-3' (forward), 5'-TTG CAA ACC TTC AAT GGT CA-3' (reverse)

hRplP0: 5′-GTG GGA GCA GACAAT GTG GG-3′ (forward), 5′-TGC GCA TCA TGG TGT TCT TG-3′ (reverse)

hTGFβ1: 5′-GCA GGG ATA ACA CAC TGC AA-3′ (forward), 5′-GGT GGC CAT GAG AAG CAG-3′ (reverse)

Real-time PCR was performed using the CFX 96 Real-Time System (Bio-Rad, Hercules, CA, USA) in a 10 µl total volume, using the iTaq SYBR Green Supermix (Bio-Rad), and with 500 nm primers. PCR cycling conditions were as follows: 94°C for 10 min, 40 cycles at 94°C for 15 s and 60°C for 1 min. Melting curve analysis was performed at the end of each PCR assay as a control for specificity. Data were expressed as C_t values and used for the relative quantification of targets with the $\Delta\Delta C_t$ calculation. To exclude potential bias due to averaging data transformed through the equation $2-\Delta\Delta Ct$ to give *N*-fold changes in gene expression, all statistics were performed with ΔC_t values.

GRIP-STRENGTH ANALYSIS

Mice were brought to the testing room and allowed to acclimatize for 10 minutes. A Grip Strength Meter (Ugo Basile) was used to measure forelimb grip strength. The grip strength meter was positioned horizontally, and mice were held by the tail and lowered toward the apparatus. Mice were allowed to grasp the smooth metal pull bar with their forelimbs only and then were pulled backward in the horizontal plane. The force applied to the bar at the moment of grasping release was recorded as the peak tension (grams). The test was performed weekly, repeated five consecutive times within the same session, discarding the highest and the lowest values from the five trials and recording the mean value of the three remaining measurements.

ROTAROD ANALYSIS

The rotarod test is one of the oldest used in assessing the effects of a drug on animal behavior. It provides a rapid and simple first estimation of any effect on neuromuscular coordination. The rotarod consists of a circular rod turning at a constant or increasing speed. Animals placed on the rotating rod try to remain on it rather than fall onto a platform 15 cm below. This test is easily automated with several animals being tested simultaneously on the same rod. Vertical barriers are used to separate the animals from one to another. Locomotor coordination on the rotarod is not a measure of muscle strength but an initial screen for neuromuscular impairment.

Two trials were performed weekly using the Ugo Basile ROTA-ROD for mice (Ugo Basile). Mice were put on the rod at speed of 30 rpm for a maximum period of 600 s, and the best performance for each mouse was recorded

HISTOLOGICAL ANALYSIS

Tissues (seminal vesicle and muscle) were collected immediately after euthanasia, muscle were flash-frozen in isopentane precooled, and stored at − 80 °C until further processing. Frozen muscles were embedded in optimal cutting temperature (OCT) compound (Tissue Tek, Sakura, Torrance, CA), and cross sections (40 µm thick) were cut with a cryostat (CM1850 UV, Leica Microsystem, Wetzlar, Germany). Cryosections of quadriceps were stained for hematoxylin and eosin (H&E). For hematoxylin and eosin staining, sections were air-dried and incubated in hematoxylin (Sigma-Aldrich) for 3 minutes, then washed in water and incubated in eosin (Roth, Karlsruhe, Germany) for 1 minute. After incubation, sections were washed in water and dehydrated rapidly in 70, 80 and 100% ethanol, and xylene. Sections were mounted with di-Nbutyle phthalate in xylene (DPX) mounting media (Sigma-Aldrich). Images were taken using a Nikon Eclipse 90i upright microscope and analyzed by Neurolucida® software (mbf-bioscience).

MASS SPECTROMETRY ANALYSIS

HPLC operating conditions (Trehalose)

A Shimadzu (Shimadzu, Koyoto, Japan) SIL series LC system equipped with degasser (DGU-20A3), isopump (LC-20AD) and column oven (CTO-10AS) along with an auto-sampler (SIL-HTc) was used to inject 10 µL aliquots of the processed samples on an ACQUITY UPLC BEH AMIDE column (100 × 2,1 mm, 3,5 µm; Waters, Dublin, Ireland, UK), which was maintained at 35 ± 1°C. An isocratic mobile phase comprising 0.1% ammonium hydroxide, 25% H_20, 74,9% acid–acetonitrile (35:65, v/v) delivered at a flow-rate of 0.3 mL/min was used for chromatographic resolution of trehalose and IS.

HPLC operating conditions (Bicalutamide)

A Shimadzu (Shimadzu, Koyoto, Japan) SIL series LC system equipped with degasser (DGU-20A3), isopump (LC-20AD) and column oven (CTO-10AS) along with an auto-sampler (SIL-HTc) was used to inject 2 µL aliquots of the processed samples on an Atlantis dC_{18} column (50 × 4.6 mm, 3 µm; Waters, Dublin, Ireland, UK), which was maintained at 40 ± 1°C. An isocratic mobile phase comprising 0.2% formic acid–acetonitrile (35:65, v/v) delivered at a flow-rate of 0.5 mL/min was used for chromatographic resolution of bicalutamide and IS.

Mass spectrometry operating condition

Quantitation was achieved by MS/MS detection in negative ion mode for bicalutamide and trehalose and IS using an MDS Sciex (Foster City, CA, USA) API-4000 mass spectrometer, equipped with a Turboionspray™ interface at 500°C. The common parameters, viz. curtain gas, GS1 gas and GS2 gas, were set at 20, 35 and 45 L/min, respectively, whereas the CAD gas was set at 6.0 L/min. The compound parameters, viz. de-clustering potential, enhanced potential, collision energy and collision exit potential, for bicalutamide and IS were: −45, −10, −22, −13 V and −55, −10, −26, −15 V, respectively. Detection of the ions was performed in the multiple reaction monitoring (MRM) mode, monitoring the transition of the *m/z* 429.8 precursor ion to the *m/z* 254.7 product ion for bicalutamide and *m/z* 269.0 precursor ion to the *m/z* 169.6 product ion for IS. *M/z* 316, 119 *m/z* and 88,8 for trehalose. Quadrupole Q1 and Q3 were set on unit resolution. The analytical data were processed using Analyst software.

Sample preparation and calibration curves

A simple protein precipitation method was utilized for extraction of bicalutamide from mouse plasma. To an aliquot of 50 µL plasma sample or spinal cord lysate (obtained by homogenizing 15mg of tissue with TissueLyser system (Quiagen)), 200 µL of precipitation solution (i.e. acetonitrile with 100 ng/mL IS) was added, and the mix vortexed for 15 s on a cyclo mixer (Remi Instruments, Mumbai, India). Then samples were centrifuged at 14,000 rpm for 10 and clear supernatant (2 µL or 10 µL) was injected onto the LC-MS/MS system for analysis.

The point calibration curve (0-10-50-100-150-200 ng/10µL trehalose or 0-10-100 ng/10µL) was constructed by plotting the peak area ratio of compound–IS against the nominal concentration of compound standards in control mouse plasma or tissue lysate. Following the evaluation of different weighting factors, the results were fitted to linear regression analysis with the use of a $1/x^2$ (x = concentration) weighting factor. The calibration curve had to have a correlation coefficient (r) of 0.99 or better.

STATISTICAL ANALYSIS

Statistical analysis was performed through two-tailed Student *t-test* for comparisons between two groups (Control vs. axotomized, NTg vs. SBMA), one way analysis of variance (ANOVA) followed by Tukey *post-hoc* test for group comparison (pcDNA3 vs. wt-SOD1 and G93A-SOD1), two-way ANOVA for group comparisons followed by Bonferroni *post-hoc* test to determine specific group pair(s) statistical difference and the survival length were statistically evaluated by the Log-rank test to compare probabilities using the PRISM software (GraphPad, San Diego, CA, USA).

Bibliography

Bibliography

1. Finsterer J, Stöllberger C. Emergencies in motoneuron disease. *Intern Emerg Med*. 2017;12(5):641-650. doi:10.1007/s11739-017-1644-6

2. Niedermeyer S, Murn M, Choi PJ. Respiratory Failure in Amyotrophic Lateral Sclerosis. *Chest*. 2018;(August):1-8. doi:10.1016/j.chest.2018.06.035

3. Miller A, Pratt H, Schiffer RB. Pseudobulbar affect: The spectrum of clinical presentations, etiologies and treatments. *Expert Rev Neurother*. 2011;11(7):1077-1088. doi:10.1586/ern.11.68

4. Messina S. New Directions for SMA Therapy. *J Clin Med*. 2018;7(9):251. doi:10.3390/jcm7090251

5. Finsterer J, Soraru G. Onset Manifestations of Spinal and Bulbar Muscular Atrophy (Kennedy's Disease). *J Mol Neurosci*. 2016;58(3):321-329. doi:10.1007/s12031-015-0663-x

6. Tanaka F, Katsuno M, Banno H, Suzuki K, Adachi H, Sobue G. Current status of treatment of spinal and bulbar muscular atrophy. *Neural Plast*. 2012;2012. doi:10.1155/2012/369284

7. Young JE, Garden GA, Martinez RA, et al. Polyglutamine-Expanded Androgen Receptor Truncation Fragments Activate a Bax-Dependent Apoptotic Cascade Mediated by DP5/Hrk. *J Neurosci*. 2009;29(7):1987-1997. doi:10.1523/JNEUROSCI.4072-08.2009

8. Gouin A, Bloch-Gallego E, Tanaka H, Rosenthal A, Henderson CE. Transforming growth factor-beta 3, glial cell line-derived neurotrophic factor, and fibroblast growth factor-2, act in different manners to promote motoneuron survival in vitro. *J Neurosci Res*. 1996;43(4):454-464. doi:10.1002/(SICI)1097-4547(19960215)43:4<454::AID-JNR6>3.0.CO;2-E

9. Udd B, Juvonen V, Hakamies L, et al. High prevalence of Kennedy's disease in Western Finland -- is the syndrome underdiagnosed? *Acta Neurol Scand*. 1998;98(2):128-133.

10. Katsuno M, Tanaka F, Adachi H, et al. Pathogenesis and therapy of spinal and bulbar muscular atrophy (SBMA). *Prog Neurobiol*. 2012;99(3):246-256. doi:10.1016/j.pneurobio.2012.05.007

11. Guidetti D, Sabadini R, Ferlini A, Torrente I. Epidemiological survey of X-linked bulbar and spinal muscular atrophy, or Kennedy disease, in the province of Reggio Emilia, Italy. *Eur J Epidemiol*. 2001;17(6):587-591. doi:10.1023/A:1014580219761

12. Takeyama KI, Ito S, Yamamoto A, et al. Androgen-dependent neurodegeneration by polyglutamine-expanded human androgen receptor in Drosophila. *Neuron*. 2002;35(5):855-864. doi:10.1016/S0896-6273(02)00875-9

13. Adachi H, Katsuno M, Minamiyama M, et al. Widespread nuclear and cytoplasmic accumulation of mutant androgen receptor in SBMA patients. *Brain*. 2005;128(3):659-670. doi:10.1093/brain/awh381

14. Katsuno M, Adachi H, Kume A, et al. Testosterone reduction prevents phenotypic expression in a transgenic mouse model of spinal and bulbar muscular atrophy. *Neuron*. 2002;35(5):843-854. doi:10.1016/S0896-6273(02)00834-6

15. Poletti A. The polyglutamine tract of androgen receptor: From functions to dysfunctions in motor neurons. *Front Neuroendocrinol*. 2004;25(1):1-26. doi:10.1016/j.yfrne.2004.03.001

16. Stenoien DL, Cummings CJ, Adams HP, et al. Polyglutamine-expanded androgen receptors form aggregates that sequester heat shock proteins, proteasome components and SRC-1, and are

suppressed by the HDJ-2 chaperone. *Hum Mol Genet*. 1999;8(5):731-741. doi:10.1093/hmg/8.5.731

17. Taylor JP, Tanaka F, Robitschek J, et al. Aggresomes protect cells by enhancing the degradation of toxic polyglutamine-containing protein. *Hum Mol Genet*. 2003;12(7):749-757. doi:10.1093/hmg/ddg074

18. Heinlein CA, Chang C. The Roles of Androgen Receptors and Androgen-Binding Proteins in Nongenomic Androgen Actions. *Mol Endocrinol*. 2002;16(10):2181-2187. doi:10.1210/me.2002-0070

19. Tan ME, Li J, Xu HE, Melcher K, Yong EL. Androgen receptor: Structure, role in prostate cancer and drug discovery. *Acta Pharmacol Sin*. 2015;36(1):3-23. doi:10.1038/aps.2014.18

20. Jenster G, van der Korput HA, Trapman J, Brinkmann AO. Identification of two transcription activation units in the N-terminal domain of the human androgen receptor. *J Biol Chem*. 1995;270(13):7341-7346. doi:10.1074/JBC.270.13.7341

21. Koryakina Y, Ta HQ, Gioeli D. Androgen receptor phosphorylation: Biological context and functional consequences. *Endocr Relat Cancer*. 2014;21(4). doi:10.1530/ERC-13-0472

22. Palazzolo I, Gliozzi A, Rusmini P, et al. The role of the polyglutamine tract in androgen receptor. *J Steroid Biochem Mol Biol*. 2008;108(3-5):245-253. doi:10.1016/j.jsbmb.2007.09.016

23. Jochum T, Ritz ME, Schuster C, et al. Toxic and non-toxic aggregates from the SBMA and normal forms of androgen receptor have distinct oligomeric structures. *Biochim Biophys Acta - Mol Basis Dis*. 2012;1822(6):1070-1078. doi:10.1016/j.bbadis.2012.02.006

24. Atsuta N, Watanabe H, Ito M, et al. Natural history of spinal and bulbar muscular atrophy (SBMA): A study of 223 Japanese patients. *Brain*. 2006;129(6):1446-1455. doi:10.1093/brain/awl096

25. Verhovshek T, Cai Y, Osborne MC, Sengelaub DR. Androgen regulates brain-derived neurotrophic factor in spinal motoneurons and their target musculature. *Endocrinology*. 2010;151(1):253-261. doi:10.1210/en.2009-1036

26. Brinkmann AO. Molecular basis of androgen insensitivity. *Mol Cell Endocrinol*. 2001;179(1-2):105-109. doi:10.1016/S0303-7207(01)00466-X

27. Li M, Miwa S, Kobayashi Y, et al. Nuclear inclusions of the androgen receptor protein in spinal and bulbar muscular atrophy. *Ann Neurol*. 1998;44(2):249-254. doi:10.1002/ana.410440216

28. Kemp MQ, Poort JL, Baqri RM, et al. Impaired motoneuronal retrograde transport in two models of SBMA implicates two sites of androgen action. *Hum Mol Genet*. 2011;20(22):4475-4490. doi:10.1093/hmg/ddr380

29. Banno H, Adachi H, Katsuno M, et al. Mutant androgen receptor accumulation in spinal and bulbar muscular atrophy scrotal skin: A pathogenic marker. *Ann Neurol*. 2006;59(3):520-526. doi:10.1002/ana.20735

30. Suzuki K, Katsuno M, Banno H, et al. CAG repeat size correlates to electrophysiological motor and sensory phenotypes in SBMA. *Brain*. 2008;131(1):229-239. doi:10.1093/brain/awm289

31. Wyttenbach A. Role of heat shock proteins during polyglutamine neurodegeneration: mechanisms and hypothesis. *J Mol Neurosci*. 2004;23(1-2):69-96. doi:10.1385/JMN:23:1-2:069

32. Taylor JP, Taye AA, Campbell C, Kazemi-Esfarjani P, Fischbeck KH, Min KT. Aberrant histone acetylation, altered transcription, and retinal degeneration in a Drosophila model of

polyglutamine disease are rescued by CREB-binding protein. *Genes Dev*. 2003;17(12):1463-1468. doi:10.1101/gad.1087503

33. Li M, Chevalier-Larsen ES, Merry DE, Diamond MI. Soluble androgen receptor oligomers underlie pathology in a mouse model of spinobulbar muscular atrophy. *J Biol Chem*. 2007;282(5):3157-3164. doi:10.1074/jbc.M609972200

34. Peters MF, Nucifora FC, Kushi J, et al. Nuclear targeting of mutant huntingtin increases toxicity. *Mol Cell Neurosci*. 1999;14(2):121-128. doi:10.1006/mcne.1999.0773

35. Piccioni F, Pinton P, Simeoni S, et al. Androgen receptor with elongated polyglutamine tract forms aggregates that block mitochondrial trafficking in motoneuronal processess. *FASEB J*. 2002;16(11):1418-1420. doi:10.1096/fj.01-1035fje

36. Katsuno M, Adachi H, Tanaka F, Sobue G. Spinal and bulbar muscular atrophy: Ligand-dependent pathogenesis and therapeutic perspectives. *J Mol Med*. 2004;82(5):298-307. doi:10.1007/s00109-004-0530-7

37. Katsuno M, Adachi H, Waza M, et al. Pathogenesis, animal models and therapeutics in Spinal and bulbar muscular atrophy (SBMA). *Exp Neurol*. 2006;200(1):8-18. doi:10.1016/j.expneurol.2006.01.021

38. Schmidt BJ, Greenberg CR, Allingham-Hawkins DJ, Spriggs EL. Expression of X-linked bulbospinal muscular atrophy (Kennedy disease) in two homozygous women. *Neurology*. 2002;59(5):770-772. doi:10.1212/WNL.59.5.770

39. Lomen-Hoerth C, Murphy J, Langmore S, Kramer JH, Olney RK, Miller B. Are amyotrophic lateral sclerosis patients cognitively normal? *Neurology*. 2003;60(7):1094-1097. doi:10.1016/j.neuron.2010.08.034.Native

40. Palazzolo I, Burnett BG, Young JE, et al. Akt blocks ligand binding and protects against expanded polyglutamine androgen receptor toxicity. *Hum Mol Genet*. 2007;16(13):1593-1603. doi:10.1093/hmg/ddm109

41. Palazzolo I, Stack C, Kong L, et al. Overexpression of IGF-1 in muscle attenuates disease in a mouse model of spinal and bulbar muscular atrophy. *Neuron*. 2009;63(3):316-328. doi:10.1016/j.neuron.2009.07.019

42. Montie HL, Pestell RG, Merry DE. SIRT1 Modulates Aggregation and Toxicity through Deacetylation of the Androgen Receptor in Cell Models of SBMA. *J Neurosci*. 2011;31(48):17425-17436. doi:10.1523/JNEUROSCI.3958-11.2011

43. Thomas M, Dadgar N, Aphale A, et al. Androgen Receptor Acetylation Site Mutations Cause Trafficking Defects, Misfolding, and Aggregation Similar to Expanded Glutamine Tracts. *J Biol Chem*. 2004;279(9):8389-8395. doi:10.1074/jbc.M311761200

44. Mukherjee S, Thomas M, Dadgar N, Lieberman AP, Iñiguez-Lluhi JA. Small ubiquitin-like modifier (SUMO) modification of the androgen receptor attenuates polyglutamine-mediated aggregation. *J Biol Chem*. 2009;284(32):21296-21306. doi:10.1074/jbc.M109.011494

45. Katsuno M, Sang C, Adachi H, et al. Pharmacological induction of heat-shock proteins alleviates polyglutamine-mediated motor neuron disease. *Proc Natl Acad Sci U S A*. 2005;102(46):16801-16806. doi:10.1073/pnas.0506249102

46. Nucifora FC, Sasaki M, Peters MF, et al. Interference by Huntingtin and Atrophin -1 with CBP-Mediated Transcription Leading to Cellular Toxicity. *Science (80-)*. 2001;291(March):2423-2428.

47. Minamiyama M, Katsuno M, Adachi H, et al. Sodium butyrate ameliorates phenotypic expression in a transgenic mouse model of spinal and bulbar muscular atrophy. *Hum Mol Genet*. 2004;13(11):1183-1192. doi:10.1093/hmg/ddh131

48. Suzuki E, Zhao Y, Ito S, et al. Aberrant E2F activation by polyglutamine expansion of androgen receptor in SBMA neurotoxicity. *Proc Natl Acad Sci U S A*. 2009;106(10):3818-3822. doi:10.1073/pnas.0809819106

49. Hafezparast M, Klocke R, Ruhrberg C, et al. Mutations in dynein link motor neuron degeneration to defects in retrograde transport. *Science (80-)*. 2003;300(5620):808-812. doi:10.1126/science.1083129

50. Szebenyi G, Morfini GA, Babcock A, et al. Neuropathogenic forms of huntingtin and androgen receptor inhibit fast axonal transport. *Neuron*. 2003;40(1):41-52. doi:10.1016/S0896-6273(03)00569-5

51. Morfini G, Pigino G, Szebenyi G, You Y, Pollema S, Brady ST. JNK mediates pathogenic effects of polyglutamine-expanded androgen receptor on fast axonal transport. *Nat Neurosci*. 2006;9(7):907-916. doi:10.1038/nn1717

52. Ranganathan S, Harmison GG, Meyertholen K, Pennuto M, Burnett BG, Fischbeck KH. Mitochondrial abnormalities in spinal and bulbar muscular atrophy. *Hum Mol Genet*. 2009;18(1):27-42. doi:10.1093/hmg/ddn310

53. Fratta P, Nirmalananthan N, Masset L, et al. Correlation of clinical and molecular features in spinal bulbar muscular atrophy. *Neurology*. 2014;82(23):2077-2084. doi:10.1212/WNL.0000000000000507

54. Aicua I, Verhagen O, Arenaza N, Cubo E. Head and Arm Tremor in X-linked Spinal and Bulbar Muscular Atrophy. *Tremor Other Hyperkinet Mov (N Y)*. 2014;4(Figure 1):265. doi:10.7916/D8959FVJ

55. Nishiyama A, Sugeno N, Tateyama M, Nishiyama S, Kato M, Aoki M. Postural leg tremor in X-linked spinal and bulbar muscular atrophy. *J Clin Neurosci*. 2014;21(5):799-802. doi:10.1016/j.jocn.2013.07.026

56. Sumner CJ, Fischbeck KH. Jaw drop in Kennedy's disease. *Neurology*. 2002;59(9):1471-1472. doi:10.1212/01.WNL.0000033325.01878.13

57. Warnecke T, Oelenberg S, Teismann I, et al. Dysphagia in X-linked bulbospinal muscular atrophy (Kennedy disease). *Neuromuscul Disord*. 2009;19(10):704-708. doi:10.1016/j.nmd.2009.06.371

58. Sperfeld AD, Hanemann CO, Ludolph AC, Kassubek J. Laryngospasm: An underdiagnosed symptom of X-linked spinobulbar muscular atrophy. *Neurology*. 2005;64(4):753-754. doi:10.1212/01.WNL.0000151978.74467.E7

59. Tanaka S, Banno H, Katsuno M, et al. Distinct acoustic features in spinal and bulbar muscular atrophy patients with laryngospasm. *J Neurol Sci*. 2014;337(1-2):193-200. doi:10.1016/j.jns.2013.12.010

60. Lund A, Udd B, Juvonen V, et al. Multiple founder effects in spinal and bulbar muscular atrophy (SBMA, Kennedy disease) around the world. *Eur J Hum Genet*. 2001;9(6):431-436. doi:10.1038/sj.ejhg.5200656

61. Antonini G, Gragnani F, Romaniello A, et al. Sensory involvement in spinal-bulbar muscular atrophy (Kennedy's disease). *Muscle and Nerve*. 2000;23(2):252-258. doi:10.1002/(SICI)1097-

4598(200002)23:2<252::AID-MUS17>3.0.CO;2-P

62. Fratta P, Collins T, Cortese A, et al. Correlation of clinical and molecular features in spinal bulbar muscular atrophy. *Neurology*. 2014;82:2077-2084.

63. Thomas PS, Fraley GS, Damien V, et al. Loss of endogenous androgen receptor protein accelerates motor neuron degeneration and accentuates androgen insensitivity in a mouse model of X-linked spinal and bulbar muscular atrophy. *Hum Mol Genet*. 2006;15(14):2225-2238. doi:10.1093/hmg/ddl148

64. Dejager S, Bry-Gauillard H, Bruckert E, et al. A comprehensive endocrine description of Kennedy's disease revealing androgen insensitivity linked to CAG repeat length. *J Clin Endocrinol Metab*. 2002;87(8):3893-3901. doi:10.1210/jc.87.8.3893

65. Querin G, Bertolin C, Da Re E, et al. Non-neural phenotype of spinal and bulbar muscular atrophy: Results from a large cohort of Italian patients. *J Neurol Neurosurg Psychiatry*. 2016;87(8):810-816. doi:10.1136/jnnp-2015-311305

66. Araki A, Katsuno M, Suzuki K, et al. Brugada syndrome in spinal and bulbar muscular atrophy. *Neurology*. 2014;82(20):1813-1821. doi:10.1212/WNL.0000000000000434

67. Querin G, Melacini P, D'Ascenzo C, et al. No evidence of cardiomyopathy in spinal and bulbar muscular atrophy. *Acta Neurol Scand*. 2013;128(6):30-32. doi:10.1111/ane.12140

68. Soukup GR, Sperfeld AD, Uttner I, et al. Frontotemporal cognitive function in X-linked spinal and bulbar muscular atrophy (SBMA): A controlled neuropsychological study of 20 patients. *J Neurol*. 2009;256(11):1869-1875. doi:10.1007/s00415-009-5212-5

69. Di Rosa E, Sorarù G, Kleinbub JR, et al. Theory of mind, empathy and neuropsychological functioning in X-linked Spinal and Bulbar Muscular Atrophy: a controlled study of 20 patients. *J Neurol*. 2015;262(2):394-401. doi:10.1007/s00415-014-7567-5

70. Kassubek J, Juengling FD, Sperfeld A-D. Widespread white matter changes in Kennedy disease: a voxel based morphometry study. *J Neurol Neurosurg & Psychiatry*. 2007;78(11):1209-1212. doi:10.1136/jnnp.2006.112532

71. Unrath A, Müller HP, Riecker A, Ludolph AC, Sperfeld AD, Kassubek J. Whole brain-based analysis of regional white matter tract alterations in rare motor neuron diseases by diffusion tensor imaging. *Hum Brain Mapp*. 2010;31(11):1727-1740. doi:10.1002/hbm.20971

72. Lai TH, Liu RS, Yang BH, et al. Cerebral involvement in spinal and bulbar muscular atrophy (Kennedy's disease): A pilot study of PET. *J Neurol Sci*. 2013;335(1-2):139-144. doi:10.1016/j.jns.2013.09.016

73. Sorarù G, D'Ascenzo C, Polo A, et al. Spinal and bulbar muscular atrophy: Skeletal muscle pathology in male patients and heterozygous females. *J Neurol Sci*. 2008;264(1-2):100-105. doi:10.1016/j.jns.2007.08.012

74. Chevalier-Larsen ES. Castration Restores Function and Neurofilament Alterations of Aged Symptomatic Males in a Transgenic Mouse Model of Spinal and Bulbar Muscular Atrophy. *J Neurosci*. 2004;24(20):4778-4786. doi:10.1523/JNEUROSCI.0808-04.2004

75. Yu Z, Dadgar N, Albertelli M, et al. Androgen-dependent pathology demonstrates myopathic contribution to the Kennedy disease phenotype in a mouse knock-in model. *J Clin Invest*. 2006;116(10):2663-2672. doi:10.1172/JCI28773

76. Monks DA, Johansen JA, Mo K, et al. Overexpression of wild-type androgen receptor in muscle recapitulates polyglutamine disease. *Proc Natl Acad Sci*. 2007;104(46):18259-18264.

doi:10.1073/pnas.0705501104

77. Giorgetti E, Lieberman AP. Polyglutamine androgen receptor-mediated neuromuscular disease. *Cell Mol Life Sci*. 2016;73(21):3991-3999. doi:10.1007/s00018-016-2275-1

78. Sinha-Hikim I, Taylor WE, Gonzalez-Cadavid NF, Zheng W, Bhasin S. Androgen Receptor in Human Skeletal Muscle and Cultured Muscle Satellite Cells: Up-Regulation by Androgen Treatment. *J Clin Endocrinol Metab*. 2004;89(10):5245-5255. doi:10.1210/jc.2004-0084

79. I. S-H, J. A, L. W, et al. Testosterone-induced increase in muscle size in healthy young men is associated with muscle fiber hypertrophy. *Am J Physiol - Endocrinol Metab*. 2002;283(1 46-1):E154-E164. doi:10.1152/ajpendo.00502.2001

80. Sopher BL, Thomas PS, Lafevre-Bernt MA, et al. Androgen receptor YAC transgenic mice recapitulate SBMA motor neuronopathy and implicate VEGF164 in the motor neuron degeneration. *Neuron*. 2004;41(5):687-699. doi:10.1016/S0896-6273(04)00082-0

81. Querin G, Sorarù G, Pradat PF. Kennedy disease (X-linked recessive bulbospinal neuronopathy): A comprehensive review from pathophysiology to therapy. *Rev Neurol (Paris)*. 2017;173(5):326-337. doi:10.1016/j.neurol.2017.03.019

82. Mariotti C, Castellotti B, Pareyson D, et al. Phenotypic manifestations associated with CAG-repeat expansion in the androgen receptor gene in male patients and heterozygous females: A clinical and molecular study of 30 families. *Neuromuscul Disord*. 2000;10(6):391-397. doi:10.1016/S0960-8966(99)00132-7

83. Darras BT, Finkel RS. Natural History of Spinal Muscular Atrophy. *Spinal Muscular Atrophy Dis Mech Ther*. 2016:399-421. doi:10.1016/B978-0-12-803685-3.00025-2

84. Fernández-rhodes LE, Kokkinis AD, White MJ, et al. NIH Public Access. *Lancet Neurol*. 2011;10(2):140-147. doi:10.1016/S1474-4422(10)70321-5.A

85. Katsuno M, Adachi H, Doyu M, et al. Leuprorelin rescues polyglutamine-dependent phenotypes in a transgenic mouse model of spinal and bulbar muscular atrophy. *Nat Med*. 2003;9(6):768-773. doi:10.1038/nm878

86. Miyazaki Y, Adachi H, Katsuno M, et al. Viral delivery of miR-196a ameliorates the SBMA phenotype via the silencing of CELF2. *Nat Med*. 2012;18(7):1136-1141. doi:10.1038/nm.2791

87. Giorgetti E, Rusmini P, Crippa V, et al. Synergic prodegradative activity of Bicalutamide and trehalose on the mutant androgen receptor responsible for spinal and bulbar muscular atrophy. *Hum Mol Genet*. 2015;24(1):64-75. doi:10.1093/hmg/ddu419

88. Yu Z, Wang AM, Adachi H, et al. Macroautophagy is regulated by the UPR-mediator CHOP and accentuates the phenotype of SBMA mice. *PLoS Genet*. 2011;7(10). doi:10.1371/journal.pgen.1002321

89. Galluzzi L, Pietrocola F, Bravo-San Pedro JM, et al. Autophagy in malignant transformation and cancer progression. *EMBO J*. 2015;34(7):856-880. doi:10.15252/embj.201490784

90. Baker M, Mackenzie IR, Pickering-Brown SM, et al. Mutations in progranulin cause tau-negative frontotemporal dementia linked to chromosome 17. *Nature*. 2006;442(7105):916-919. doi:10.1038/nature05016

91. Menzies FM, Huebener J, Renna M, Bonin M, Riess O, Rubinsztein DC. Autophagy induction reduces mutant ataxin-3 levels and toxicity in a mouse model of spinocerebellar ataxia type 3. *Brain*. 2010;133(1):93-104. doi:10.1093/brain/awp292

92. Hara T, Nakamura K, Matsui M, et al. Suppression of basal autophagy in neural cells causes neurodegenerative disease in mice. *Nature*. 2006;441(7095):885-889. doi:10.1038/nature04724

93. Mizushima N, Noda T, Yoshimori T, et al. A protein conjugation system essential for autophagy. *Nature*. 1998;395(6700):395-398. doi:10.1038/26506

94. Gomes LR, Menck CFM, Leandro GS. Autophagy roles in the modulation of DNA repair pathways. *Int J Mol Sci*. 2017;18(11). doi:10.3390/ijms18112351

95. Feng Y, He D, Yao Z, Klionsky DJ. The machinery of macroautophagy. *Cell Res*. 2014;24(1):24-41. doi:10.1038/cr.2013.168

96. Galluzzi L, Baehrecke EH, Ballabio A, et al. Molecular definitions of autophagy and related processes. *EMBO J*. 2017;36(13):1811-1836. doi:10.15252/embj.201796697

97. Farré JC, Krick R, Subramani S, Thumm M. Turnover of organelles by autophagy in yeast. *Curr Opin Cell Biol*. 2009;21(4):522-530. doi:10.1016/j.ceb.2009.04.015

98. Hosseinpour-Moghaddam K, Caraglia M, Sahebkar A. Autophagy induction by trehalose: Molecular mechanisms and therapeutic impacts. *J Cell Physiol*. 2018;233(9):6524-6543. doi:10.1002/jcp.26583

99. Uytterhoeven V, Lauwers E, Maes I, et al. Hsc70-4 Deforms Membranes to Promote Synaptic Protein Turnover by Endosomal Microautophagy. *Neuron*. 2015;88(4):735-748. doi:10.1016/j.neuron.2015.10.012

100. Sahu R, Kaushik S, Clement CC, et al. Microautophagy of Cytosolic Proteins by Late Endosomes. *Dev Cell*. 2011;20(1):131-139. doi:10.1016/j.devcel.2010.12.003

101. Morozova K, Clement CC, Kaushik S, et al. Structural and biological interaction of HSC-70 protein with phosphatidylserine in endosomal microautophagy. *J Biol Chem*. 2016;291(35):18096-18106. doi:10.1074/jbc.M116.736744

102. Vevea JD, Garcia EJ, Chan RB, et al. Role for Lipid Droplet Biogenesis and Microlipophagy in Adaptation to Lipid Imbalance in Yeast. *Dev Cell*. 2015;35(5):584-599. doi:10.1016/j.devcel.2015.11.010

103. Liu XM, Du LL. A selective autophagy pathway takes an unconventional route. *Autophagy*. 2015;11(12):2381-2382. doi:10.1080/15548627.2015.1110669

104. Bandyopadhyay U, Kaushik S, Varticovski L, Cuervo AM. The Chaperone-Mediated Autophagy Receptor Organizes in Dynamic Protein Complexes at the Lysosomal Membrane. *Mol Cell Biol*. 2008;28(18):5747-5763. doi:10.1128/MCB.02070-07

105. Salvador N. JBC Papers in Press. Published on June 20, 2000 as Manuscript M001394200 1. *J Biol Chem*. 2000.

106. Park JM, Jung CH, Seo M, et al. The ULK1 complex mediates MTORC1 signaling to the autophagy initiation machinery via binding and phosphorylating ATG14. *Autophagy*. 2016;12(3):547-564. doi:10.1080/15548627.2016.1140293

107. Kon M, Kiffin R, Koga H, et al. Chaperone-mediated autophagy is required for tumor growth. *Sci Transl Med*. 2011;3(109):1-30. doi:10.1126/scitranslmed.3003182

108. Arias E, Koga H, Diaz A, Mocholi E, Patel B, Cuervo AM. Lysosomal mTORC2/PHLPP1/Akt Regulate Chaperone-Mediated Autophagy. *Mol Cell*. 2015;59(2):270-284. doi:10.1016/j.molcel.2015.05.030

109. Eskelinen EL. Doctor Jekyll and Mister Hyde: Autophagy can promote both cell survival and cell death. *Cell Death Differ*. 2005;12:1468-1472. doi:10.1038/sj.cdd.4401721

110. Antonioli M, Di Rienzo M, Piacentini M, Fimia GM. Emerging Mechanisms in Initiating and Terminating Autophagy. *Trends Biochem Sci*. 2017;42(1):28-41. doi:10.1016/j.tibs.2016.09.008

111. Yang Q, Mao Z. Parkinson disease: A role for autophagy? *Neuroscientist*. 2010;16(4):335-341. doi:10.1177/1073858409357118

112. Cherra SJ, Dagda RK, Chu CT. Review: Autophagy and neurodegeneration: Survival at a cost? *Neuropathol Appl Neurobiol*. 2010;36(2):125-132. doi:10.1111/j.1365-2990.2009.01062.x

113. Ichimura Y, Kirisako T, Takao T, et al. A ubiquitin-like system mediates protein lipidation. *Nature*. 2000;408(6811):488-492. doi:10.1038/35044114

114. Wild P, McEwan DG, Dikic I. The LC3 interactome at a glance. *J Cell Sci*. 2014;127(1):3-9. doi:10.1242/jcs.140426

115. Karanasios E, Walker SA, Okkenhaug H, et al. Autophagy initiation by ULK complex assembly on ER tubulovesicular regions marked by ATG9 vesicles. *Nat Commun*. 2016;7:1-17. doi:10.1038/ncomms12420

116. Lamb CA, Yoshimori T, Tooze SA. The autophagosome: Origins unknown, biogenesis complex. *Nat Rev Mol Cell Biol*. 2013;14(12):759-774. doi:10.1038/nrm3696

117. Kihara A, Noda T, Ishihara N, Ohsumi Y. Two distinct Vps34 phosphatidylinositol 3-kinase complexes function in autophagy and carboxypeptidase y sorting in Saccharomyces cerevisiae. *J Cell Biol*. 2001;153(3):519-530. doi:10.1083/jcb.152.3.519

118. Zhang J, Yin X, Zhao L, et al. Regional alterations in cortical thickness and white matter integrity in amyotrophic lateral sclerosis. *J Neurol*. 2014;261(2):412-421. doi:10.1007/s00415-013-7215-5

119. Proikas-Cezanne T, Takacs Z, Donnes P, Kohlbacher O. WIPI proteins: essential PtdIns3P effectors at the nascent autophagosome. *J Cell Sci*. 2015;128(2):207-217. doi:10.1242/jcs.146258

120. Jung JM, Kwon JY, Kim HJ, et al. Ischemic lesion burden and characteristics of aortic atheroma. *J Stroke Cerebrovasc Dis*. 2014;23(2):278-282. doi:10.1016/j.jstrokecerebrovasdis.2013.02.013

121. Settembre C, Polito VA, Garcia M, et al. Europe PMC Funders Group Europe PMC Funders Author Manuscripts TFEB Links Autophagy to Lysosomal Biogenesis. *Science (80-)*. 2013;332(6036):1429-1433. doi:10.1126/science.1204592.TFEB

122. Inoki K, Li Y, Zhu T, Wu J, Guan KL. TSC2 is phosphorylated and inhibited by Akt and suppresses mTOR signalling. *Nat Cell Biol*. 2002;4(9):648-657. doi:10.1038/ncb839

123. Traxinger K, Kelly C, Johnson BA, Lyles RH, Glass JD. Prognosis and epidemiology of amyotrophic lateral sclerosis Analysis of a clinic population, 1997-2011. *Neurol Clin Pract*. 2013;3(4):313-320. doi:10.1212/CPJ.0b013e3182a1b8ab

124. Rubinstein AD, Eisenstein M, Ber Y, Bialik S, Kimchi A. The autophagy protein atg12 associates with antiapoptotic Bcl-2 family members to promote mitochondrial apoptosis. *Mol Cell*. 2011;44(5):698-709. doi:10.1016/j.molcel.2011.10.014

125. Amaya C, Fader CM, Colombo MI. Autophagy and proteins involved in vesicular trafficking. *FEBS Lett*. 2015;589(22):3343-3353. doi:10.1016/j.febslet.2015.09.021

126. Gutierrez MG. Rab7 is required for the normal progression of the autophagic pathway in mammalian cells. *J Cell Sci*. 2004;117(13):2687-2697. doi:10.1242/jcs.01114

127. Hasegawa J, Iwamoto R, Otomo T, Nezu A, Hamasaki M, Yoshimori T. Autophagosome–lysosome fusion in neurons requires INPP5E, a protein associated with Joubert syndrome. *EMBO J*. 2016;35(17):1853-1867. doi:10.15252/embj.201593148

128. McEwan DG, Popovic D, Gubas A, et al. PLEKHM1 regulates autophagosome-lysosome fusion through HOPS complex and LC3/GABARAP proteins. *Mol Cell*. 2015;57(1):39-54. doi:10.1016/j.molcel.2014.11.006

129. Tien NT, Karaca I, Tamboli IY, Walter J. Trehalose alters subcellular trafficking and the metabolism of the Alzheimer-associated amyloid precursor protein. *J Biol Chem*. 2016;291(20):10528-10540. doi:10.1074/jbc.M116.719286

130. Matsunaga K, Saitoh T, Tabata K, et al. Two Beclin 1-binding proteins, Atg14L and Rubicon, reciprocally regulate autophagy at different stages. *Nat Cell Biol*. 2009;11(4):385-396. doi:10.1038/ncb1846

131. Tsuboyama K, Koyama-Honda I, Sakamaki Y, Koike M, Morishita H, Mizushima N. The ATG conjugation systems are important for degradation of the inner autophagosomal membrane. *Science (80-)*. 2016;354(6315):1036-1041. doi:10.1126/science.aaf6136

132. Yu L, McPhee CK, Zheng L, et al. Autophagy termination and lysosome reformation regulated by mTOR. *Nature*. 2010;465(7300):942-946. doi:10.1038/nature09076.Autophagy

133. Chen Q. Role of trehalose phosphate synthase and trehalose during hypoxia: from flies to mammals. *J Exp Biol*. 2004;207(18):3125-3129. doi:10.1242/jeb.01133

134. Corradini D, Strekalova EG, Eugene Stanley H, Gallo P. Microscopic mechanism of protein cryopreservation in an aqueous solution with trehalose. *Sci Rep*. 2013;3. doi:10.1038/srep01218

135. Kang YL, Saleem MA, Chan KW, Yung BYM, Law HKW. Trehalose, an mTOR independent autophagy inducer, alleviates human podocyte injury after puromycin aminonucleoside treatment. *PLoS One*. 2014;9(11):1-9. doi:10.1371/journal.pone.0113520

136. Sarkar S, Chigurupati S, Raymick J, et al. Neuroprotective effect of the chemical chaperone, trehalose in a chronic MPTP-induced Parkinson's disease mouse model. *Neurotoxicology*. 2014;44:250-262. doi:10.1016/j.neuro.2014.07.006

137. Sarkar S, Davies JE, Huang Z, Tunnacliffe A, Rubinsztein DC. Trehalose, a novel mTOR-independent autophagy enhancer, accelerates the clearance of mutant huntingtin and α-synuclein. *J Biol Chem*. 2007;282(8):5641-5652. doi:10.1074/jbc.M609532200

138. Casarejos MJ, Solano RM, Gómez A, Perucho J, De Yébenes JG, Mena MA. The accumulation of neurotoxic proteins, induced by proteasome inhibition, is reverted by trehalose, an enhancer of autophagy, in human neuroblastoma cells. *Neurochem Int*. 2011;58(4):512-520. doi:10.1016/j.neuint.2011.01.008

139. Mardones P, Rubinsztein DC, Hetz C. Mystery solved: Trehalose kickstarts autophagy by blocking glucose transport. *Sci Signal*. 2016;9(416):1-4. doi:10.1126/scisignal.aaf1937

140. DeBosch BJ, Heitmeier MR, Mayer AL, et al. Trehalose inhibits solute carrier 2A (SLC2A) proteins to induce autophagy and prevent hepatic steatosis. *Sci Signal*. 2016;9(416):ra21. doi:10.1126/scisignal.aac5472

141. Tanaka M, Machida Y, Niu S, et al. Trehalose alleviates polyglutamine-mediated pathology in a

mouse model of Huntington disease. *Nat Med*. 2004;10(2):148-154. doi:10.1038/nm985

142. Schaeffer V, Lavenir I, Ozcelik S, Tolnay M, Winkler DT, Goedert M. Stimulation of autophagy reduces neurodegeneration in a mouse model of human tauopathy. *Brain*. 2012;135(7):2169-2177. doi:10.1093/brain/aws143

143. Castillo K, Nassif M, Valenzuela V, et al. Trehalose delays the progression of amyotrophic lateral sclerosis by enhancing autophagy in motoneurons. *Autophagy*. 2013;9(9):1308-1320. doi:10.4161/auto.25188

144. Vidal RL, Matus S, Bargsted L, Hetz C. Targeting autophagy in neurodegenerative diseases. *Trends Pharmacol Sci*. 2014;35(11):583-591. doi:10.1016/j.tips.2014.09.002

145. Appl T, Kaltenbach L, Lo DC, Terstappen GC. Targeting mutant huntingtin for the development of disease-modifying therapy. *Drug Discov Today*. 2012;17(21-22):1217-1223. doi:10.1016/j.drudis.2012.06.017

146. Ross CA, Tabrizi SJ. Huntington's disease: From molecular pathogenesis to clinical treatment. *Lancet Neurol*. 2011;10(1):83-98. doi:10.1016/S1474-4422(10)70245-3

147. Zuccato C, Valenza M, Cattaneo E. Molecular Mechanisms and Potential Therapeutical Targets in Huntington ' s Disease. *Physiol Rev*. 2010;90(3):905-981. doi:10.1152/physrev.00041.2009.

148. Chaudhary RK, Patel KA, Patel MK, Joshi RH, Roy I. Inhibition of Aggregation of Mutant Huntingtin by Nucleic Acid Aptamers in Vitro and in a Yeast Model of Huntington's Disease. *Mol Ther*. 2015;23(12):1912-1926. doi:10.1038/mt.2015.157

149. Fernandez-Estevez MA, Casarejos MJ, Sendon JL, et al. Trehalose reverses cell malfunction in fibroblasts from normal and huntington's disease patients caused by proteosome inhibition. *PLoS One*. 2014;9(2):1-9. doi:10.1371/journal.pone.0090202

150. Bradford J, Shin J-Y, Roberts M, et al. Mutant Huntingtin in Glial Cells Exacerbates Neurological Symptoms of Huntington Disease Mice. *J Biol Chem*. 2010;285(14):10653-10661. doi:10.1074/jbc.M109.083287

151. Perucho J, Gómez A, Muñoz MP, de Yébenes JG, Mena MÁ, Casarejos MJ. Trehalose rescues glial cell dysfunction in striatal cultures from HD R6/1 mice at early postnatal development. *Mol Cell Neurosci*. 2016;74:128-145. doi:10.1016/j.mcn.2016.05.002

152. Collinge J. P RION D ISEASES OF H UMANS AND A NIMALS : Their Causes and Molecular Basis. *Annu Rev*. 2001;24(McGowan 1922):519–50. doi:10.1146/annurev.neuro.24.1.519

153. Aguzzi A, Miele G. Recent advances in prion biology. *Curr Opin Neurol*. 2004;17(3):337-342. doi:10.1097/00019052-200406000-00015

154. Heiseke A, Aguib Y, Schatzl HM. Autophagy, prion infection and their mutual interactions. *Curr Issues Mol Biol*. 2010;12(2):87-98.

155. Bosco D a, Morfini G, Karabacak NM, et al. NIH Public Access. *Nat Neurosci*. 2011;13(11):1396-1403. doi:10.1038/nn.2660.Wild-type

156. Pasinelli P, Brown RH. Molecular biology of amyotrophic lateral sclerosis: Insights from genetics. *Nat Rev Neurosci*. 2006;7(9):710-723. doi:10.1038/nrn1971

157. Gomes C, Escrevente C, Costa J. Mutant superoxide dismutase 1 overexpression in NSC-34 cells: Effect of trehalose on aggregation, TDP-43 localization and levels of co-expressed glycoproteins. *Neurosci Lett*. 2010;475(3):145-149. doi:10.1016/j.neulet.2010.03.065

158. Lan DM, Liu FT, Zhao J, et al. Effect of trehalose on PC12 cells overexpressing wild-type or A53T mutant α-synuclein. *Neurochem Res*. 2012;37(9):2025-2032. doi:10.1007/s11064-012-0823-0

159. Kitada T, Asakawa S, Hattori N, et al. Mutations in the parkin gene cause autosomal recessive juvenile parkinsonism. *Nature*. 1998;392(6676):605-608. doi:10.1038/33416

160. Webb JL, Ravikumar B, Atkins J, Skepper JN, Rubinsztein DC. α-synuclein Is Degraded by Both Autophagy and the Proteasome. *J Biol Chem*. 2003;278(27):25009-25013. doi:10.1074/jbc.M300227200

161. Rott R, Szargel R, Haskin J, et al. Monoubiquitylation of α-Synuclein by seven in absentia homolog (SIAH) promotes its aggregation in dopaminergic cells. *J Biol Chem*. 2008;283(6):3316-3328. doi:10.1074/jbc.M704809200

162. Honda Y, Tanaka M, Honda S. Trehalose extends longevity in the nematode Caenorhabditis elegans. *Aging Cell*. 2010;9(4):558-569. doi:10.1111/j.1474-9726.2010.00582.x

163. Redmann M, Wani WY, Volpicelli-Daley L, Darley-Usmar V, Zhang J. Trehalose does not improve neuronal survival on exposure to alpha-synuclein pre-formed fibrils. *Redox Biol*. 2017;11(December 2016):429-437. doi:10.1016/j.redox.2016.12.032

164. Eckenhoff RG, Johansson JS, Wei H, et al. Inhaled anesthetic enhancement of amyloid-β oligomerization and cytotoxicity. *Anesthesiology*. 2004;101(3):703-709. doi:10.1097/00000542-200409000-00019

165. Ramirez-Bermudez J. Alzheimer's disease: critical notes on the history of a medical concept. *Arch Med Res*. 2012;43(8):595-599. doi:10.1016/j.arcmed.2012.11.008

166. De Bona P, Giuffrida ML, Caraci F, et al. Design and synthesis of new trehalose-conjugated pentapeptides as inhibitors of Aβ(1-42) fibrillogenesis and toxicity. *J Pept Sci*. 2009;15(3):220-228. doi:10.1002/psc.1109

167. Arora A, Ha C, Park CB. Inhibition of insulin amyloid formation by small stress molecules. *FEBS Lett*. 2004;564(1-2):121-125. doi:10.1016/S0014-5793(04)00326-6

168. Rodríguez-Navarro JA, Rodríguez L, Casarejos MJ, et al. Trehalose ameliorates dopaminergic and tau pathology in parkin deleted/tau overexpressing mice through autophagy activation. *Neurobiol Dis*. 2010;39(3):423-438. doi:10.1016/j.nbd.2010.05.014

169. Avila J, Lucas JJ, Perez M, Hernandez F. Role of tau protein in both physiological and pathological conditions. *Physiol Rev*. 2004;84(2):361-384. doi:10.1152/physrev.00024.2003

170. Ittner LM, Götz J. Amyloid-β and tau - A toxic pas de deux in Alzheimer's disease. *Nat Rev Neurosci*. 2011;12(2):67-72. doi:10.1038/nrn2967

171. Krüger U, Wang Y, Kumar S, Mandelkow EM. Autophagic degradation of tau in primary neurons and its enhancement by trehalose. *Neurobiol Aging*. 2012;33(10):2291-2305. doi:10.1016/j.neurobiolaging.2011.11.009

172. Dickey CA, Kamal A, Lundgren K, et al. The high-affinity HSP90-CHIP complex recognizes and selectively degrades phosphorylated tau client proteins. *J Clin Invest*. 2007;117(3):648-658. doi:10.1172/JCI29715

173. Bettencourt C, Lima M. "Mimicking" capacity of spinocerebellar ataxia type 3: The details matter. *J Neurol Sci*. 2013;326(1-2):120-121. doi:10.1016/j.jns.2013.01.022

174. Casarejos MJ, Perucho J, López-Sendón JL, et al. Trehalose improves human fibroblast deficits in a new CHIP-mutation related ataxia. *PLoS One*. 2014;9(9):1-13.

doi:10.1371/journal.pone.0106931

175. Shen C, Sun Z, Chen D, et al. Developing Urinary Metabolomic Signatures as Early Bladder Cancer Diagnostic Markers. *Omi A J Integr Biol*. 2015;19(1):1-11. doi:10.1089/omi.2014.0116

176. Toh H, Chitramuthu BP, Bennett HPJ, Bateman A. Structure, function, and mechanism of progranulin; The brain and beyond. *J Mol Neurosci*. 2011;45(3):538-548. doi:10.1007/s12031-011-9569-4

177. Holler CJ, Taylor G, McEachin ZT, et al. Trehalose upregulates progranulin expression in human and mouse models of GRN haploinsufficiency: A novel therapeutic lead to treat frontotemporal dementia. *Mol Neurodegener*. 2016;11(1):1-17. doi:10.1186/s13024-016-0114-3

178. Albertelli MA, Scheller A, Brogley M, Robins DM. Replacing the Mouse Androgen Receptor with Human Alleles Demonstrates Glutamine Tract Length-Dependent Effects on Physiology and Tumorigenesis in Mice. *Mol Endocrinol*. 2006;20(6):1248-1260. doi:10.1210/me.2006-0021

179. Méjat A, Ramond F, Bassel-Duby R, Khochbin S, Olson EN, Schaeffer L. Histone deacetylase 9 couples neuronal activity to muscle chromatin acetylation and gene expression. *Nat Neurosci*. 2005;8(3):313-321. doi:10.1038/nn1408

180. Klotz L. Maximal androgen blockade for advanced prostate cancer. *Best Pract Res Clin Endocrinol Metab*. 2008;22(2):331-340. doi:10.1016/j.beem.2008.01.004

181. Chua JP, Reddy SL, Merry DE, et al. Transcriptional activation of TFEB/ZKSCAN3 target genes underlies enhanced autophagy in spinobulbar muscular atrophy. *Hum Mol Genet*. 2014;23(5):1376-1386. doi:10.1093/hmg/ddt527

182. Crippa V, Carra S, Rusmini P, et al. A role of small heat shock protein B8 (HspB8) in the autophagic removal of misfolded proteins responsible for neurodegenerative diseases. *Autophagy*. 2010;6(7):958-960. doi:10.4161/auto.6.7.13042

183. Chau J, Lieberman A. Pathogenic mechanisms and therapeutic strategies in spinobulbar muscular atrophy. *CNS Neurol Disord Drug Targets*. 2013;12(8):1146-1156. doi:10.1038/nature13314.A

184. Rusmini P, Polanco MJ, Cristofani R, et al. Aberrant Autophagic Response in the Muscle of A Knock-in Mouse Model of Spinal and Bulbar Muscular Atrophy. *Sci Rep*. 2015;5(September):1-21. doi:10.1038/srep15174

185. Robberecht W, Philips T. The changing scene of amyotrophic lateral sclerosis. *Nat Rev Neurosci*. 2013;14(4):248-264. doi:10.1038/nrn3430

186. Matus S, Medinas DB, Hetz C. Common ground: Stem cell approaches find shared pathways underlying ALS. *Cell Stem Cell*. 2014;14(6):697-699. doi:10.1016/j.stem.2014.05.001

187. Hirano M, Angelini C, Montagna P, et al. Amyotrophic lateral sclerosis with ragged-red fibers. *Arch Neurol*. 2008;65(3):403-406. doi:10.1001/archneurol.2007.65

188. Simon NG, Turner MR, Vucic S, et al. Quantifying disease progression in amyotrophic lateral sclerosis. *Ann Neurol*. 2014;76(5):643-657. doi:10.1002/ana.24273

189. Paez-Colasante X, Seaberg B, Martinez TL, Kong L, Sumner CJ, Rimer M. Improvement of Neuromuscular Synaptic Phenotypes without Enhanced Survival and Motor Function in Severe Spinal Muscular Atrophy Mice Selectively Rescued in Motor Neurons. *PLoS One*. 2013;8(9). doi:10.1371/journal.pone.0075866

190. Rusina R, Ridzoň P, Kulišťák P, et al. Relationship between ALS and the degree of cognitive

impairment, markers of neurodegeneration and predictors for poor outcome. A prospective study. *Eur J Neurol*. 2010;17(1):23-30. doi:10.1111/j.1468-1331.2009.02717.x

191. Figueroa-Romero C, Hur J, Bender DE, et al. Identification of Epigenetically Altered Genes in Sporadic Amyotrophic Lateral Sclerosis. *PLoS One*. 2012;7(12). doi:10.1371/journal.pone.0052672

192. Kanekura K, Suzuki H, Aiso S, Matsuoka M. ER stress and unfolded protein response in amyotrophic lateral sclerosis. *Mol Neurobiol*. 2009;39(2):81-89. doi:10.1007/s12035-009-8054-3

193. Voigt A, Herholz D, Fiesel FC, et al. TDP-43-mediated neuron loss In Vivo requires RNA-binding activity. *PLoS One*. 2010;5(8). doi:10.1371/journal.pone.0012247

194. Katsuno M, Tanaka F, Sobue G. Perspectives on molecular targeted therapies and clinical trials for neurodegenerative diseases. *J Neurol Neurosurg Psychiatry*. 2012;83(3):329-335. doi:10.1136/jnnp-2011-301307

195. Wijesekera LC, Leigh PN. Amyotrophic lateral sclerosis. *Orphanet J Rare Dis*. 2009;4(1):1-22. doi:10.1186/1750-1172-4-3

196. Jones AR, Woollacott I, Shatunov A, et al. Residual association at C9orf72 suggests an alternative amyotrophic lateral sclerosis-causing hexanucleotide repeat. *Neurobiol Aging*. 2013;34(9):1-7. doi:10.1016/j.neurobiolaging.2013.03.003

197. Chiò A, Logroscino G, Hardiman O, et al. Prognostic factors in ALS: A critical review. *Amyotroph Lateral Scler*. 2009;10(5-6):310-323. doi:10.3109/17482960802566824

198. Lobsiger CS, Boillee S, McAlonis-Downes M, et al. Schwann cells expressing dismutase active mutant SOD1 unexpectedly slow disease progression in ALS mice. *Proc Natl Acad Sci U S A*. 2009;106(11):4465-4470. doi:10.1073/pnas.0813339106

199. Su XW, Broach JR, Connor JR, Gerhard GS, Simmons Z. Genetic heterogeneity of amyotrophic lateral sclerosis: Implications for clinical practice and research. *Muscle Nerve*. 2014;49(6):786-803. doi:10.1002/mus.24198

200. Okado-Matsumoto A, Fridovich I. Amyotrophic lateral sclerosis: a proposed mechanism. *Proc Natl Acad Sci U S A*. 2002;99(13):9010-9014. doi:10.1073/pnas.132260399

201. Polymenidou M, Cleveland DW. Prion-like spread of protein aggregates in neurodegeneration: Figure 1. *J Exp Med*. 2012;209(5):889-893. doi:10.1084/jem.20120741

202. Toivonen JM, Manzano R, Oliván S, Zaragoza P, García-Redondo A, Osta R. MicroRNA-206: A potential circulating biomarker candidate for amyotrophic lateral sclerosis. *PLoS One*. 2014;9(2). doi:10.1371/journal.pone.0089065

203. Honda D, Ishigaki S, Iguchi Y, et al. The ALS/FTLD-related RNA-binding proteins TDP-43 and FUS have common downstream RNA targets in cortical neurons. *FEBS Open Bio*. 2014;4:1-10. doi:10.1016/j.fob.2013.11.001

204. Johnson BS, Snead D, Lee JJ, McCaffery JM, Shorter J, Gitler AD. TDP-43 is intrinsically aggregation-prone, and amyotrophic lateral sclerosis-linked mutations accelerate aggregation and increase toxicity. *J Biol Chem*. 2009;284(30):20329-20339. doi:10.1074/jbc.M109.010264

205. Lattante S, Rouleau GA, Kabashi E. TARDBP and FUS Mutations Associated with Amyotrophic Lateral Sclerosis: Summary and Update. *Hum Mutat*. 2013;34(6):812-826. doi:10.1002/humu.22319

206. Vance C, Rogelj B, Hortobágyi T, et al. Mutations in FUS, an RNA processing protein, cause familial amyotrophic lateral sclerosis type 6. *Science*. 2009;323(5918):1208-1211. doi:10.1126/science.1165942

207. Groen EJN, Fumoto K, Blokhuis AM, et al. ALS-associated mutations in FUS disrupt the axonal distribution and function of SMN. *Hum Mol Genet*. 2013;22(18):3690-3704. doi:10.1093/hmg/ddt222

208. Droppelmann CA, Campos-Melo D, Volkening K, Strong MJ. The emerging role of guanine nucleotide exchange factors in ALS and other neurodegenerative diseases. *Front Cell Neurosci*. 2014;8(September):1-14. doi:10.3389/fncel.2014.00282

209. Meyerowitz J, Parker SJ, Vella LJ, et al. C-Jun N-terminal kinase controls TDP-43 accumulation in stress granules induced by oxidative stress. *Mol Neurodegener*. 2011;6(1):57. doi:10.1186/1750-1326-6-57

210. Renton AE, Majounie E, Waite A, et al. A hexanucleotide repeat expansion in C9ORF72 is the cause of chromosome 9p21-linked ALS-FTD. *Neuron*. 2011;72(2):257-268. doi:10.1016/j.neuron.2011.09.010

211. DeJesus-Hernandez M, Mackenzie IR, Boeve BF, et al. Expanded GGGGCC hexanucleotide repeat in noncoding region of C9ORF72 causes chromosome 9p-linked FTD and ALS. *Neuron*. 2011;72(2):245-256. doi:10.1016/j.neuron.2011.09.011

212. Xi Z, Zinman L, Moreno D, et al. Hypermethylation of the CpG island near the G4C2 repeat in ALS with a C9orf72 expansion. *Am J Hum Genet*. 2013;92(6):981-989. doi:10.1016/j.ajhg.2013.04.017

213. Al-Chalabi A, Fang F, Hanby MF, et al. An estimate of amyotrophic lateral sclerosis heritability using twin data. *J Neurol Neurosurg Psychiatry*. 2010;81(12):1324-1326. doi:10.1136/jnnp.2010.207464

214. Al-Chalabi A, Calvo A, Chio A, et al. Analysis of amyotrophic lateral sclerosis as a multistep process: A population-based modelling study. *Lancet Neurol*. 2014;13(11):1108-1113. doi:10.1016/S1474-4422(14)70219-4

215. Perl DP. Exposure to aluminium and the subsequent development of a disorder with features of Alzheimer's disease. *J Neurol Neurosurg Psychiatry*. 2006;77(7):811. doi:10.1136/jnnp.2006.090613

216. Paez-Colasante X, Figueroa-Romero C, Sakowski SA, Goutman SA, Feldman EL. Amyotrophic lateral sclerosis: Mechanisms and therapeutics in the epigenomic era. *Nat Rev Neurol*. 2015;11(5):266-279. doi:10.1038/nrneurol.2015.57

217. Desplats P, Patel P, Kosberg K, et al. Combined exposure to Maneb and Paraquat alters transcriptional regulation of neurogenesis-related genes in mice models of Parkinsons disease. *Mol Neurodegener*. 2012;7(1):1. doi:10.1186/1750-1326-7-49

218. Alonso A, Logroscino G, Jick SS, Hernan MA. Association of smoking with amyotrophic lateral sclerosis risk and survival in men and women: a prospective study. *BMC Neurol*. 2010;10:6. doi:10.1186/1471-2377-10-6\r1471-2377-10-6 [pii]

219. Bird A. Perceptions of epigenetics. *Nature*. 2007;447(7143):396-398. doi:10.1038/nature05913

220. Qureshi IA, Mehler MF. Epigenetic mechanisms governing the process of neurodegeneration. *Mol Aspects Med*. 2013;34(4):875-882. doi:10.1016/j.mam.2012.06.011

221. Chestnut B a., Chang Q, Price A, Lesuisse C, Wong M, Martin LJ. Epigenetic Regulation of Motor

Neuron Cell Death Through DNA Methylation. *J Neurosci*. 2011;31(46):16619-16636. doi:10.1523/JNEUROSCI.1639-11.2011.Epigenetic

222. Urdinguio RG, Sanchez-Mut J V., Esteller M. Epigenetic mechanisms in neurological diseases: genes, syndromes, and therapies. *Lancet Neurol*. 2009;8(11):1056-1072. doi:10.1016/S1474-4422(09)70262-5

223. Feng J, Fouse S, Fan G. Epigenetic regulation of neural gene expression and neuronal function. *Pediatr Res*. 2007;61(5 PART 2 SUPPL.):58-63. doi:10.1203/pdr.0b013e3180457635

224. Fuso A, Nicolia V, Cavallaro RA, Scarpa S. DNA methylase and demethylase activities are modulated by one-carbon metabolism in Alzheimer's disease models. *J Nutr Biochem*. 2011;22(3):242-251. doi:10.1016/j.jnutbio.2010.01.010

225. Lagali PS, Picketts DJ. Matters of life and death: The role of chromatin remodeling proteins in retinal neuron survival. *J Ocul Biol Dis Infor*. 2011;4(3):111-120. doi:10.1007/s12177-012-9080-3

226. Martin C, Zhang Y. The diverse functions of histone lysine methylation. *Nat Rev Mol Cell Biol*. 2005;6(11):838-849. doi:10.1038/nrm1761

227. Janssen C, Schmalbach S, Boeselt S, Sarlette A, Dengler R, Petri S. Differential histone deacetylase mRNA expression patterns in amyotrophic lateral sclerosis. *J Neuropathol Exp Neurol*. 2010;69(6):573-581. doi:10.1097/NEN.0b013e3181ddd404

228. Kwak S, Hideyama T, Yamashita T, Aizawa H. AMPA receptor-mediated neuronal death in sporadic ALS. *Neuropathology*. 2010;30(2):182-188. doi:10.1111/j.1440-1789.2009.01090.x

229. Hideyama T, Yamashita T, Aizawa H, et al. Profound downregulation of the RNA editing enzyme ADAR2 in ALS spinal motor neurons. *Neurobiol Dis*. 2012;45(3):1121-1128. doi:10.1016/j.nbd.2011.12.033

230. Lewis BP, Burge CB, Bartel DP. Conserved seed pairing, often flanked by adenosines, indicates that thousands of human genes are microRNA targets. *Cell*. 2005;120(1):15-20. doi:10.1016/j.cell.2004.12.035

231. Lagos-Quintana M, Rauhut R, Lendeckel W, Tuschl T. Identification of novel genes Coding for RNAs of Small expressed RNAs. *Science (80-)*. 2001;294(5543):853-858. doi:10.1126/science.1064921

232. Hansen TB, Wiklund ED, Bramsen JB, et al. MiRNA-dependent gene silencing involving Ago2-mediated cleavage of a circular antisense RNA. *EMBO J*. 2011;30(21):4414-4422. doi:10.1038/emboj.2011.359

233. Haramati S, Chapnik E, Sztainberg Y, et al. miRNA malfunction causes spinal motor neuron disease. *Proc Natl Acad Sci*. 2010;107(29):13111-13116. doi:10.1073/pnas.1006151107

234. Rüegger S, Großhans H. MicroRNA turnover: When, how, and why. *Trends Biochem Sci*. 2012;37(10):436-446. doi:10.1016/j.tibs.2012.07.002

235. Freischmidt A, Müller K, Ludolph AC, Weishaupt JH. Systemic dysregulation of TDP-43 binding microRNAs in amyotrophic lateral sclerosis. *Acta Neuropathol Commun*. 2013;1(1):42. doi:10.1186/2051-5960-1-42

236. Williams AH, Valdez G, Moresi V, et al. MicroRNA-206 delays ALS progression and promotes regeneration of neuromuscular synapses in mice. *Science*. 2009;326(5959):1549-1554. doi:10.1126/science.1181046

237. Logroscino G, Traynor BJ, Hardiman O, et al. Descriptive epidemiology of amyotrophic lateral sclerosis: New evidence and unsolved issues. *J Neurol Neurosurg Psychiatry*. 2008;79(1):6-11. doi:10.1136/jnnp.2006.104828

238. Lacomblez L, Bensimon G, Leigh PN, Guillet P, Meininger V. Dose-ranging study of riluzole in amyotrophic lateral sclerosis. Amyotrophic Lateral Sclerosis/Riluzole Study Group II. *Lancet*. 1996;347(9013):1425-1431. doi:10.1016/S0140-6736(96)91680-3

239. Gordon PH, Salachas F, Bruneteau G, et al. Improving survival in a large French ALS center cohort. *J Neurol*. 2012;259(9):1788-1792. doi:10.1007/s00415-011-6403-4

240. Olney RK, Murphy J, Forshew D, et al. The effects of executive and behavioral dysfunction on the course of ALS. *Neurology*. 2005;65(11):1774-1777. doi:10.1212/01.wnl.0000188759.87240.8b

241. Gordon PH. Amyotrophic lateral sclerosis: Pathophysiology, diagnosis and management. *CNS Drugs*. 2011;25(1):1-15. doi:10.2165/11586000-000000000-00000

242. Rabkin JG, Albert SM, Rowland LP, Mitsumoto H. How common is depression among ALS caregivers? A longitudinal study. *Amyotroph Lateral Scler*. 2010;10(5-6):448-455. doi:10.1080/17482960802459889

243. Lou J, Reeves A, Benice T, Sexton G. Fatigue and depression are associated with poor quality of life in ALS. *Neurology*. 2003;60(1):122-123. http://www.ncbi.nlm.nih.gov/pubmed/12525733.

244. Wu MY, Hill CS. TGF-β Superfamily Signaling in Embryonic Development and Homeostasis. *Dev Cell*. 2009;16(3):329-343. doi:10.1016/j.devcel.2009.02.012

245. Pardali E, Goumans MJ, ten Dijke P. Signaling by members of the TGF-β family in vascular morphogenesis and disease. *Trends Cell Biol*. 2010;20(9):556-567. doi:10.1016/j.tcb.2010.06.006

246. Kang JS, Liu C, Derynck R. New regulatory mechanisms of TGF-β receptor function. *Trends Cell Biol*. 2009;19(8):385-394. doi:10.1016/j.tcb.2009.05.008

247. Heldin CH, Moustakas A. Role of Smads in TGFβ signaling. *Cell Tissue Res*. 2012;347(1):21-36. doi:10.1007/s00441-011-1190-x

248. Flanders KC, Ren RF, Lippa CF. Transforming growth factor-betas in neurodegenerative disease. *Prog Neurobiol*. 1998;54(1):71-85. doi:S0301-0082(97)00066-X [pii]

249. Chin J, Angers a, Cleary LJ, Eskin a, Byrne JH. Transforming growth factor beta1 alters synapsin distribution and modulates synaptic depression in Aplysia. *J Neurosci*. 2002;22(9):RC220. doi:20026363

250. Brionne TC, Tesseur I, Masliah E, Wyss-Coray T. Loss of TGF-beta 1 leads to increased neuronal cell death and microgliosis in mouse brain. *Neuron*. 2003;40(6):1133-1145. doi:10.1016/S0896-6273(03)00766-9

251. Strelau J, Strzelczyk A, Rusu P, et al. Progressive Postnatal Motoneuron Loss in Mice Lacking GDF-15. *J Neurosci*. 2009;29(43):13640-13648. doi:10.1523/JNEUROSCI.1133-09.2009

252. Fong SW, McLennan IS, McIntyre A, Reid J, Shennan KIJ, Bewick GS. TGF- 2 alters the characteristics of the neuromuscular junction by regulating presynaptic quantal size. *Proc Natl Acad Sci*. 2010;107(30):13515-13519. doi:10.1073/pnas.1001695107

253. McPherron AC, Lawler AM, Lee S-J. Regulation of skeletal muscle mass in mice by a new TGF-p superfamily member. *Nature*. 1997;387(6628):83-90. doi:10.1038/387083a0

254. Cohn RD, Erp C Van, Habashi JP, et al. Angiotensin II type 1 receptor blockade attenuates TGF-β– induced failure of muscle regeneration in multiple myopathic states. *Nat Med*. 2007;13(2):204-210. doi:10.1038/nm1536.Angiotensin

255. Katsuno M, Adachi H, Banno H, Suzuki K, Tanaka F, Sobue G. Transforming growth factor-β signaling in motor neuron diseases. *Curr Mol Med*. 2011;11(1):48-56. doi:10.2174/156652411794474356

256. Jiang Y, Zhang M, Koishi K, McLennan IS. TGF-β2 attenuates the injury-induced death of mature motoneurons. *J Neurosci Res*. 2000;62(6):809-813. doi:10.1002/1097-4547(20001215)62:6<809::AID-JNR7>3.0.CO;2-4

257. Houi K, Kobayashi T, Kato S, Mochio S, Inoue K. Increased plasma TGF-beta1 in patients with amyotrophic lateral sclerosis. *Acta Neurol Scand*. 2002;106(5):299-301. doi:10.1034/j.1600-0404.2002.01301.x

258. Jiang Y-M, Yamamoto M, Kobayashi Y, et al. Gene expression profile of spinal motor neurons in sporadic amyotrophic lateral sclerosis. *Ann Neurol*. 2005;57(2):236-251. doi:10.1002/ana.20379

259. Nakamura M, Ito H, Wate R, Nakano S, Hirano A, Kusaka H. Phosphorylated Smad2/3 immunoreactivity in sporadic and familial amyotrophic lateral sclerosis and its mouse model. *Acta Neuropathol*. 2008;115(3):327-334. doi:10.1007/s00401-007-0337-z

260. Vivien D, Ali C. Transforming growth factor-β signalling in brain disorders. *Cytokine Growth Factor Rev*. 2006;17(1-2):121-128. doi:10.1016/j.cytogfr.2005.09.011

261. Fernandes HB, Baimbridge KG, Church J, Hayden MR, Raymond LA. Mitochondrial Sensitivity and Altered Calcium Handling Underlie Enhanced NMDA-Induced Apoptosis in YAC128 Model of Huntington's Disease. *J Neurosci*. 2007;27(50):13614-13623. doi:10.1523/JNEUROSCI.3455-07.2007

262. Holzbaur ELF, Howland DS, Weber N, et al. Myostatin inhibition slows muscle atrophy in rodent models of amyotrophic lateral sclerosis. *Neurobiol Dis*. 2006;23(3):697-707. doi:10.1016/j.nbd.2006.05.009

263. Miller TM, Kim SH, Yamanaka K, et al. Gene transfer demonstrates that muscle is not a primary target for non-cell-autonomous toxicity in familial amyotrophic lateral sclerosis. *Proc Natl Acad Sci*. 2006;103(51):19546-19551. doi:10.1073/pnas.0609411103

264. Zhong Z, Ilieva H, Hallagan L, et al. Activated protein C therapy slows ALS-like disease in mice by transcriptionally inhibiting SOD1 in motor neurons and microglia cells. *J Clin Invest*. 2009;119(11):3437-3449. doi:10.1172/JCI38476

265. Galbiati M, Crippa V, Rusmini P, et al. ALS-related misfolded protein management in motor neurons and muscle cells. *Neurochem Int*. 2014;79:70-78. doi:10.1016/j.neuint.2014.10.007 Mini review

266. Galbiati M, Onesto E, Zito A, et al. The anabolic/androgenic steroid nandrolone exacerbates gene expression modifications induced by mutant SOD1 in muscles of mice models of amyotrophic lateral sclerosis. *Pharmacol Res*. 2012;65(2):221-230. doi:10.1016/j.phrs.2011.12.001

267. Bierie B, Moses HL. TGF-β and cancer. *Cytokine Growth Factor Rev*. 2006;17(1-2):29-40. doi:10.1016/j.cytogfr.2005.09.006

268. Shi Y, Massagué J. Mechanisms of TGF-beta signaling from cell membrane to the nucleus. *Cell*.

2003;113(6):685-700. doi:10.1016/S0092-8674(03)00432-X

269. Mo K, Razak Z, Rao P, et al. Microarray analysis of gene expression by skeletal muscle of three mouse models of Kennedy disease/spinal bulbar muscular atrophy. *PLoS One*. 2010;5(9):1-8. doi:10.1371/journal.pone.0012922

270. Ueberham U, Ueberham E, Gruschka H, Arendt T. Altered subcellular location of phosphorylated Smads in Alzheimer's disease. *Eur J Neurosci*. 2006;24(8):2327-2334. doi:10.1111/j.1460-9568.2006.05109.x

271. Phatnani HP, Guarnieri P, Friedman BA, et al. Intricate interplay between astrocytes and motor neurons in ALS. *Proc Natl Acad Sci*. 2013;110(8):E756-E765. doi:10.1073/pnas.1222361110

272. Krieglstein K, Strelau J, Schober A, Sullivan A, Unsicker K. TGF-β and the regulation of neuron survival and death. *J Physiol Paris*. 2002;96(1-2):25-30. doi:10.1016/S0928-4257(01)00077-8

273. Tesseur I, Zou K, Berber E, Zhang H, Wyss-Coray T. Highly sensitive and specific bioassay for measuring bioactive TGF-β. *BMC Cell Biol*. 2006;7:1-7. doi:10.1186/1471-2121-7-15

274. Ahtikoski AM, Koskinen SOA, Virtanen P, Kovanen V, Risteli J, Takala TES. Synthesis and degradation of type IV collagen in rat skeletal muscle during immobilization in shortened and lengthened positions. *Acta Physiol Scand*. 2003;177(4):473-481. doi:10.1046/j.1365-201X.2003.01061.x

275. Fragiadaki M, Ikeda T, Witherden A, Mason RM, Abraham D, Bou-Gharios G. High doses of TGF- potently suppress type I collagen via the transcription factor CUX1. *Mol Biol Cell*. 2011;22(11):1836-1844. doi:10.1091/mbc.E10-08-0669

276. Miller J, Arrasate M, Brooks E, et al. Identifying polyglutamine protein species in situ that best predict neurodegeneration. *Nat Chem Biol*. 2011;7(12):925-934. doi:10.1038/nchembio.694